6-19-2018

Free-Radical Polymerization of Acid-Containing Deep Eutectic Solvents

Kylee Fazende

Louisiana State University and Agricultural and Mechanical College, kfazen2@lsu.edu

FREE-RADICAL POLYMERIZATION OF ACID-CONTAINING DEEP EUTECTIC
SOLVENTS

A Dissertation

Submitted to the Graduate Faculty of the
Louisiana State University and
Agricultural and Mechanical College
in partial fulfillment of the
requirements for the degree of
Doctor of Philosophy

in

The Department of Chemistry

by
Kylee Fazende
B.S., University of Southern Mississippi, 2013
August 2018

ACKNOWLEDGEMENTS

TABLE OF CONTENTS

LIST OF ABBREVIATIONS

AA	Acrylic acid
AIBN	2,2′-azobis(2-methylpropionitrile)
aIL	Advanced ionic liquid
APS	Ammonium persulfate
ATR	Attenuated total reflectance
ATRP	Atom-transfer radical polymerization
BPO	Benzoyl peroxide
ChBr	Choline bromide
ChBT	Choline bitartrate
ChCl	Choline chloride
CQ	Camphorquinone
CRP	Controlled radical polymerization
CTA	Chain transfer agent
DES	Deep eutectic solvent
DMF	Dimethyl formamide
DMSO	Dimethyl sulfoxide
FP	Frontal polymerization
FRP	Free-radical polymerization
FS	Fumed silica
FT	Front temperature
FTIR	Fourier transform-infrared spectroscopy
FV	Front velocity

HBA	Hydrogen bond acceptor
HBD	Hydrogen bond donor
HEMA	Hydroxyethyl methacrylate
HIPE	High internal phase emulsion
IBA	Isobutyric acid
IL	Ionic liquid
iPCM	Inert phase change material
k_p	Propagation rate constant
L231	Luperox ® 231
LA	Lauric acid
MAA	Methacrylic acid
MeA	Methyl acrylate
MMA	Methyl methacrylate
MWCNT	Multi-wall carbon nanotube
NDF	Neutral density filter
NMP	Nitroxide-mediated polymerization
OD	Optical density
PA	Propionic acid
PLP	Pulsed-laser initiated polymerization
RAFT	Reversible addition-fragmentation chain transfer polymerization
ROMP	Ring opening metathesis polymerization
RTIL	Room temperature ionic liquid

RTIR	Real-time infrared spectroscopy
SA	Stearic acid
SARA ATRP	Supplemental activation reducing agent atom-transfer radical polymerization
TMACl	Tetramethylammonium chloride
TPO	Diphenyl(2,4,6-trimethylbenzoyl) phosphine oxide

ABSTRACT

The forefront of this study explored polymerization, specifically thermally-initiated, free-radical frontal polymerization of (meth)acrylic acid monomers while the monomers acted as a hydrogen bond donor of a deep eutectic solvent. These frontal polymerizations were shown to exhibit unusual front velocities and, in some cases, lower front temperatures than the frontal polymerization of the neat monomers or systems containing inert analogs in the place of the hydrogen bond acceptor of these monomer-containing deep eutectic solvents. The frontal polymerization will occur with a range of initiator concentrations including ones that were too low for the pure monomer systems to sustain a front. Because of the unusual behavior of these frontal systems, an isothermal photopolymerization was performed using these acid-monomer systems.

The second half of this work focuses on the studying kinetics of photopolymerization of these monomer-containing deep eutectic solvents using real-time infrared spectroscopy. Analysis of this real-time reaction monitoring indicated increases in polymerization rate that span orders of magnitude when comparing the deep eutectic solvent polymerization to pure monomer polymerization. A significant increase in polymerization rate was also seen in systems that include a methyl ester derivative of the hydrogen bond donor monomer in a nonpolymerizable deep eutectic solvent. Because the increase in rate was present in systems in which the monomer is a component of the deep eutectic solvent as well as when the monomer is just within a deep eutectic solvent, it can be determined that in addition to increased solvent viscosity, both preorganization due to hydrogen bonding and the polarity of the deep eutectic solvent around the monomer play a role in the enhancement of the rate.

I. INTRODUCTION

1.1 FREE-RADICAL POLYMERIZATION

Polymerizations can occur in a number of ways, but one that is extremely common (and the focus of this work) is free-radical polymerization (FRP). FRP is a type of addition polymerization meaning each polymer chain is grown one monomer addition at a time, and the polymer typically only grows from one end when producing linear polymer. The pool of FRP monomers is quite large because, in theory, any C-C double bond can form a radical. In practice, less substituted alkenes make better monomers because less substitutions lead to more reactive, less stable radicals as well as producing radicals that are less sterically hindered against attack.[1]

FRP typically occurs in three steps: initiation, propagation and termination; a summary of which can be seen in Scheme 1.1. Initiation is the beginning of an FRP and determines how the polymerization is started. Initiation is the process of fragmenting a molecule and forming radicals on the fragments that can then react with polymerizable molecules. The three main types of initiation are thermal, photo, and redox; some commonly used initiators from each category can been seen in Figure 1.1.[2]

Initiation: $I-I \rightarrow 2I\cdot$
Propagation: $I\cdot + M \rightarrow M\cdot$
                        $M\cdot + M \rightarrow P\cdot$
Termination: $P_1\cdot + P_2\cdot \rightarrow P_{12}$ (combination)
                        $P_1\cdot + P_2\cdot \rightarrow P_1 + P_2$ (disproportionation)
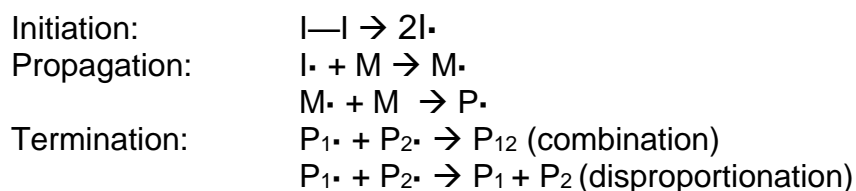
Scheme 1.1. The general process of initiation, propagation, and termination as seen in FRP.
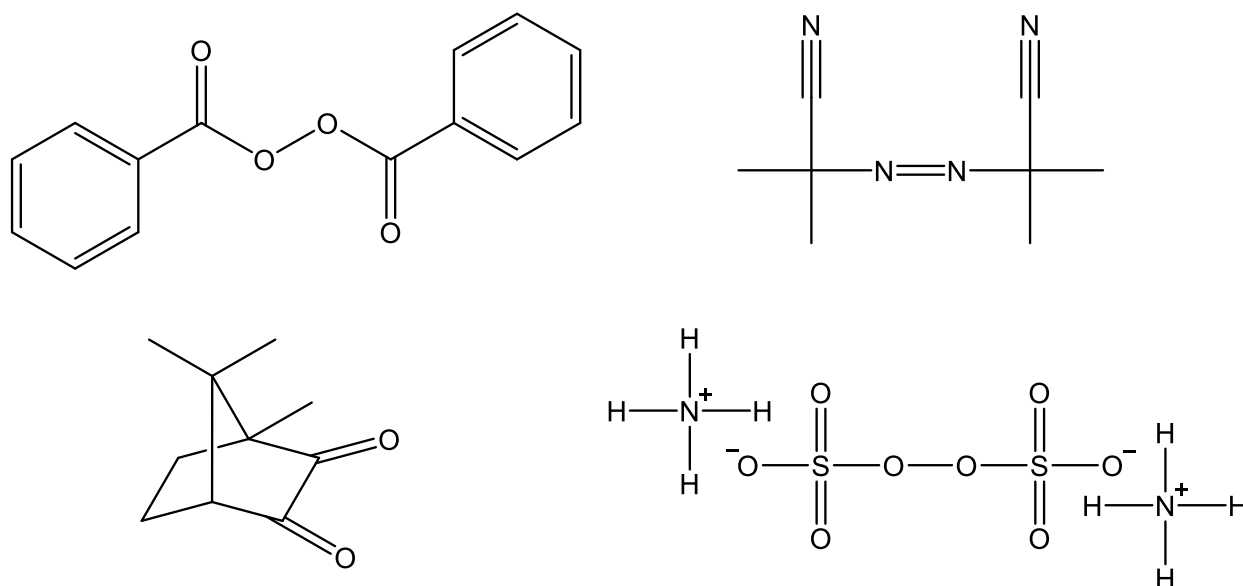
Figure 1.1. Commonly used FRP initiators (clockwise from top left): benzoyl peroxide (BPO, thermal) 2,2′-azobis(2-methylpropionitrile) (AIBN, thermal), ammonium persulfate (APS, redox) and camphorquinone (CQ, photo).

This work employs both thermal and photoinitiators as can be seen in Chapters 2 and 3, respectively. Initiator concentration determines the number of polymer chains that can be produced as well as influencing how fast the polymerization can occur. Propagation occurs when the initiator radical (I·) combines with a single electron from a monomer's pi bond to break the double bond and form a new, more stable single bond between the initiator fragment and monomer along with a new radical (M·, Scheme 1.1). This new monomer radical then combines with the alkene of a different monomer to keep the polymer chain growing (P·). Eventually termination occurs during which radicals react in such a way that a new radical is not produced, thus ending the polymerization reaction. Termination can occur by two mechanisms: combination and disproportionation. Combination termination happens when the radicals of two polymer chains react together to form a single, longer polymer chain. Disproportionation termination is a reaction in which a growing chain radical abstracts a hydrogen from

another growing chain, thus killing the growth of both chains without increasing either chain's length.[2] The kinetics of this type of polymerization dictate the almost instantaneous growth of large chains as soon as initiation takes place, and the number of these large chains increases over time (see Figure 1.2). For more information on the kinetics of FRP, see Chapter 3.

Within the realm of radical-addition polymerization also exists controlled radical polymerization (CRP). Unlike during FRP, radicals in CRP do not exist freely until they can react with the next monomer. Additional molecules are added to a CRP system to limit the radical concentration that exists at any one time. Because of this, CRP produces polymers that are more monodisperse in size and exhibit different kinetics than FRP polymerizations. Ideally, all chains within a CRP system are initiated simultaneously, grow linearly with time, and never terminate. The lack of termination in a true CRP leads to these also being called "living" polymerizations.[2] The differences in the kinetic profiles of FRP and CRP can be seen in Figure 1.2.
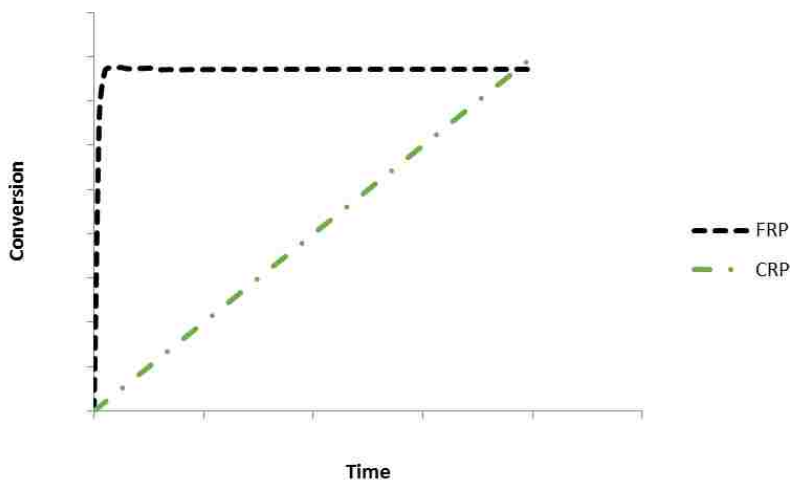

Figure 1.2. Generalized kinetic profiles of controlled and free-radical addition polymerizations.

Three main types of CRP exist: nitroxide-mediated polymerization (NMP),[3] atom-transfer radial polymerization (ATRP),[4] and reversible addition-fragmentation chain transfer polymerization (RAFT);[5] each with their own control process, advantages, and disadvantages. NMP uses stable nitroxide radicals to react with the radicals of growing chains to minimize the number of active growing chains and therefore minimize termination. ATRP uses redox chemistry between an activated metal (usually Cu or Fe) and metal halide to react with growing chain radicals and reversibly deactivate the growing chains.[4] RAFT uses chain transfer agents (CTAs) to cap the majority of growing chains during the polymerization process keeping them from terminating.[5]

1.2 IONIC LIQUIDS

Ionic liquids (ILs) have in recent decades become a large contender in the field of polymers because of their ability to solvate polymers and monomers for polymerization reactions. Kubisa has written an excellent review on the subject highlighting both the utility and limitations of ILs in relation to polymerizations.[6] Ionic liquids are ionic complexes that can form a molten salt at some temperature below 100 °C. Room temperature ionic liquids (RTILs) are desirable for most applications. These ionic complexes are typically comprised of a large, organic cation and a smaller anion (see Figure 1.3 for some commonly employed RTIL components). Imidazolium cations are arguably the most commonly used for RTILs. Initially, RTIL anions were quite air and water sensitive which minimized their usefulness in real world applications. By the 1990s a second generation of ILs had emerged that were much more stable to ambient conditions, but the anions tended to have weaker complexation ability than the more sensitive first-generation anions. After the turn of the century, a third generation of ILs

emerged. This third generation included what Gorke deemed "advanced ILs" (aILs).[7] Many aILs contained quaternary ammonium salts and tended to be more biodegradable and nontoxic than their older, IL predecessors. These aILs, in some cases, do not performs like traditional ILs because they require a second molecule as part of their complex that contains no charged groups. A specific type of these aILs that contains one charged and one uncharged molecule are deep eutectic solvents (DESs).

Commonly used IL cations   **Commonly used IL anions**
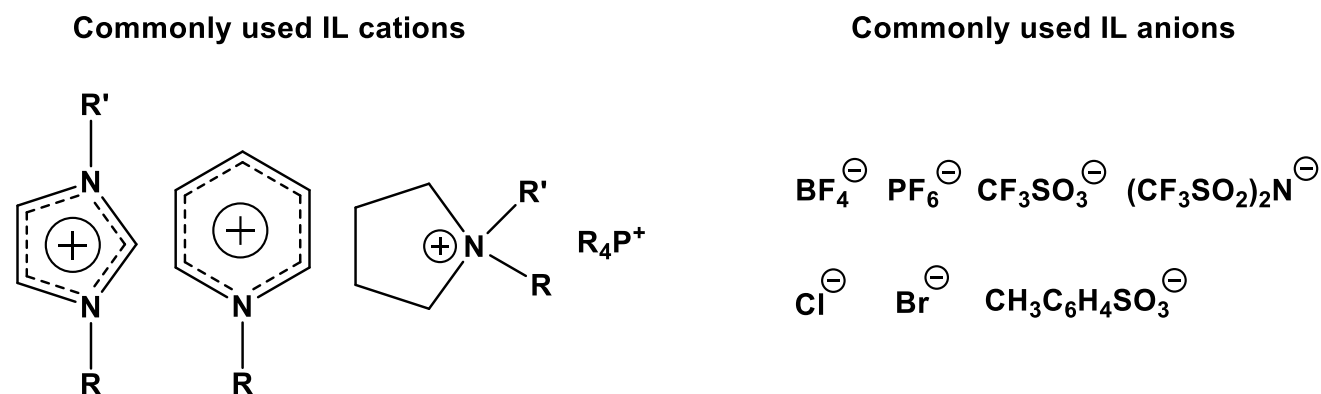
Figure 1.3. Commonly used IL components.

1.3 DEEP EUTECTIC SOLVENTS
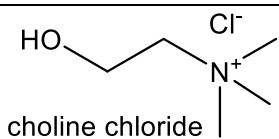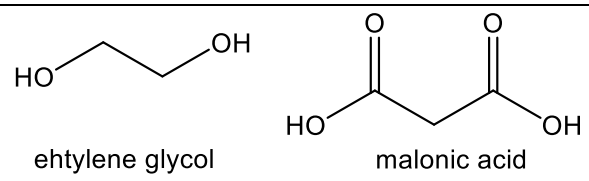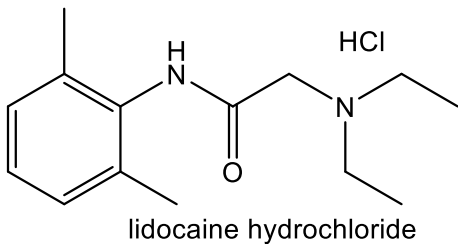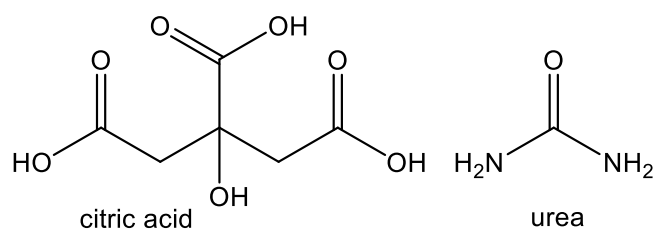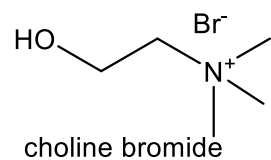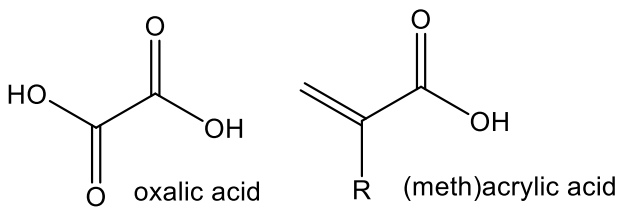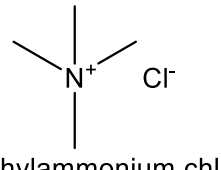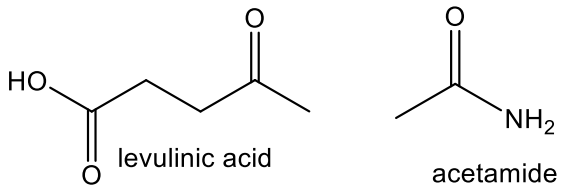
Though eutectics have been used in various forms for over two decades, Abbott pioneered DESs as we know them today in the early 2000s.[8] DESs are becoming increasingly popular in a variety of fields. Multiple reviews regarding DESs and their various uses and properties have been written in the past decade.[9-15] DESs can be divided into several classes depending on their components (see Table 1.1). Because of the variety of the types of DESs and versatility within the types of DESs, they have the ability to be more tunable than traditional ILs while maintaining many of the desirable qualities of ILs like low vapor pressure, high temperature stability, and (in many cases) higher viscosity than small molecule, organic solvents.[6] The commonly accepted complexation found in DESs is seen in Figure 1.4. In Type III DESs, the

5

hydrogen bond acceptor (HBA) is the quaternary ammonium salt, and the hydrogen

bond donor (HBD) is an organic molecule that is capable of hydrogen bonding. Many

types of HBDs have been studied including alcohols,[16, 17] amides,[8] and carboxylic

acids.[18, 19] Table 1.2 shows some commonly used DES components. This work focuses

on HBDs that are exclusively carboxylic acids. Because of the hydrogen bonding nature

of DESs, they tend to be quite hydrophilic. Hydrophobic eutectics based on menthol and

a variety of carboxylic acids have been reported,[20] but to classify these as DESs is

debatable since the eutectics contain no charged species.

Table 1.1. The types of DESs.[9]

Type	General Formula	Formula Terms and Components
I	$Cat^+X^-zMCl_x$	M = Zn, Sn, Fe, Al, Ga, In
II	$Cat^+X^-zMCl_x \cdot yH_2O$	M = Cr, Co, Cu, Ni, Fe
III	Cat^+X^-RZ	Z = COOH, $CONH_2$, OH, NH_2CONH_2
IV	$MCl_x + RZ = MCl_{x-1}^+ \cdot RZ + MCl_{x+1}^-$	M = Al or Zn Z = $CONH_2$ or OH

Table 1.2. Type III DES components.

HBA	HBD
choline chloride lidocaine hydrochloride choline bromide tetramethylammonium chloride	ehtylene glycol malonic acid citric acid urea oxalic acid (meth)acrylic acid levulinic acid acetamide

The formation of the DESs itself is generally believe to be due to a massive depression in freezing point (see Figure 1.4) caused by charge delocalization because of the strong hydrogen bonding interactions between the halide anion and the HBD.[21] In some cases, the decrease in freezing point can be greater than 200 ⁰C.[18] DESs have been applied to an number of fields including CO_2 capture,[21-23] drug solubilization and release,[24-26] biomass and biopolymer processing,[27-31] oil separation,[32, 33] and many more.
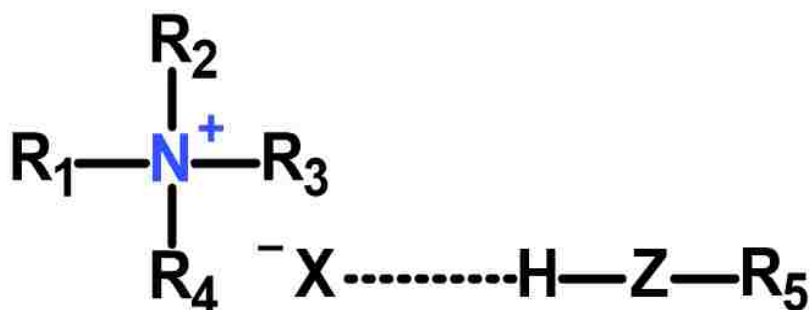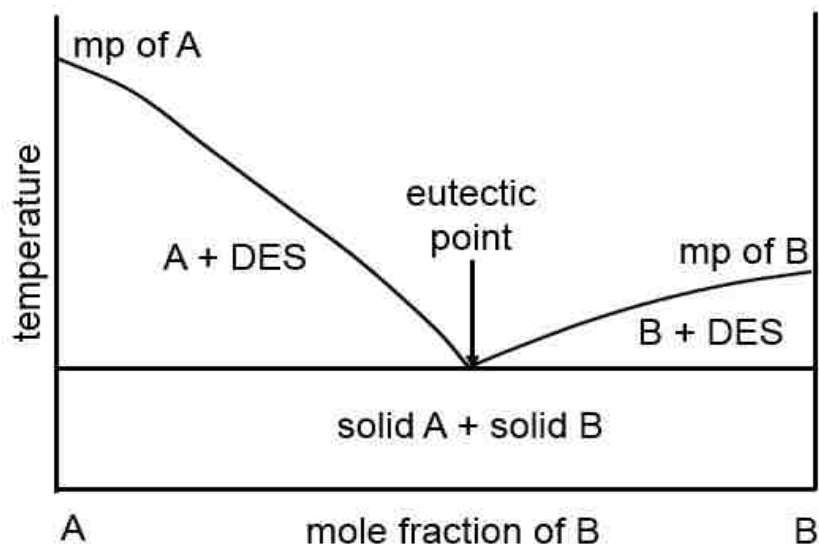
Figure 1.4. A model phase diagram of a DES (top), and the bimolecular complexation found in a Type III DES (bottom).

With the increase in popularity of these complex solvents has come those who seek to understand and hope to predict the molecular interactions that influence and dictate the properties of DESs. It is generally recognized that for many, if not most DESs, the eutectic point is at a molar ratio of 2:1, HBD:HBA, thus, many DES researchers consider 2:1 to be the "ideal" ratio for a DES. Little is known or understood about this ratio or why this occurs at this specific ratio, though an argument can be made for the number of hydrogen bond capable hydrogens in relation to the number of HBA anions. Bednarz noted in their publication on itaconic acid DESs that the most

successful ratio was 1:1 as opposed to 2:1,[34] but since itaconic acid is a difunctional carboxylic acid, the ratio of 2 hydrogens per Cl⁻ anion is conserved.

Without a complete understanding of the molecular interactions within DESs, the ability to predict properties and DESs behavior is not possible. Several researchers are making progress in this area using a variety of tools including molecular dynamic simulations,[35, 36] neutron scattering,[37, 38] nuclear magnetic resonance spectroscopy,[39] and infrared spectroscopy.[36, 40] Kuroda's 2D FTIR work is specifically interesting because they propose a heterogeneous molecular structure within the DES that if properly understood, could largely influence and expand the utility of DESs in the future. Quasi-elastic neutron scattering has also been used to examine DESs at the molecular level and, in that case, the typical bimolecular complexation model (Figure 1.4) of DESs is also questioned.[37] Similar conclusions have been reached about RTILs.[6] Much more exploration into DES structure is left to be completed before DES properties will be able to be predicted.

Another advantage of DESs over their RTIL counterparts is that DES components can quite easily be derived from biomass and other natural sources, making them desirable as "green" solvents. Because of these more naturally derived components, DESs (like some of their aIL counterparts) tend to have lower toxicity and better biodegradability than many RTILs. Examples of these more "green" DES components previously seen in literature are fructose,[26] glycerol,[41] citric acid,[42] lactic acid,[42] levulinic acid,[19] and probably most commonly urea.[8] The most commonly used HBA is choline chloride (ChCl) which can be considered quite green due to its being a B vitamin derivative (and having provitamin status in Europe) making it a common additive

9

to livestock feed.[9] DESs like RTILs are also recyclable as solvents under the correct conditions[43] further increasing their "green" character. One area in which "greenness" as well as DESs' other previously mentioned desirable qualities are being taken advantage of as solvents (and in some cases, reactants) is in polymerization reactions. DESs have been shown to be especially useful in the realm of polymerization. Below, the concept of the polymerization in and of DESs will be addressed with a special emphasis given to free-radical polymerization, which is the focus of this work.

1.3.1 Polymerization in DESs

One of the many advantages to DESs is their ability to solvate materials and be used in reactions where traditional organic solvents would not perform well—high heat, partial vacuum, or high viscosity. Because of this, DESs are ideal for use as solvents in polymerization reactions.

Gutierrez et al. demonstrated that furfuryl alcohol and formaldehyde can undergo polycondensation within a p-toluenesulfonic acid-choline chloride DES.[44] This work is worth noting for two reasons: one, because this is one of the earliest examples of DES polycondensation without diluting the DES, and two, because that particular DES had quite a low viscosity allowing MWCNTs to be homogeneously dispersed into the DES. After post-polymerization pyrolysis, it was found that the MWCNTs were homogeneously incorporated into the polymer network due to condensation with the furfuryl alcohol carbons.

In 2011, Mota-Morales et al. began the trend of performing FRP in DESs.[45] (Though in that particular case, which is discussed in more detail below and then in Chapter 2, the monomer was part of the DES, thus making it a polymerization of the

10

DES as opposed to in the DES.) This work showed that FRP can be successful in DESs, and many researchers have expanded upon that finding by using DESs as inert solvents for FRP reactions. Hydroxyethylmethacrylate (HEMA) is a common monomer used in DESs and has been polymerized in fructose-ChCl,[26] orcinol-ChCl,[46] and ethylene glycol-ChCl[16] DESs. The resulting materials were quite interesting and applied to drug delivery (fructose-ChCl) and gel electrolytes that can be used as flexible supercapacitors (orcinol-ChCl and ethylene glycol-ChCl). Methyl methacrylate,[47] HEMA,[48] and methyl acrylate[49] have both been polymerized via ATRP in DESs.[47] One interesting note about the aforementioned ATRP of methyl methacrylate is that the reaction was performed without a traditional ATRP ligand.[47] The DESs were also shown to enhance the recovery of the metallic ATRP catalyst.[49] Both acrylate and methacrylate monomers have been shown to exhibit controlled polymerization behavior during SARA ATRP in DESs as well.[48]

Another interesting type of radical polymerization that has been performed in DESs is enzyme-mediated radical polymerization. Sanchez-Leija and coworkers showed that acrylamide within a DES could be polymerized and that the polymerization was mediated by the enzyme.[50] Polymerization within the DES did occur at low temperature (4 °C) while in pure aqueous environment, no polymer was obtained.[50]

One last and rather interesting application of free-radical polymerization in DESs is that of heterogeneous FRP. In a series of papers spearheaded by Carranza of the Pojman team, high internal phase emulsions that contained DESs were polymerized. DESs were the internal phase of the HIPEs while the continuous phase consisted of monomer and crosslinker.[43] A number of monomers including lauryl acrylate, styrene,

methyl methacrylate, and stearyl acrylate were applied to these HIPE systems. Upon polymerization and crosslinking of the continuous phase, the internal phase was able to be removed and recycled. The resulting crosslinked material was porous, and the porosity corresponded quite well to the dispersion and droplet size within the unpolymerized HIPEs. This concept was advanced a step further by incorporating nanomaterials including nitrogen doped MWCNTs[51] or nanohydroxyapetite[52] to produce nanocomposites with defined and predictable porosity.

1.3.2 Polymerizations of DESs

Because of the wide variety of molecules that can be used in DESs, it is only reasonable to assume that some monomers, whether readily available or specifically synthesized for the purpose, can be used as DES components. In this case, the DES, or at least one of its components, functions as a monomer and participates in the polymerization reaction. The idea of polymerization of a DES is the focus of this work, but many have already successfully polymerized DESs and, in some cases, created very interesting materials in the process.

Polycondensations of resorcinol-choline chloride DESs with formaldehyde were among the first polymerization reactions performed within and of DESs. This makes sense as the HBDs are often molecules that can participate in polycondensation reactions (alcohols and carboxylic acids). The poly(DES) monoliths had bimodal porosity with both meso and micropores.[53] Carriazo then expanded this work to ternary DESs containing urea, resorcinol, and choline chloride to create high surface area materials.[54] Resorcinol-choline chloride DESs can also be polymerized in the presence of 3-hydroxypyridine to create a monolith that contains significant nitrogen content with

the high carbon content.[55] Another example of polycondensation of a DES is that of the octanediol-lidocaine DES which when polymerized with citric acid, creates an elastomeric material that is capable of drug release of the lidocaine.[25] Octanediol, combined a number of HBAs including ChCl and tetraethylammonium bromide, was also used for polycondensation with citric acid to produce biodegradable polyester elastomers which showed some antimicrobial properties due to the presence of the HBA cation.[56]

As previously stated, CO_2 capture is an area where DESs have been found useful. Isik et al. have taken the concept a step further by polymerizing DESs that contain special monomeric components for CO_2 capture.[21, 22] In this case two very different monomers were employed. The first was a quaternary ammonium methacrylate synthesized by starting with an amine containing methacrylate that was then quaternized to produce the polymerizable quaternary ammonium HBA. The methacrylate HBA was used with amidoxime as the HBD and was polymerized using photopolymerization and an additional crosslinker. The second type of HBA monomer was multifunctional alcohols (both tri and tetrafunctional) that were used in condensation polymerization with citric acid, which acted as the HBD for those systems. It is worth nothing that similar to the polycondensations performed by Serrano et al,[25] these polycondensation reactions were performed over a matter of days as opposed to the almost instantaneous crosslinking seen in a photopolymerization. After the polymerization and characterization of the resulting polymers only the methacrylate-amidoxime system was selected to be applied in CO_2 capture.[21] This nonporous

poly(DES) material was shown to have better CO_2 absorption than analogous

poly(amines) functionalized with amidoximes that had been previously reported.[22]

Recently, Li and colleagues reported the polymerization of an acrylic acid-choline

chloride DES with a crosslinker using photopolymerization.[57] The use of

photopolymerization allowed for a 3D patternable material that was elastomeric and

transparent. Because this material also exhibited conductivity, the poly(DES) was

applied to strain and tactile sensors using changes in resistance to indicate changes in

the polymer network that corresponded to the respective stimuli.[57]

Mota-Morales was able to perform free-radical polymerizations in DESs. This

case is unique, however, because those polymerizations were performed using frontal

polymerization (FP),[45] which is discussed in more detail in Chapter 2. Over several

years, a series of publications by Mota-Morales and coworkers showed that FP and

DESs can be quite successful when used in tandem,[58] including in the production of

nanocomposites.[59] The success of these free-radical, and specifically frontal,

polymerizations inspired this work.

1.3.3 Choline activation of polymerization reactions

In a few cases, choline chloride has been shown to have a catalytic effect on

reactions. The first case is that of epoxide ring opening by nucleophilic attack in the

presence of a $SnCl_2$/ChCl DES.[60] Though, not performed as a polymerization, epoxide

ring opening polymerizations are extremely common and useful, so the relevance to

polymerization is present. Most of the epoxide ring openings that were performed in the

DES produced a greater than 90% yield of ring opened product in less than two hours

without the addition of any additional heat regardless of the type of nucleophile used. Some thiol nucleophiles reached greater than 90% yield in just 10 minutes.

The second and more relevant case to this manuscript is the report of choline chloride affecting the decomposition of a free-radical initiator.[61] Itaconic acid DESs were shown by the same group to be able to be polymerized using redox-initiated FRP, These itaconic acid-choline chloride DESs were able to be crosslinked and produce hydrogels.[34] The interesting thing is that in the aqueous solution polymerization, choline chloride was shown to activate the redox decomposition of the ammonium persulfate initiator (seen in Figure 1.1).[61] This activation led to a higher molecular weight of the resulting polymer but also a larger polydispersity. The activation also led to the oxidation of the choline cation to form an aldehyde as can be seen in Figure 1.5.
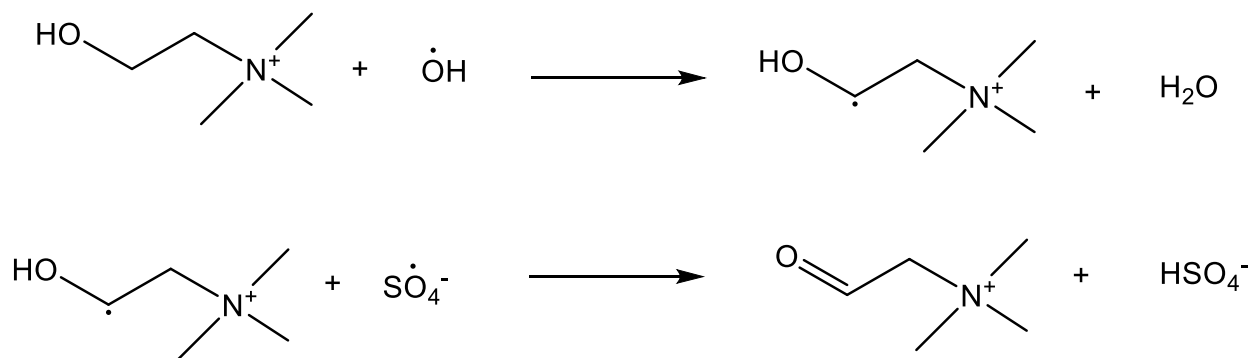
Figure 1.5. One proposed route for the oxidation of choline to betaine aldehyde during the redox FRP of itaconic acid.

II. FRONTAL POLYMERIZATION OF AN ACID-MONOMER-CONTAINING DEEP EUTECTIC SOLVENT

2.1 INTRODUCTION

Frontal polymerization (FP) is a polymerization method during which the site of reaction is localized and propagates through the monomer. FP falls into three categories: thermal, isothermal, and photofrontal; with each relying on a different phenomenon to allow the front to propagate. Thermal frontal polymerization—the focus of this manuscript—relies on the Arrhenius dependence of an exothermic reaction coupled with heat transport in the system.[62] Isothermal frontal polymerization occurs when the Trommsdorff-Norrish gel effect creates a localized area of low termination that propagates through the system.[63-65] The front in a photofrontal polymerization propagates due to a continuous flux of radiation (most commonly UV light).[66, 67] FP was first studied by Soviet scientists Chechlio, et al. in the mid-1970s using benzoyl peroxide initiated methyl methacrylate polymerization.[68] In the case of that particular system, pressure was needed to ensure that the front occurred,[69] but there are many monomers that can be polymerized using FP under ambient conditions. Since then, research on FP has expanded significantly to include cure-on-demand materials,[70, 71] synthesis of gels[34, 72-78] and gradient materials,[79-81] and epoxide polymerizations,[82-85] composite materials,[59, 86-89] and many other applications.

One of the most commonly studied types of FP (and the focus of this work) is thermal free-radical frontal polymerization of acrylic monomers. Acrylic (also called

acrylate) FP is typically performed via free-radical polymerization, but many other types

of polymerizations have also been applied in FP including cationic[90-93], ROMP[94, 95],

controlled free radical[96], and thiol-ene.[65, 97, 98] Multifunctional monomers are especially

popular in FP studies[70, 99-102] due to their increased reactivity and crosslinked nature

which makes the polymerization less susceptible to convective instabilities. The type of

polymerization and its corresponding initiator typically dictates whether the reaction is

classified as thermal, isothermal, or photofrontal. Monomers that can be polymerized

using a free-radical mechanism, such as acrylates, can be thermal or photofrontal, as

the corresponding initiator can be obtained in both thermally initiated and photoinitiated

varieties. This work utilizes peroxide, thermal initiators.

Two major values are used to determine the usefulness of a frontal reaction: front

temperature (FT) and front velocity (FV); these two values give the ability to

quantitatively compare one frontal system to another as long as factors that affect the

values are taken into account. Front temperature is the maximum temperature recorded

during front propagation. As will be seen in the section 2.3.4 (as well as Appendix B),

the temperature profile in a thermal FP system is well defined; for any specific point in

the monomer mixture, the temperature does not drastically change until the front

propagates through and then FT is reached. Front velocity is the determination of how

quickly the front propagates through a system. Section 2.3.4 will provide details on how

this is determined using video recording and the position versus time graphs that are

obtained to determine FV.

All types of FP have certain requirements to allow the front to propagate, but as

this work focuses on thermal FP (from this point forward, "FP"), those requirements are

the most pertinent. The polymerization reaction must be exothermic, and its rate of reaction must exhibit an Arrhenius dependence as well as being drastically larger at the front temperature than at ambient temperature (or storage temperature if not stored at ambient conditions). Zero reaction at ambient temperature is ideal, but any reaction with a sufficiently low reaction rate at ambient temperature can produce a front. Sufficiently high viscosity is also desired so that convection does not decrease the amount of heat at the front to the point that propagation ceases.

These requirements for FP create limitations for the utility of frontal systems. Oftentimes, due to the need for such a drastic increase in reaction rate, front temperatures are very high, some reaching over 200 ºC,[62] too high to be used in many biological systems and many other applications. (Though Totaro et al. have found ways to decrease FT by using thiol-ene comonomer systems.[71]) Due to these high temperatures (as well as viscosity limitations that will be discussed further on), solvent selection for solution FP is very limited. High boiling point solvents such as dimethyl sulfoxide (DMSO)[103, 104] and dimethyl formamide (DMF)[104] are some of the organic solvents that have been successfully used in FP, but even these have limitations due to viscosity. Diluting a monomer for FP can be advantageous because it can decrease front temperature,[105] but it can also decrease solution viscosity and front velocity.[104] The front velocity is decreased by the dilution of the reactants and by the absorption of heat. If the monomer solution viscosity is too low, an inert viscosity modifier must be added to inhibit convection, which can quench the front.[70]

Two types of convection are commonly observed in FP: buoyancy-driven and surface-tension-induced. Buoyancy-driven convection typically occurs when a front is not

18

propagating directly downward, hence why all fronts in this work are descending. Surface-tension-induced convection (also known as Marangoni convection) occurs due to localized changes in surface tension. Of the two types of convection, Marangoni convection limits the utility of FP more drastically. In thin layers, buoyancy-driven convection is quite minimal, but heat loss due to the Marangoni effect can be devastating to the front.[106] As mentioned above, inert fillers can be used to overcome convection and other limitations of FP.

Fillers can cause some systems to meet requirements for frontal polymerization when they normally would not. Fumed silica, for example, is an excellent viscosity modifier for frontal polymerization; while kaolin or talc can act as both viscosity modifier and heat sink. The disadvantage to adding viscosity modifier is that, oftentimes, this addition slows the front even further.[100] A low vapor pressure, high viscosity, and high temperature stable solvent is therefore ideal for FP, and ILs easily meet these criteria.[107, 108] ILs are oftentimes, and rather unfortunately, expensive and difficult to synthesize. An alternative to traditional ILs is a similar but fundamentally different system known as deep eutectic solvents.

First reported by Abbott less than two decades ago, DESs are greener, cheaper, and, in many cases, easier to synthesize than traditional ILs. Several excellent reviews have been published on DESs in recent years.[9-11] The fundamental difference between DESs and ILs lies in the type of interactions that occur within the liquid. DESs contain hydrogen bond interactions while ILs contain short lived ion pair interactions. By employing these hydrogen bond interactions—instead of ionic interactions—DES components are usually easier to obtain commercially than IL components.

DESs consist of a hydrogen bond donor (HBD) and hydrogen bond acceptor (HBA). The HBD can be a variety of molecules, including chlorometalate salts,[109] amides,[8] and carboxylic acids.[18, 19] These HBDs can also be polymerizable molecules such as acrylic acid[45, 58, 59] and acrylamide.[58] The HBA is usually a halogen-containing, ammonium salt. The most common HBA is choline chloride (ChCl). Because of its provitamin status in several European countries as well as its being a common animal food additive, ChCl is produced on a very large industrial scale making it an inexpensive and easily accessible DES component.[10]

Frontal polymerization of DESs, i.e., one of the DES components is the monomer, has been reported previously,[45, 58, 59] but little research has been done into why or how the presence of the DES affects the behavior of the front. Herein we do just that by examining the FP behavior of DESs as well as the FP behavior of systems that contain analogs of ChCl to mimic the non-chemical effects that the ChCl may impart on the polymerization. Specifically, we added talc to mimic the effect of the heat absorption by ChCl, or a solvent (DMSO) to mimic the dilution and heat absorption by ChCl and added stearic acid or lauric acid to mimic the effect of heat absorption and hydrogen bonding. The effect of initiator concentration on the front velocity and front temperature was also studied.

2.2 MATERIALS AND METHODS

2.2.1 Materials

Acrylic acid (AA), methacrylic acid (MAA), Luperox® 231 (L231), stearic acid (SA), and lauric acid (LA) were all obtained from Sigma Aldrich. Dimethylsulfoxide (DMSO) was obtained from Fisher Scientific, and Acros Organics supplied ChCl. Talc

20

and fumed silica were supplied by U. S. Composites. All reagents and components were used as received. Chemical structures for all DES components and nonreactive analogs can be seen in Figure 2.1.
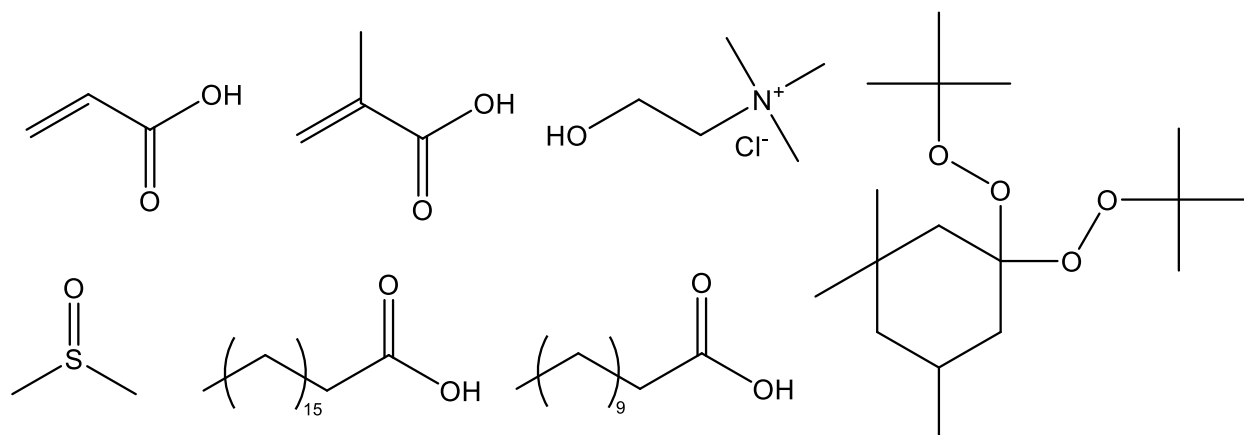
Figure 2.1. Chemical structures (clockwise from top left) acrylic acid, methacrylic acid, Luperox® 231, lauric acid, stearic acid, and DMSO.

2.2.2 DES Synthesis

DESs were formulated in molar ratios of 1.6:1 and 2:1 (HBD:HBA) for acrylic acid and methacrylic acid, respectively. As reported by Mota-Morales,[58] acrylic acid-choline chloride DESs have the highest viscosity at the 1.6:1 ratio making this ratio most suitable for frontal polymerization. DES synthesis was done by mixing the HBD and HBA, (the HBD is always added to the container first to minimize water absorption by the HBA) and then placing the mixture in a 70 °C oven until no solid was visible. Once the DES was fully synthesized, it was removed from the oven and prepared for frontal polymerization

2.2.3 Frontal Polymerization Sample Preparation

Once the DESs were fully formed, they could be used for FP. The thermal radical initiator chosen was Luperox® 231 (1,1-bis(*tert*-butylperoxy)-3,3,5-trimethylcyclohexane) and was always added to the DES first in the sample preparation.

Due to the small amounts of initiator added, a syringe and 23G needle were used to add the initiator, and it was mixed in using magnetic stirring. The stirring of the initiator and silica into the DES, in some cases, acted as a nucleation source and caused small crystals to form in the DES (Figure 2.2A)—if a stir bar is left in a DES for a long enough period, crystals will grow without stirring (Figure 2.2B).

Figure 2.2. Crystallization of a DES by A) stirring and B) after sitting with a stir bar present.

After removing the DES from the oven, it was allowed to cool for ~15 minutes to ensure that homopolymerization would not occur upon addition of initiator. Initiator was added as mol% initiator relative to double bonds present in the monomer. Fumed silica was added at 1% w/w to ensure high enough viscosity was achieved to allow the front to propagate. (It is important to note that the overall macroscopic viscosity increase caused by fumed silica has been reported to have no impact on the final results of the polymerization in relation to molecular weight or conversion.)[110, 111] Once all components were stirred in, the contents of each vial was placed into a 15 cm x 1.6 cm unsealed, borosilicate glass test tube and polymerized as a descending front.

In all samples, polymerization was initiated with a butane-fueled soldering torch without a soldering tip. The torch was applied to the exterior of the tube until the polymer covered the entire top of the monomer mixture. For the front to be considered

successful, it must have propagated without the addition of external heat for a minimum of 60 mm; though, this constraint was not necessary. The fronts examined in this work clearly did or did not exhibit frontal behavior.

2.2.4 Measurement of Frontal Properties

Front temperatures were measured by placing a wire K type thermocouple into the sample with the exposed portion of the wire approximately 2 cm from the bottom of the test tube and not touching the glass of the tube. The thermocouple was connected to a computer via a Vernier Go!Link detector, and data was recorded by Logger Pro® software. An example of a temperature profile obtained by this system can be seen in Figure 2.3 and all FT profiles can be found in Appendix B. The front temperature was taken as the maximum temperature recorded during the polymerization.
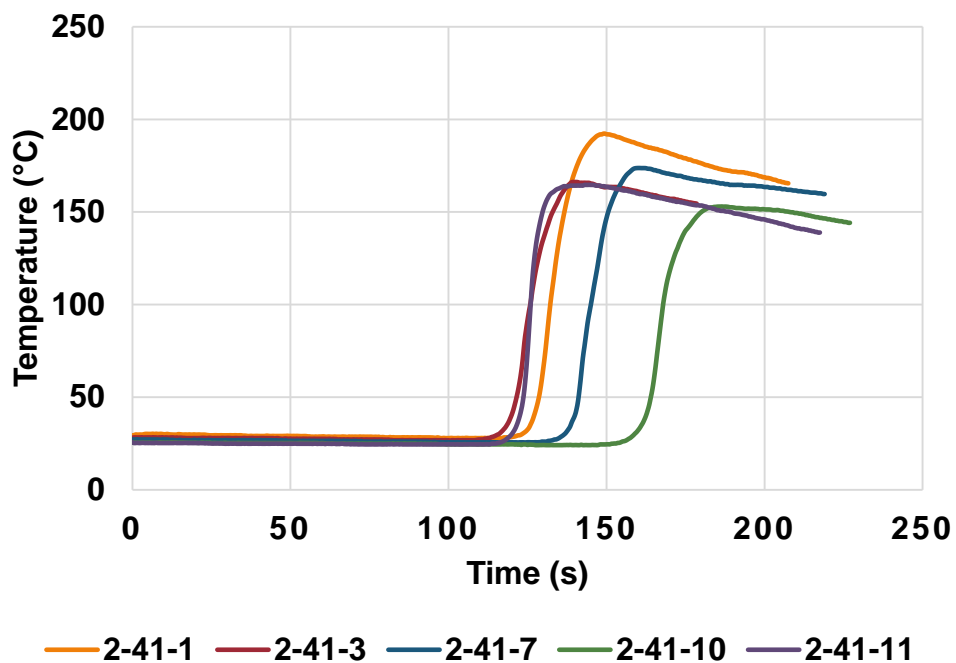
Figure 2.3. Recorded front temperature profiles for AA-ChCl samples.

To determine FV, video of each polymerization reaction was recorded. (It is important to note that samples were used for either FT or FV determination, not both, as

the presence of the thermocouple can, in some cases, alter the front velocity.) The tube

was placed on a stand next to a ruler while the FP was recorded as video (see Figure

2.4 for a photograph of the setup). Analysis of the video yielded time data recorded in

correlation to the front's position as measured by the ruler. Time data points were

recorded every 5 mm during the polymerization. These time and position data points

produce a position vs. time plot, an example of which can be seen in Figure 2.5, and all

of which can be found in Appendix C. A linear regression was performed using

Microsoft Excel, and the slope of the resulting line was taken as the front velocity.

Figure 2.4. FP setup during initiation (left) and polymerization (right).
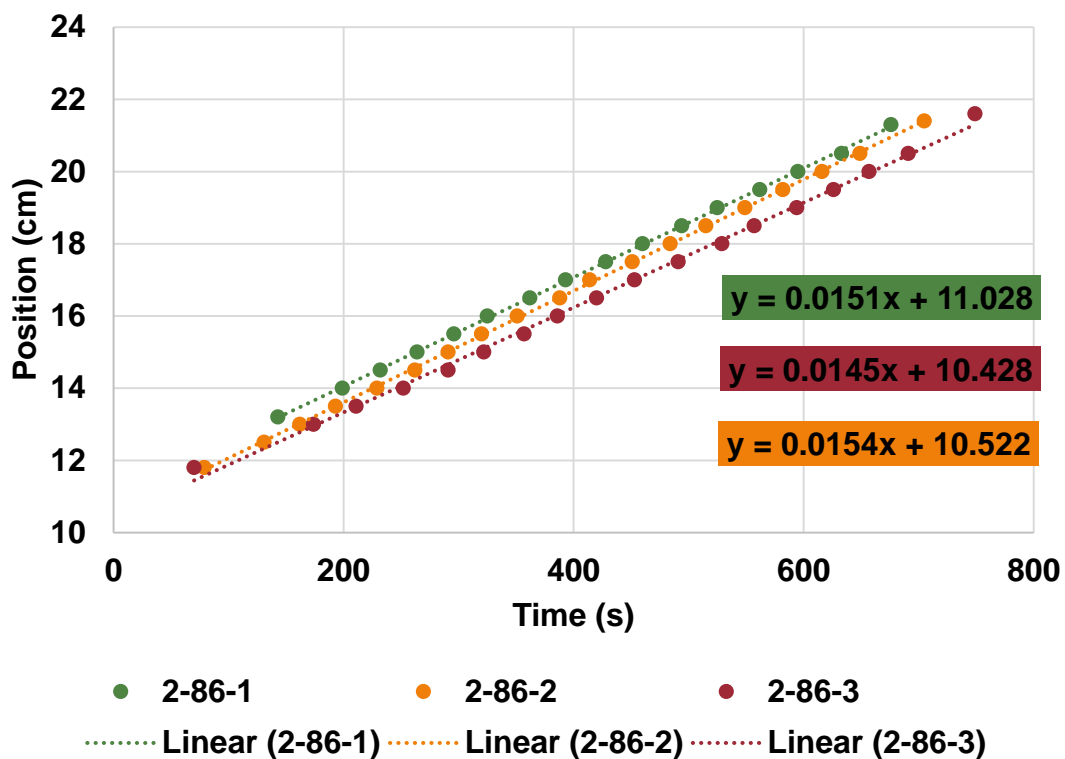
Figure 2.5. Position vs. time graph produced from video analysis of front propagation.

2.3 VARIED INITIATOR CONCENTRATION EXPERIMENTS

Initiator concentrations of 0.2%, 0.3%, 0.8%, 1.7%, 2.5%, and 3.3% were

measured for frontal properties (FV and FT). Figures 2.6 and 2.7 show the frontal

properties of AA-ChCl and MAA-ChCl, respectively, as a function of initiator

concentration. The corresponding temperature profiles (FT) position versus time graphs

(FV) that were obtained experimentally can be found in Appendices B and C,

respectively.

2.3.1 Acrylic Acid DESs Polymerized Using Various Initiator Concentrations

The velocity data in Figure 2.6 for AA indicated that ~0.7% initiator is the

solubility limit for the initiator. The opacity caused by crystal formation made the exact

limit difficult to identify, but the decrease in the data between 0.7% and 1.3% indicated

that heterogeneity in initiator dispersion is likely. The second increase in velocity beyond the solubility limit was most likely due to a decrease in distance between heterogeneous areas of high initiator concentration, thus creating a more "pseudo-homogeneous" system. The FT data shows similar trends.
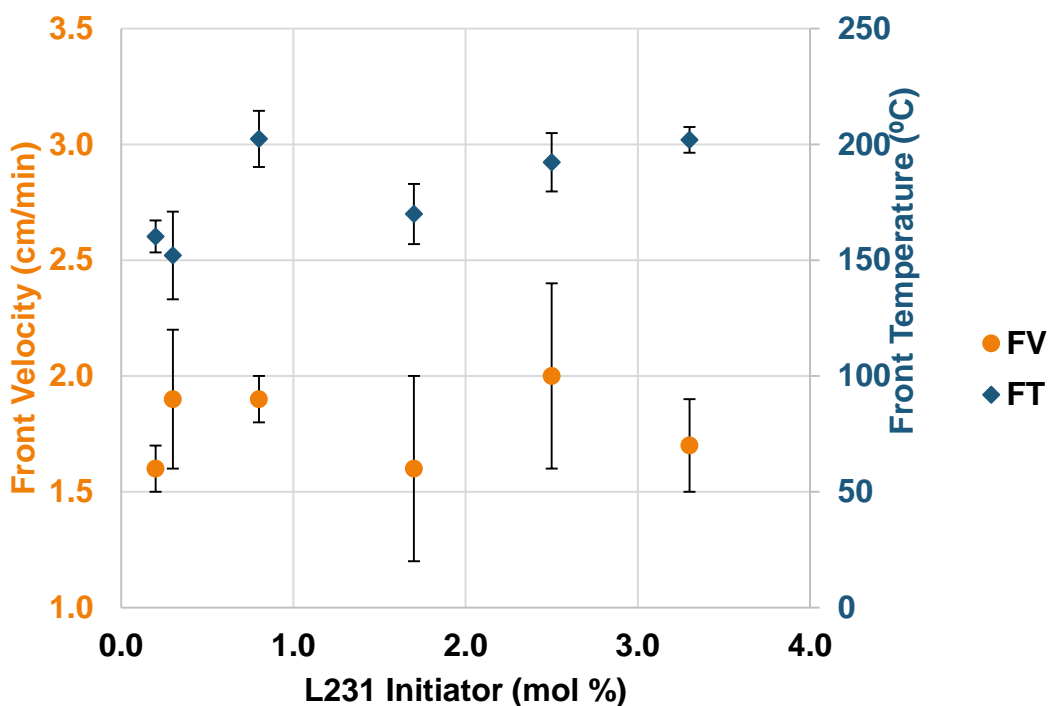
Figure 2.6. AA-ChCl front properties.

2.3.2 Methacrylic Acid DESs Polymerized Using Various Initiator Concentrations

The frontal behavior and trends for MAA-ChCl varied initiator systems were similar to the AA-ChCl samples but with lower overall values. The decrease in values between AA and MAA was expected, as MAA is inherently less reactive. Due to the similarity in the frontal behavior of these systems, further study into monomer containing DESs and their impact on polymerization was performed.
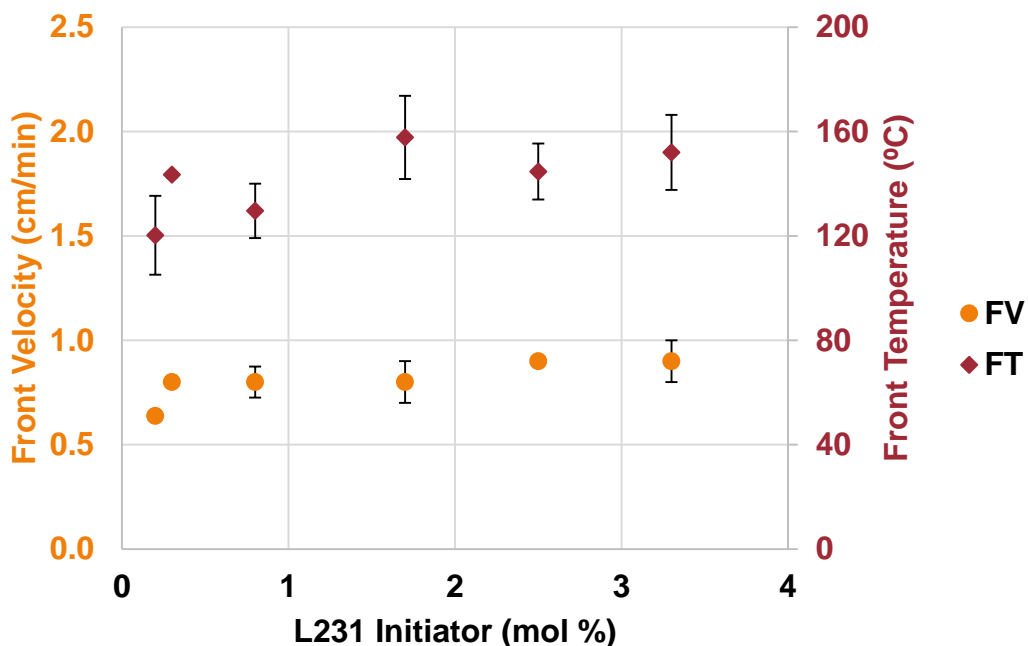
Figure 2.7. MAA-ChCl front properties.

2.4 CHOLINE CHLORIDE REPLACEMENT

In order to ascertain what kind of effect the presence of choline chloride (and therefore the DES) in the front has on the properties of the FP, analogs were used to replace the ChCl and mimic several common nonchemical effects including heat loss, dilution, and crystalline melting. The frontal properties of these analog systems can be seen in Figures 2.8 and 2.9.
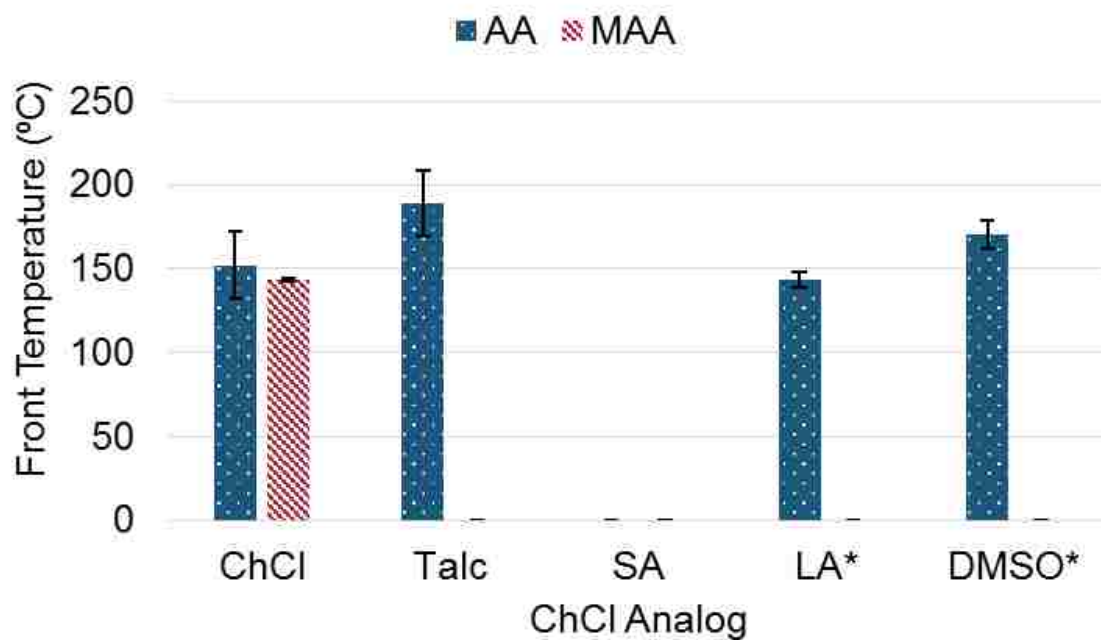
Figure 2.8. Front temperatures of monomers with ChCl analogs.
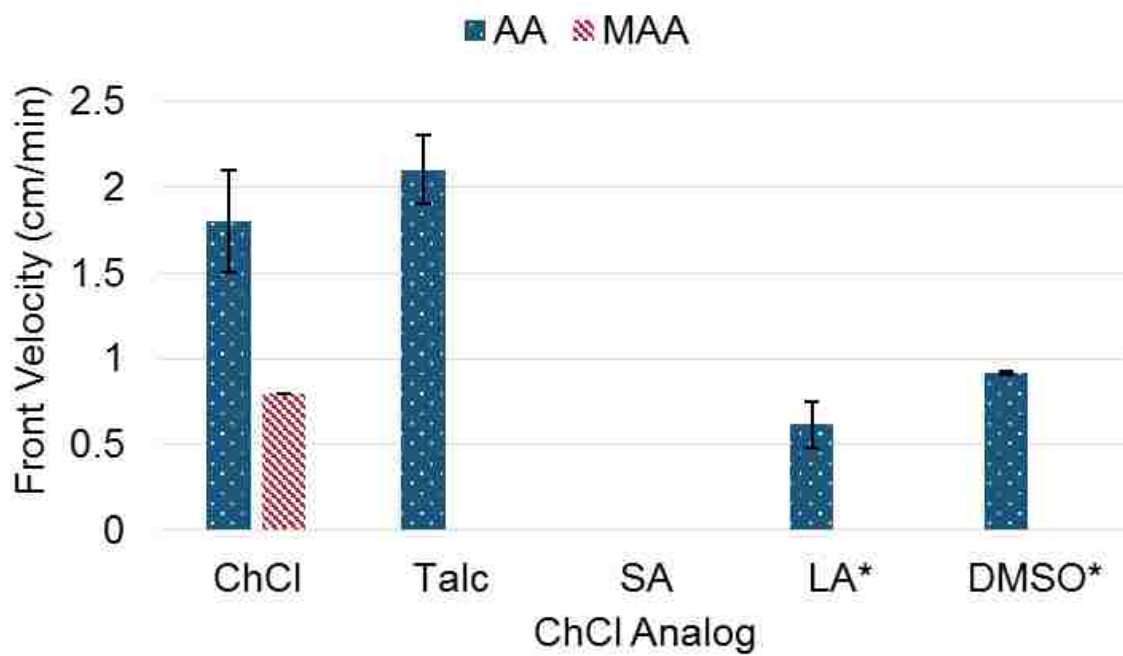
Figure 2.9. Front velocities of monomers with ChCl analogs.

2.4.1 Talc Substitution

For the talc experiments, one large batch of the talc mixture was made because the high viscosity of the mixture caused for a large amount of the mixture to stick to the sides of the container in which the mixture was prepared and therefore not be usable for the actual experimentation. The large batch was a much more effective way of producing the mixture with minimal waste. The talc samples, which were to simulate the heat absorption effect by the ChCl, behaved more similarly to the pure AA polymerization than to the AA-DES polymerization with violent bubbling and popping throughout the propagation of the front. However, the front velocity was slightly higher with talc as with ChCl. This is consistent with talc acting only as a heat sink but not as diluent. However, the methacrylic acid samples would not polymerize frontally with talc.

2.4.2 Inert Phase Change Material (iPCM) Substitution

Due to the crystallization of DES seen in mixing, it was realized that a comparison needed to be made to an inert filler that would also melt during the propagation of the front. Stearic acid (SA) was selected as the inert phase change material (iPCM), based on the work of Viner, et al.[112] The SA was added to the monomer and placed in a 90 ºC oven until all solid was no longer visible. Because the SA mixtures solidified upon cooling, as soon as the SA was completely melted, the vials were moved to the 60 ºC oven to keep them warm while minimizing the risk of homopolymerization. The lower temperature allowed the cooling time to be shortened to ~5 minutes before adding the silica and initiator. Once all components were mixed, the monomer-stearic acid mixture including silica and initiator was placed into a test tube where it was allowed to cool completely and solidify completely before being

polymerized. The high melting point of the SA made the samples solidify, and this prevented the frontal polymerization because the heat required to melt the stearic acid suppresses front propagation. It is important to note that even when samples were initiated before complete solidification, solidification still occurred during the initiation process and fronts would not propagate.

2.4.3 Solvent Substitution

To verify that dilution was not the sole mechanism by which the front temperature was lowered, ChCl was replaced with dimethylsulfoxide (DMSO) and lauric acid (LA). Lauric acid was originally chosen as an iPCM for its relatively low melting point, but as it was found to be soluble in both acid monomers, the lauric acid acted as a hydrogen bond capable diluent instead. The lauric acid samples were treated the same as the ChCl: mixed into the monomer, placed in the oven, removed from the oven when no solid was visible, allowed to cool, and stirred with silica and initiator before being placed into the tubes. DMSO and monomer were mixed for ~10 minutes then L231 was added. In the cases of both LA and DMSO, the fumed silica concentration had to be increased approximately five-fold to ensure high enough viscosity to minimize convective instabilities; these samples with increased silica are denoted with * in Figure 2.8 and Figure 2.9.

DMSO was an inert diluent while LA will dilute the monomers and hydrogen bond with them in a similar fashion to the ChCl. Again, the MAA samples did not polymerize. The AA samples would produce a front that was much slower than the AA-DES, and the dilute analog fronts did also require a much higher silica content. DMSO lowered the front velocity of acrylic acid below that with talc or ChCl and prevents methacrylic acid from

31

supporting frontal polymerization. DMSO had a greater effect than talc because the DMSO not only absorbs heat, it diluted the reactants, reduced the rate of reaction beyond that caused by the reduction in front temperature. Lauric acid reduced the front velocity with acrylic acid compared to ChCl, talc and DMSO and suppressed front propagation with methacrylic acid. The decrease in front velocity was greater for the LA than the DMSO relative to the AA-DES because of the hydrogen bonding capability of LA. The formation of the AA-LA solution was clearly endothermic, as the samples become cold to the touch. The dissolving of the solid LA and breaking of the hydrogen bonds already present in the pure LA required more energy than is released by the formation of the hydrogen bonds between the monomer and LA. A portion of the heat of the polymerization was absorbed by the solution to break the large number of already present hydrogen bonds. It is interesting to note, however, that while the DES formation was also endothermic, the same type of large decrease in the front velocity is not seen in the AA-DES polymerization. This fact strongly indicated that the reactivity of the acrylic acid and methacrylic acid are enhanced by the ChCl.

2.5 CONCLUSIONS

Acrylic acid and methacrylic acid will easily form polymerizable DESs that sustain a front with a range of initiator concentrations. This ability to perform a free-radical polymerization in a DES allows for a wide range of useful monomers and systems to be applied to DESs, and the ability to use FP in conjunction with a DES increases their usefulness even further. By replacing ChCl with nonreactive analogs that mimic various, common phenomena that can impact the behavior of FP in a DES made with a polymerizable HBD, it was clear that the DES has an overall positive impact on the FP

32

of the system. AA-DESs polymerized in a more controlled fashion than acrylic acid alone, and MAA-DESs polymerized as fronts while the samples that contained MAA and the analogs would not sustain a front. While the exact mechanism behind this impact is yet to be determined, the current hypothesis is that the DES altered the reactivity of the monomers within the DES. Future work will be performed to determine in more detail how this change in polymerization behavior happens.

III. KINETIC STUDIES OF PHOTOPOLYMERIZATION OF MONOMER-CONTAINING DEEP EUTECTIC SOLVENTS

3.1 INTRODUCTION

3.1.1 Free-radical Photopolymerization Kinetics

In order to understand the factors that could alter the rate of a photopolymerization, the kinetics must be examined. The equations below show the rates of the respective steps of the polymerization and show the factors that can influence the actual rate of a polymerization. Generally speaking, FRP rates are based on the disappearance of the monomer (M) (equation 3.1)

$$(3.1) \qquad -\frac{d[M]}{dt} = R_i + R_p$$

where R_i is the rate of initiation and R_p is the rate of propagation. Because R_p is significantly higher, equation 3.1 is approximated and seen in the approximated form in equation 3.2.

$$(3.2) \qquad -\frac{d[M]}{dt} = R_p$$

R_p is dependent on three main factors, the concentration of propagating radicals $[M_r]$, the concentration of monomer $[M]$, and the propagation rate constant (k_p). Equation 3.3 shows the relationship of these to the polymerization rate.

$$(3.3) \qquad R_p = k_p[M_r][M]$$

Because the radical concentration remains very low, the steady-state approximation is used which assumes that upon initiation of the polymerization system, the radical concentration instantaneously increases to a steady, constant value. This assumption leads to the equivalence of the rates of initiation R_i and termination R_t. Equation 3.4 shows this equivalence and defines R_t, where k_t is the termination rate constant, and

rearrangement to equation 3.5 gives the ability to eliminate [M_r] in calculating R_p

(equation 3.6).

(3.4) $$R_i = R_t = 2k_t[M_r]^2$$

(3.5) $$M_r = \left(\frac{R_i}{2k_t}\right)^{0.5}$$

(3.6) $$R_p = k_p \left(\frac{R_i}{2k_t}\right)^{0.5} [M]$$

At this point it is necessary to address R_i and the factors within a photopolymerization specifically that affect rate; the first being not initiator concentration as seen in other types of FRP, but rather light intensity (I). (Because of this, it often much easier to alter light intensity as opposed to initiator concentration within photopolymerization systems as will be seen in this work.) Equation 3.7 shows the simplest form of the equation for R_i as a function of light intensity where I_{abs} is the intensity of light absorbed by the initiator and ϕ_i is the quantum yield or the number of propagating chains that are actually produced per photon of light absorbed.

(3.7) $$R_i = 2I_{abs}\phi_i$$

Because the amount of light absorbed is difficult to determine I_{abs} must be presented in a way that can be measured which is the intensity of the incident light I_o. This is accomplished by incorporating the Beer-Lambert law (equation 3.8)

(3.8) $$I'_{abs} = I_0 - I_0 e^{-2.3\varepsilon D c}$$

where ε is the molar extinction coefficient, D is the penetration depth within sample, and c is the concentration of the photoinitiator. It is important to note that in samples with large D values, the differences in light absorbance at different D must be taken into account because I'_{abs} and I_{abs} are not equivalent in that case. For the purposes of this

manuscript, D is sufficiently small that the two are taken to be equivalent. Combining

equations 3.7 and 3.8 gives

(3.9)
$$R_i = 2\phi_i I_0 (1 - e^{-2.3\varepsilon Dc})$$

which when incorporated into equation 3.6 gives

(3.10)
$$R_p = k_p \left(\frac{2\phi_i I_0 (1 - e^{-2.3\varepsilon Dc})}{2k_t} \right)^{0.5} [M]$$

which shows that a photopolymerization is affected by three main factors when the

concentrations of monomer and initiator are kept constant: k_p, k_t, and I_0. In the next

section, some examples of enhancement to k_p in ionic liquids will be discussed.

Viscosity and the related Trommsdorff-Norrish effect are often the most effective way to

decrease k_t in a traditional FRP thus increasing polymerization rate.

3.1.2 Free-radical Polymerization Kinetics in Ionic Liquids

Ionic liquids, like DESs, can be used as solvents for polymerization reactions and

have been for a much longer time period. Kubisa's review on the subject is an excellent

overview,[6] but for the purposes of this chapter, the focus will be on kinetics of

polymerization in ionic liquids.

Free-radical polymerization in ILs tends to behave unlike solution polymerizations

performed in organic solvents or in the bulk. In 2006, Strehmel and coworkers reported

thermally-initiated polymerizations of n-butyl methacrylate using AIBN as the initiator in

both ILS and toluene.[113] A plethora of ILs were used including imidazolium, pyridinium,

and alkylammonium cations each coupled with multiple anions. In some cases, the

polymer was produced in higher yield in the IL than in the bulk. One interesting point the

authors make is that in the cursory kinetic studies they performed, no Trommsdorff–

Norrish effect is observed as would be observed in typical bulk polymerization. Such an

effect gives a distinctive S shape (Figure 3.1) to the resulting conversion versus time plot for the polymerization. It is also stated that increased conversions and molecular weights are obtained for the polymerizations performed in the ILs. These increases are attributed to a combination of the decrease of the termination rate, and an increase of the propagation rate. The authors claim this combination because the increases in molecular weight do not follow increases in viscosity of the ILs in which they are polymerized indicating more than one impact on the reaction kinetics. In the specific case of the n-butyl methacrylate monomer, imidazolium ILs were found to have the greatest positive impact on the polymerization and final polymer properties.
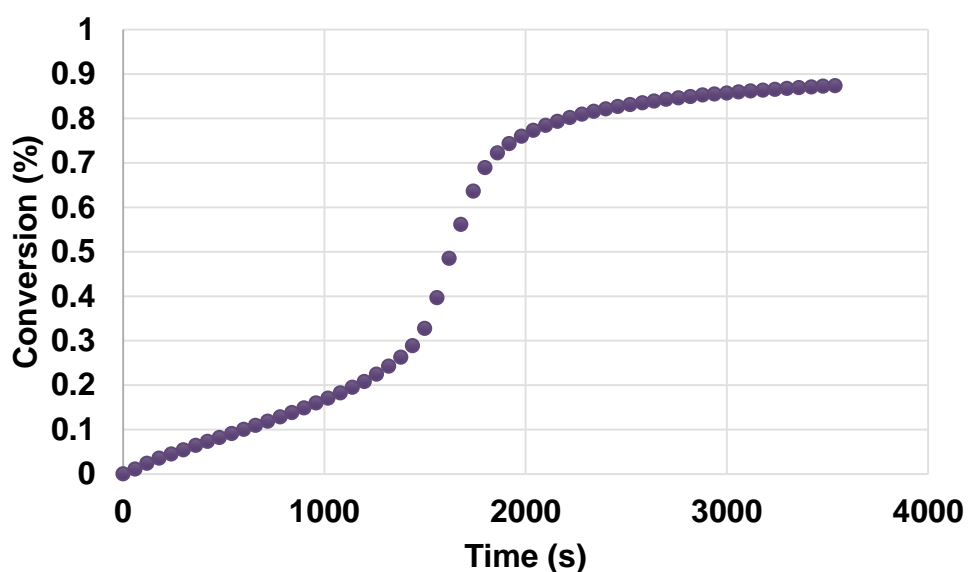

Figure 3.1. The distinct shape of a conversion versus time graph when the Trommsdorff–Norrish effect is present.

Another highly interesting example of kinetic work using pulsed-laser initiated polymerization (PLP), performed in ILs comes from a group of German scientists in 2007.[114] The authors claim that the presence of the highly polar imidazolium salt causes a decrease in the activation energy of the two monomers tested (glycidal methacrylate and methyl methacrylate) compared to the bulk polymerization. They also state that this

decrease in activation energy leads to increases of the k_p by factors of two and four, respectively, when compared to a bulk polymerization.

Another instance where PLP was used and propagation rate constants were reported to be enhanced was that of the polymerization of hydroxypropylmethacrylate in imidazolium and pyridinium ILs.[115] In solution polymerization using benzyl alcohol or toluene as the solvent, the k_p for the polymerization was the same as the k_p for the bulk polymerization, while most of the ILs used resulted in an increased k_p. In this case as well, the polarity of the solvent that increases monomer solvent interaction is attributed to the increased k_p.

3.2 MATERIALS AND METHODS

3.2.1 Materials

AA and methyl methacrylate (MMA) were supplied by Sigma Aldrich. Diphenyl(2,4,6-trimethylbenzoyl) phosphine oxide (TPO), propionic acid (PA), choline bromide (ChBr), choline bitartrate (ChBT), tetramethylammonium chloride (TMACl), and MAA were obtained from TCI America. Acros Organics supplied ChCl, isobutyric acid (IBA), methyl acrylate (MeA). All reagents and components were used as received.

3.2.2 Real-Time Infrared Spectroscopy

All spectra were obtained on a Bruker Tensor 27 Fourier transform-infrared spectrometer (FTIR) equipped with a Peak Miracle single-bounce diamond attenuated total reflectance (ATR) cell using real-time infrared spectroscopy (RTIR). The spectral range for all spectra was 4000 – 650 cm^{-1}, and all spectra were recorded at a resolution of 4 cm^{-1}. All experimental and background spectra consisted of 16 scans. The FTIR was set to take a spectrum after a specified interval of time until a total number of

spectra were taken. The total number of spectra (and therefore total time) was determined by how long it takes the reaction to reach a conversion plateau as can be seen in Figure 3.2. Table 3.1 shows all sample sets that will be discussed in the coming sections and their respective interval times and total times. (For a complete list of all sample sets tested broken down by light intensity with intervals and times, see Appendix D.) All spectra were subjected to a 9 point smooth and baseline correction using the concave rubberband method with 64 baseline points and 16 iterations using the Bruker OPUS software.

Table 3.1. RTIR sample sets with interval and total times.

Sample set	Interval time (s)	Number of spectra	Total time (min)
AA-TPO	300	120	600
AA-ChCl-TPO	45	120	90
MAA-TPO	300	120	600
MAA-ChCl-TPO	45	120	90
MeA-TPO	30	60	30
MeA-TPO-PA-ChCl	30	60	30
MMA-TPO	30	120	60
MMA-TPO-IBA-ChCl	30	60	30

3.2.3 Kinetic Analysis of RTIR Spectra

Kinetic analysis of all spectral data was performed using a spectral difference approach (integration method K of the OPUS software) using the acrylate peaks at 1625 cm^{-1} (C=C stretching vibration) and 810 cm^{-1} (C=C-H out of plane bending). The bounds for the integration of each sample were determined by visual analysis. The integration method is applied to the spectra using a premade macro kindly provided by Bruker to ensure that all spectra for a sample are analyzed using the same integration parameters and compiled into a single document. Which of the two aforementioned peaks is best suited to each sample set is specific to the sample set and monomer system in question and is indicated each respective section. All samples within a given monomer system

are analyzed using the same peak. The spectral differences were used to calculate

conversion data for the polymerization using equation 3.11. M_0 is the initial monomer

concentration at time = 0 (before irradiation), and M_t is the monomer concentration at

time = t as determined by the spectral difference analysis.

(3.11)
$$\% \ Conversion = \frac{M_0 - M_t}{M_0} * 100$$

The slope of the initial portion of the polymerization (~0 - 30% conversion) allows for
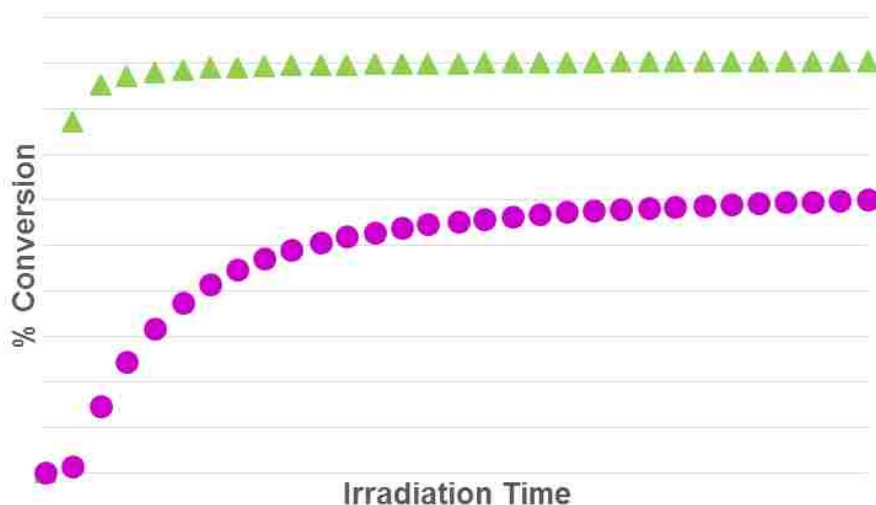
rate determination.

Figure 3.2. Conversion versus time plot for acrylic acid DES photopolymerization.

In many cases, the polymerization occurs too quickly to obtain enough data

points to calculate an initial rate. Any sample with an increase in conversion greater

than 15% in one spectral interval is considered too fast. An example of this can be seen

in the spectra seen in Figure 3.3 (keeping in mind that the spectral interval for this

samples was 30 s) and the green data set of Figure 3.2, while the purple data set in

Figure 3.2 and the spectra seen in Figure 3.4 show data from which a rate can be

calculated. These high rates were the reason that the initiator concentration was

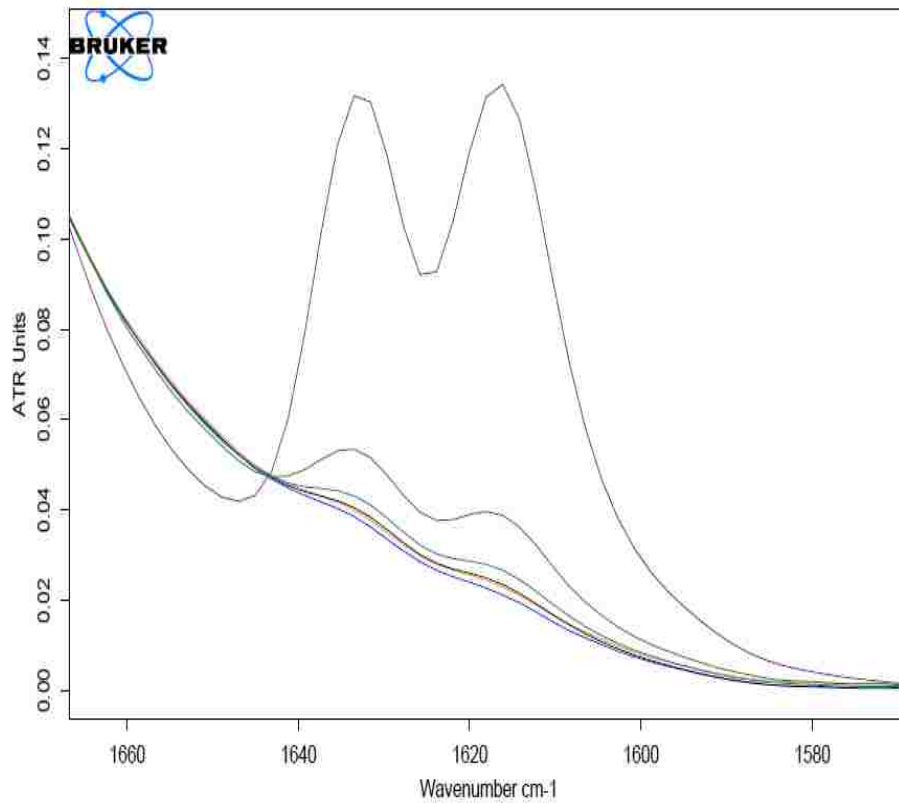decreased to 0.1%, and the neutral density filter was used.

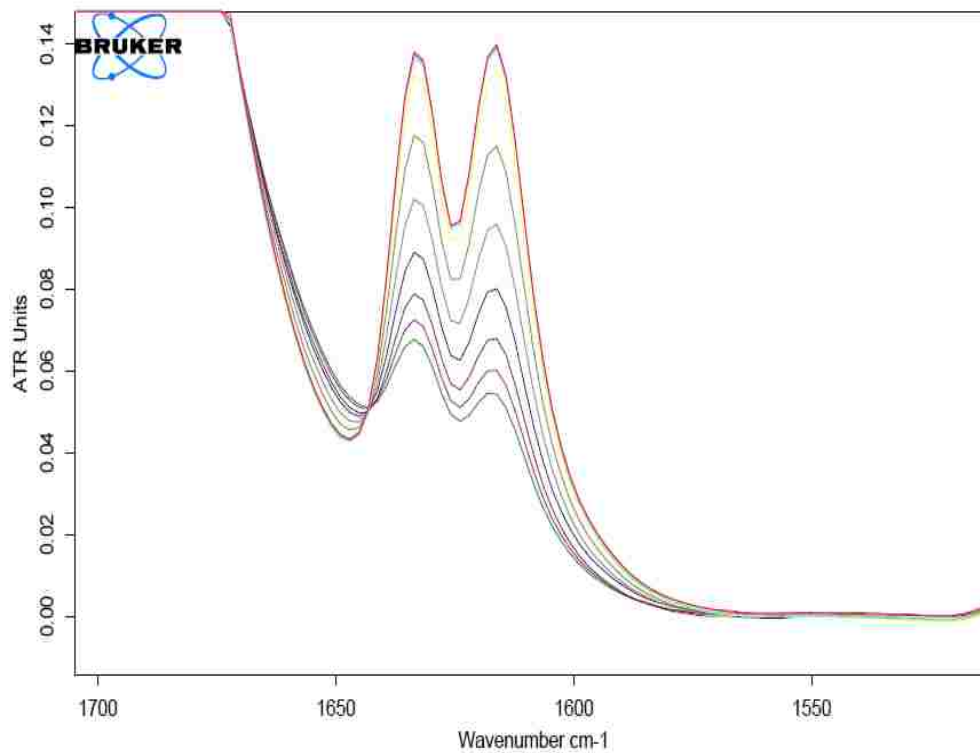Figure 3.3. The spectra of a sample too fast for rate determination.

Figure 3.4. Spectra of a sample for which a rate can be calculated.

3.2.4 Photopolymerization of DESs

In order to ensure measurable polymerization on the ATR cell, a room-temperature photopolymerization was used. Initially, camphorquinone (CQ, Figure 1.1) was chosen as the radical photoinitiator but was found to be too inefficient to initiate some of the polymerizations within a reasonable time frame for RTIR measurement. Typically, CQ is used in conjunction with an amine activator to increase the initiation efficiency. This was attempted using trimethylamine, but acid-base reactions between the amine and the HBD of the DES eliminated any activation of the CQ. Ultimately, the photopolymerization was performed using diphenyl(2,4,6-trimethylbenzoyl) phosphine oxide (TPO, Figure 3.5) as the photoinitiator. In all samples, the concentration of TPO relative to monomer double bonds is 0.1 mol% for the HDB monomer systems and 1% for the methyl ester monomer systems. Initially, a concentration of 1% was used for the HBD monomers as well, but all samples polymerized too quickly—even at the low limit of light intensity produced by the light source—to obtain a quantifiable rate.
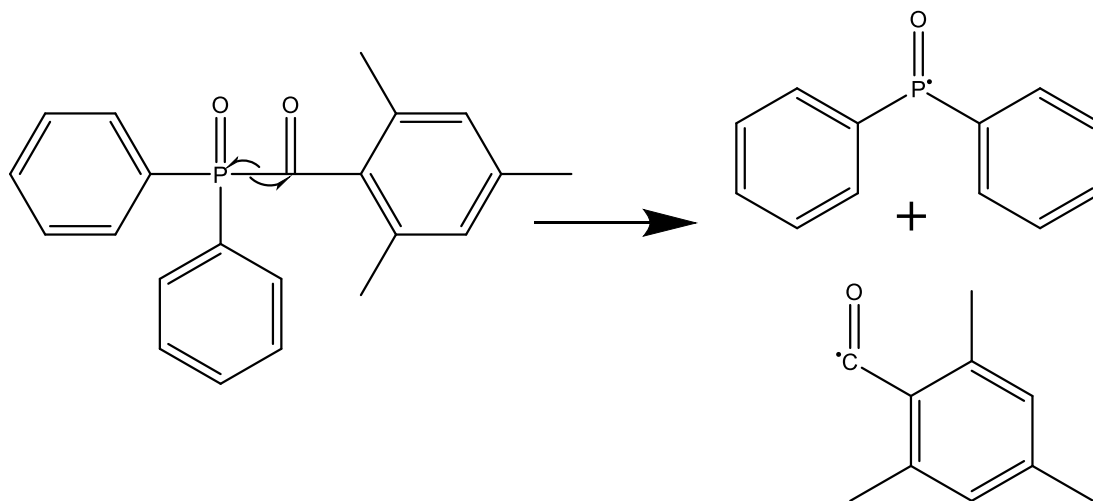

Figure 3.5.The α-cleavage initiation mechanism of TPO.

42

Figures 3.6 and 3.7 shows the coupling of the Thor Labs Broadband Halogen

Fiber Optic Illuminator (also called the light source) and the FTIR instrument. The light

source emits across the visible light spectrum using a 150 W high-output halogen lamp

coupled with a variable intensity controller and fiber bundle that allows for the direction

of the light onto the sample and ATR crystal. The fiber is mounted directly above the

ATR crystal at a height of 1.2 cm giving an illumination area of 1.9 cm^2. By using an

optical power meter also supplied by Thor Labs, the intensity of light emitted through the

fiber bundle can be measured at a specified wavelength—light intensities for this work

were measured at either 365 nm (methyl ester monomers) or 400 nm (HBD monomers).
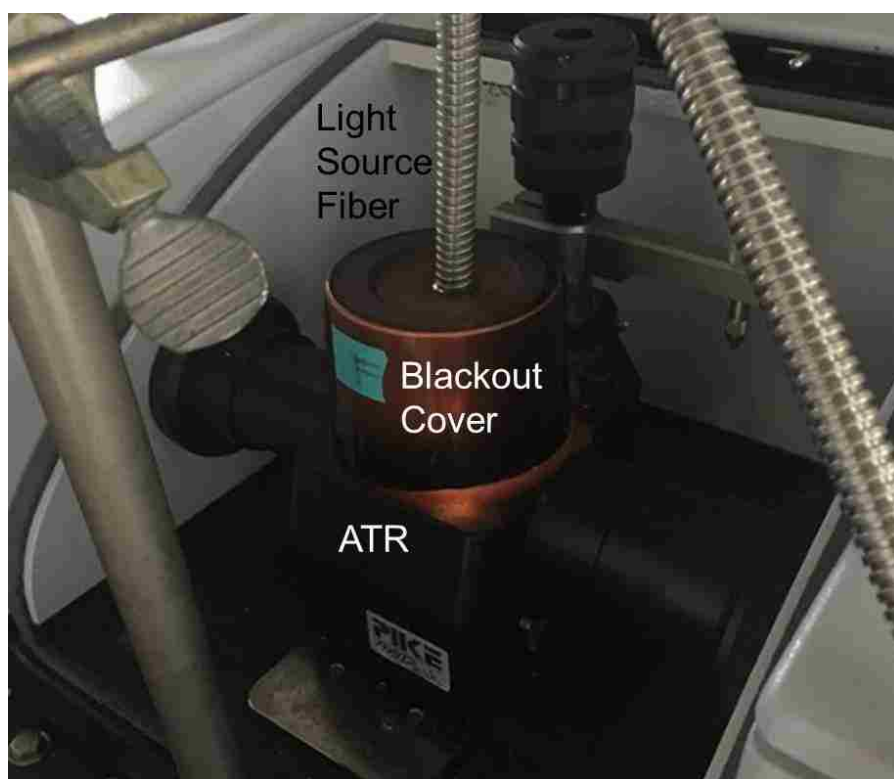

Figure 3.6. The light source fiber mounted above the ATR crystal while irradiating a sample.
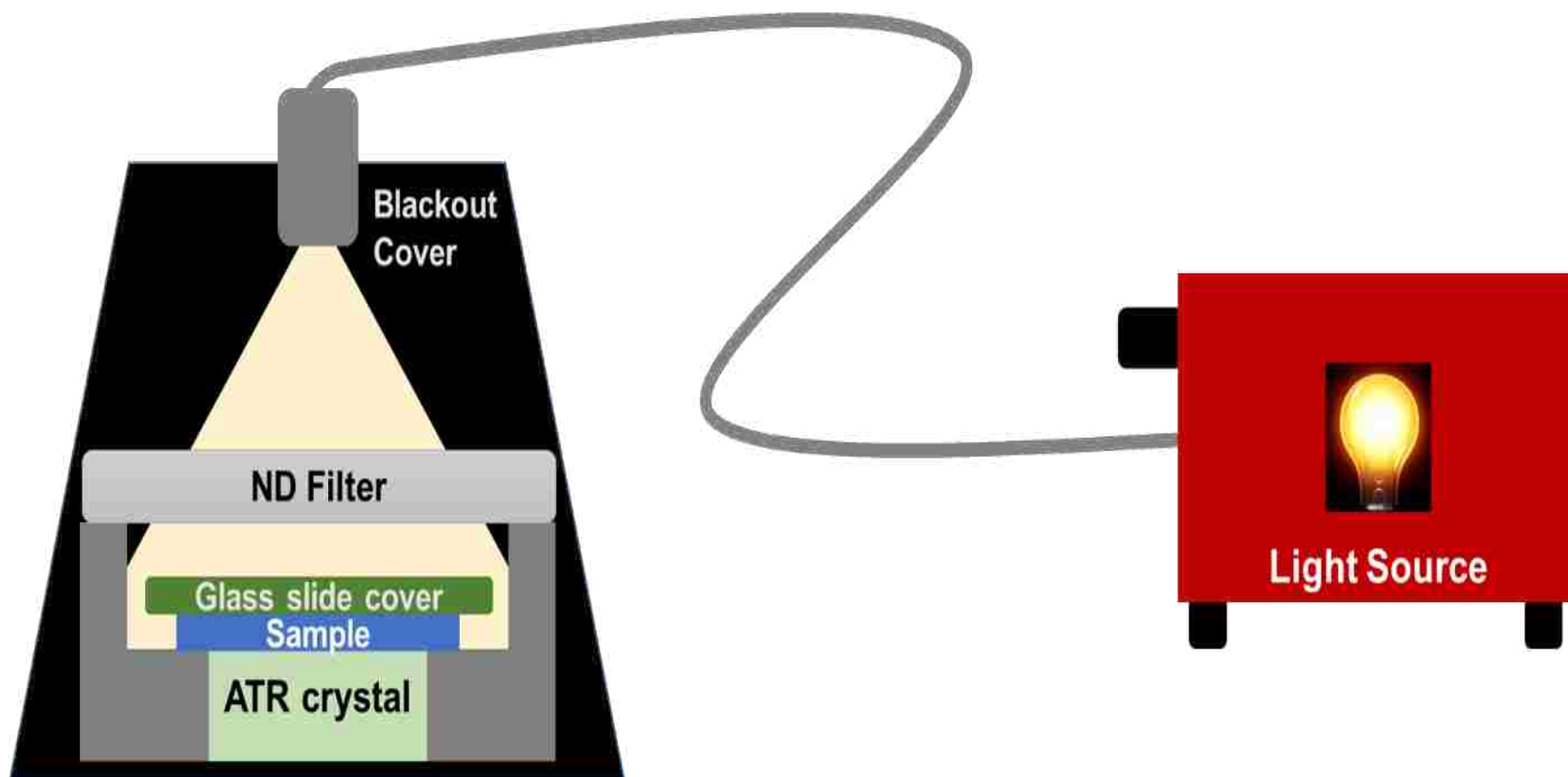
Figure 3.7. The photopolymerization-FTIR setup cross-section.

The sample was applied to the ATR crystal while the room was darkened using a plastic sample applicator and covered with a glass slide cover to minimize oxygen inhibition and, in the case of the pure monomers, sample evaporation. As can be seen in Figures 3.6 and 3.7, a black polyethylene cover was placed on the fiber and used to cover the sample cell and ensure that no outside light would interfere with the photopolymerization. The lighting of the room was not seen to have a significant impact on the photopolymerization as long as the blackout cover was properly in place.

In order to further decrease the intensity of the light beyond the low limit of the light source, a neutral density filter (NDF) was employed for the AA-ChCl and MAA-ChCl DESs. The NDF obtained from Thor Labs is a variable optical density filter with a spectral range of 240 nm – 1200 nm and contains stepped, distinct optical densities of 0.04, 0.1, 0.2, 0.3, 0.4, 0.5, 0.6, and 1.0. The formula for optical density can be seen in equation 3.12 where OD is the optical density, and T is the % transmission of the light at a specified wavelength. Thor Labs reports all ODs at 633 nm.

(3.12)
$$OD = \log_{10}\left(\frac{1}{T}\right)$$

Figure 3.8 shows the transmission spectra of the optical densities used. The reported optical densities used for this work were 0.1, 0.2, and 0.4 which correspond to decreases in 400 nm light of 21%, 37%, and 65% or ODs of 0.1, 0.2, and 0.5, respectively, at 400 nm.
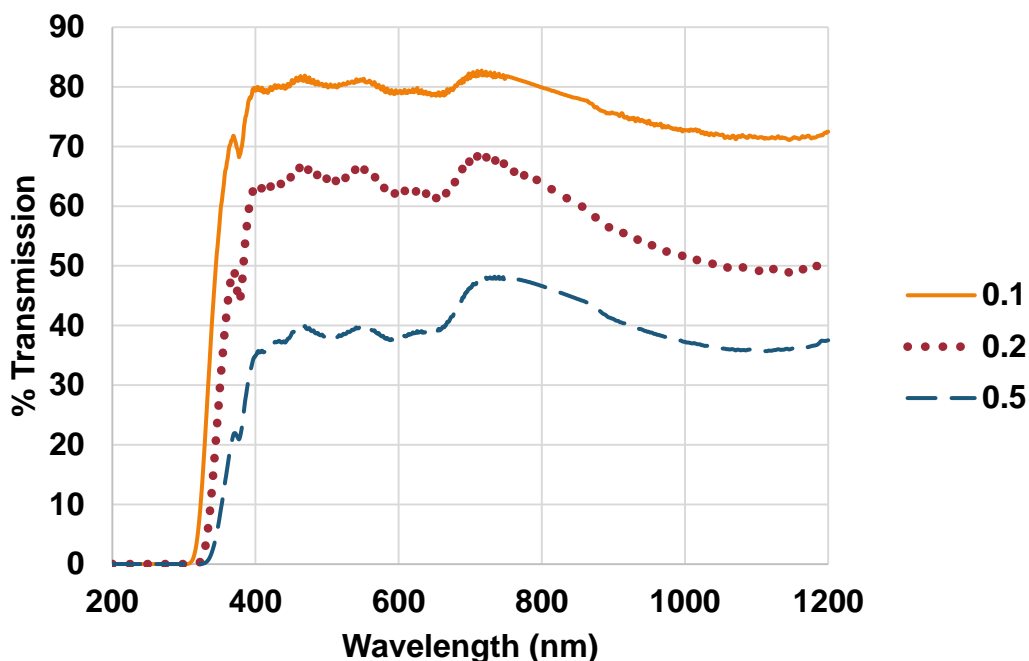
Figure 3.8. The transmission spectra for the respective optical densities used.

3.2.5 IR Sample Preparation

3.2.5.1 Polymerizable DESs

The process of DES preparation for photopolymerization was very similar to the procedure discussed in Chapter 2. The main difference is that since TPO is a solid initiator and not heat sensitive, a stock solution of monomer HBD and TPO was made first. This stock solution was then used in the same way as the pure HBD would be, being mixed with the ChCl and placed in the oven until DES formation is complete. All stock solutions were stored in amber vials and wrapped in foil. Due to size constraints of the amber vials available, DESs are produced in colorless vials but were wrapped in foil to ensure no exposure to light. Samples for RTIR analysis were transferred to 2 mL amber vials to minimize light contamination. All stock solutions and DESs were made in a darkened room under red LED light.

3.2.5.2 Nonpolymerizable DESs

In the case of the DESs used for the methyl ester monomer polymerization, the DESs were made using analogs of the HBD monomers without the C=C bond: propionic acid in the place of acrylic acid and isobutyric acid in the place of methacrylic acid (Figure 3.9). The DESs were made first and then a stock solution of methyl ester monomer containing 1 mol% TPO was added to the DES and mixed in. When not in use, the stock solutions and DES-methyl ester monomer systems were stored in a freezer in amber vials.
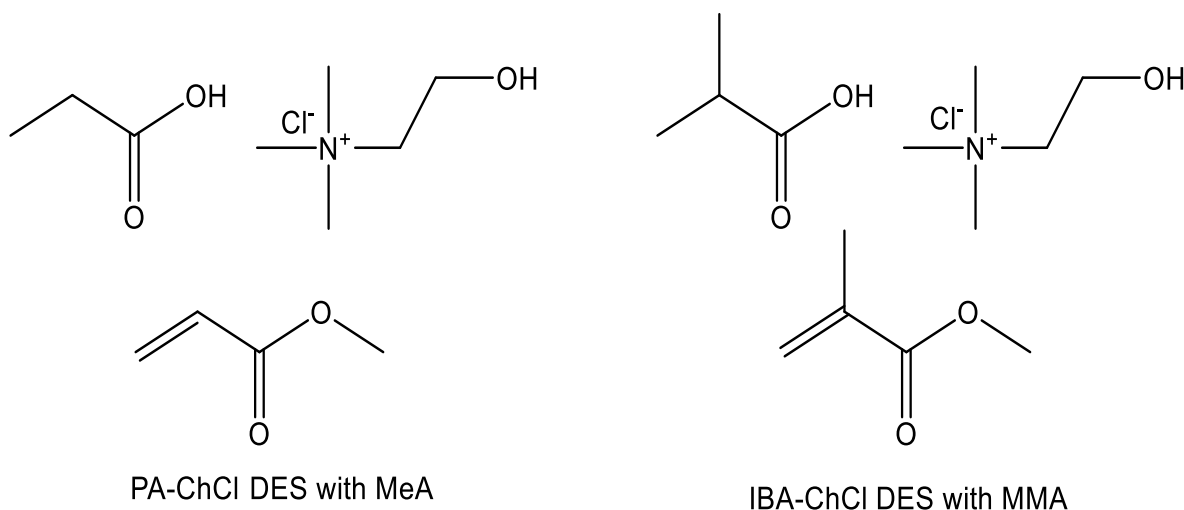

PA-ChCl DES with MeA   IBA-ChCl DES with MMA

Figure 3.9. Nonpolymerizable DES systems containing methyl ester monomers.

3.3 PHOTOPOLYMERIZATION OF ACID-MONOMER-CONTAINING DESs

The photopolymerization of the DESs and the pure monomers were polymerized and rates determined. Initially samples were polymerized at measured intensities of 14 mW*cm^{-2}, 35 mW*cm^{-2}, 70 mW*cm^{-2}, 105 mW*cm^{-2}, and 140 mW*cm^{-2}, but due to the fact that only the 14 mW*cm^{-2} (measured at 400 nm) exhibited a slow enough polymerization to calculate a rate, the neutral density filter was employed for the DESs. For both AA and MAA DESs, the 810 cm^{-1} peak was used as the analysis peak

because in these samples, the 1625 cm^{-1} peak tends to overlap with (and eventually

disappear underneath) the carbonyl peak at ~1700 cm^{-1} making the spectral difference

and therefore conversion artificially inflated.

3.3.1 Photopolymerization of Acrylic Acid DESs

3.3.1.1 AA-ChCl DES Photopolymerization at Varying Light Intensities

Table 3.2 shows the rates of polymerization for the acrylic acid DESs and pure

acrylic acid polymerization. It is clear that the increase in rate seen in Chapter 2 is

reflected in a photopolymerization system as well as an FP system. An important note is

that the conversions listed in Table 3.2 are the maximum conversions achieved during

the polymerization. Should the conversion at 90 min (the final time for the DES

samples) be compared between DES and pure monomer (80% and 4%, respectively)

the difference is much larger.

Table 3.2. Rate and conversion data for AA-TPO and AA-ChCl-TPO.

Sample Set	Intensity (mW*cm^{-2})	Initial Rate (min^{-1})	Maximum conversion (%)
AA-TPO	14	0.03 ± 0.06	41 ± 29
AA-ChCl-TPO	14	13.0 ± 6.0	79 ± 7
AA-ChCl-TPO	11	9.5 ± 1.3	71 ± 4
AA-ChCl-TPO	9	5.4 ± 2.2	69 ± 5
AA-ChCl-TPO	5	2.0 ± 1.0	43 ± 11

There is a difference in viscosity between pure AA (1.2 cP[116]) and the AA-ChCl

DES (171 cP, measured using a Brookfield viscometer), but this does not solely account

for the increase in rate. This viscosity increase may increase rate somewhat, but the

increase is not significant enough to cause gel effect like autoacceleration. Based on

Kuroda's[36] statement regarding heterogeneities within DES systems, it is possible that

heterogeneous domains exist in the DES where the monomer concentration is higher

which could lead to an increased localized rate. Such a heterogeneous system would

lead one to compare these systems to emulsion polymerizations during which polymers grow inside a particle that is monomer rich, and the polymer is typically insoluble in the solution outside the particle. Because of this, emulsion has very distinct intervals during the polymerization during which the rate behavior is very predictable. Interval I corresponds to rapid increase in rate followed by a much slower increase or a plateau in rate in interval II, and finally during interval III the rate quickly decreases due to decreasing monomer concentration at the end of the reaction. Figure 3.10 shows rate versus conversion plots for all of the AA-ChCl samples. In the case of the AA-ChCl samples, some broadening at the maximum of the plot occurs but not enough and not consistently enough to conclude that this system polymerizes in the same way as an emulsion. The 5 mW*cm^{-2} samples do seem to broaden more than the others with the slowing of the polymerization. With a further decrease in polymerization rate (by decreasing light intensity), interval II behavior might be observable, but it is doubtful.
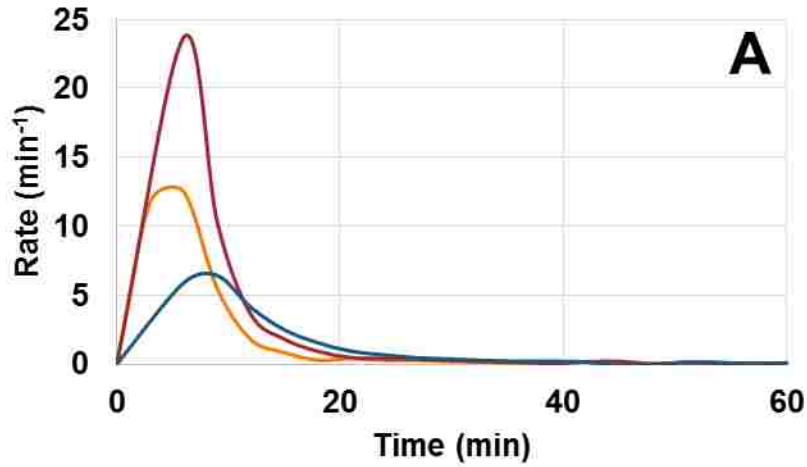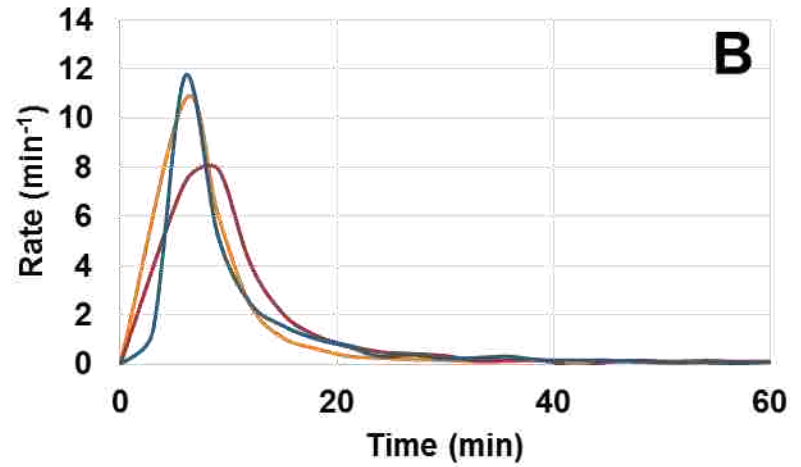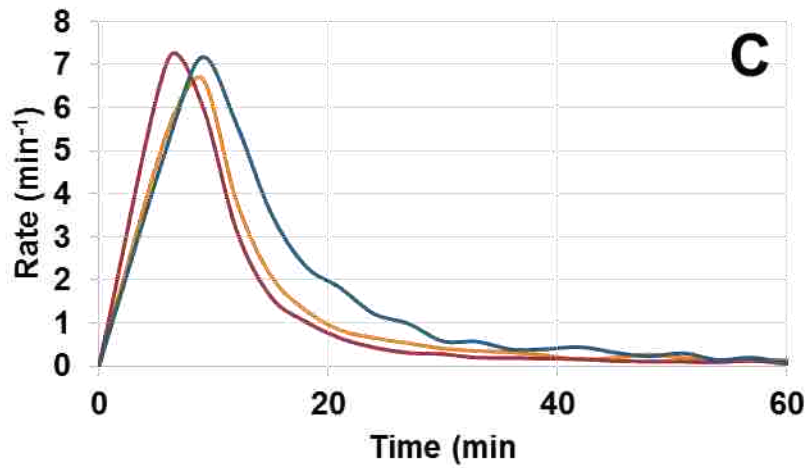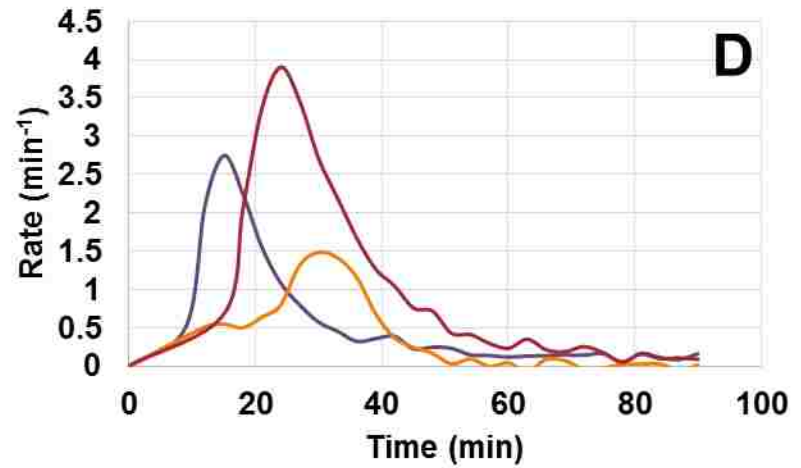
Figure 3.10. Rate versus time plots for AA-ChCl samples measured at intensities of 14 mW*cm^{-2} (A), 11 mW*cm^{-2} (B), 9 mW*cm^{-2} (C), 5 mW*cm^{-2} (D).

Another factor that is seen in polymerization in ILs (and within acrylate bulk polymerizations when comparing various monomer structures[117]) is the hydrogen bonding within the system. It is known that hydrogen bonding can cause preorganization that increases polymerization rate.[117] With the increased hydrogen bonding network seen in DESs, this is most likely the main factor that increases the rate.

3.3.1.2 Other HBAs for AA DES Photopolymerization

In order to test the idea of heterogeneous domains within the DES, a different HBA was desired for the polymerization. Three HBAs were attempted, but none were successful. Figure 3.11 shows the structures of the three.

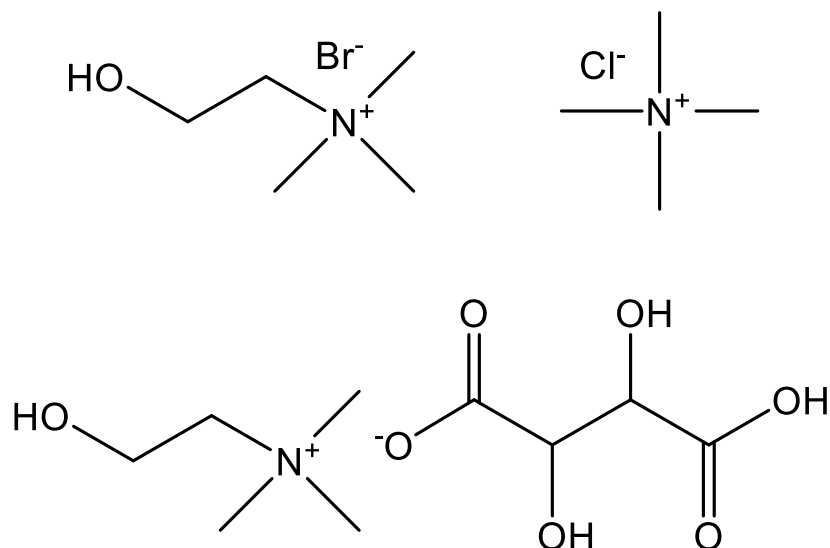Figure 3.11. Top left: choline bromide, top right: tetramethylammonium chloride, Bottom: choline bitartrate.

ChBr was the only HBA of the three to form a DES under the standard DES formation conditions at the 1.6:1 ratio, and the AA-ChBr samples all crystallized almost instantaneously after removal from the oven and formed a semi-solid material that could not be melted back to a pure liquid state.

3.3.2 Photopolymerization of Methacrylic Acid DESs

Just as is the case for the AA samples, the MAA samples show orders of magnitude increase in rate between the DES and pure monomer. Also, the 90 minute conversion between the two—55% and 4%— is larger, though not as drastic a difference as seen in the AA.

Table 3.3. Rate and conversion data for MAA-TPO and MAA-ChCl-TPO.

Sample Set	Intensity (mW*cm^{-2})	Initial Rate (min^{-1})	Maximum conversion (%)
MAA-TPO	14	0.02 ± 0.02	11 ± 8
MAA-ChCl-TPO	14	3.9 ± 1.1	55 ± 5
MAA-ChCl-TPO	11	1.4 ± 0.6	46 ± 17
MAA-ChCl-TPO	9	1.5 ± 0.4	55 ± 10
MAA-ChCl-TPO	5	0.7 ± 0.3	33 ± 12

The slower rates and lower conversions are to be expected with the less reactive MAA monomer. Again, it seems that viscosity plays some role in the rate enhancement of these samples with the MAA DES viscosity measuring 73 cP, and the pure MAA's viscosity being 1.3 cP,[118] but as was the case with the AA samples as well, it is likely that viscosity is not the main factor to play a role in the rate enhancement. By plotting the rate versus time (Figure 3.12), we can see that the MAA samples do have broader and slightly more emulsion like plots—which is reasonable because of the slightly more hydrophobic nature of MAA compared to AA—but still do not exhibit enough of an interval II behavior to be considered emulsion like. This leads to the conclusion that once again, the increased hydrogen bonding network around the monomer cause the increase in rate.
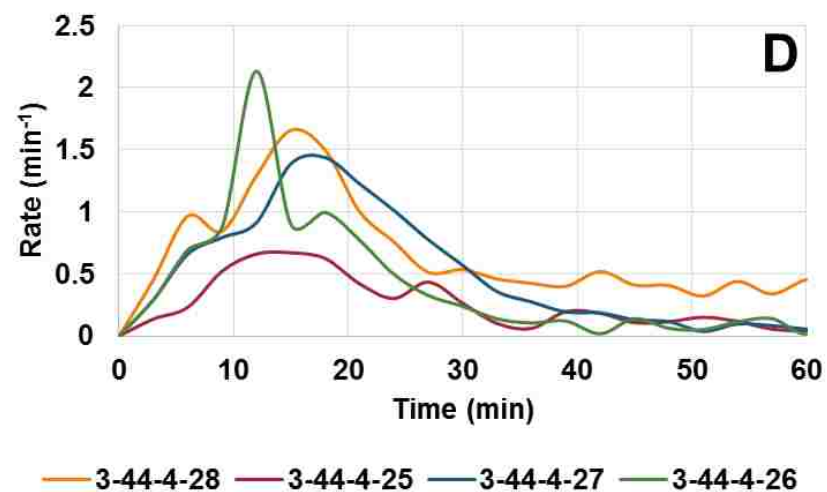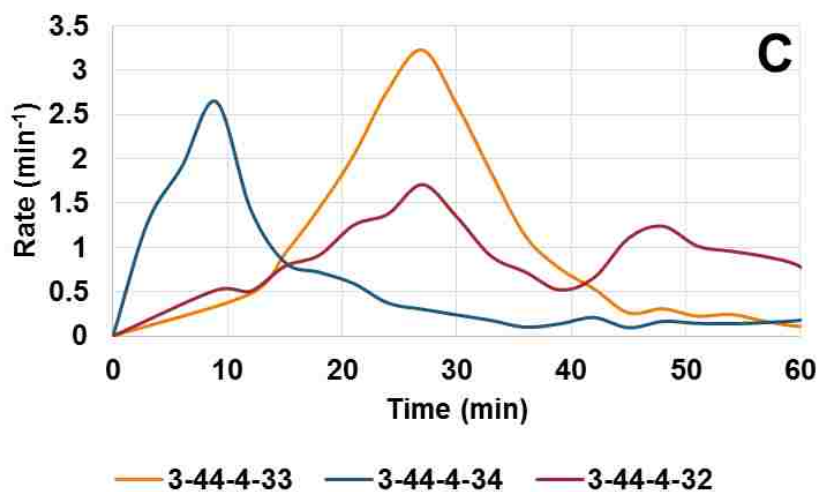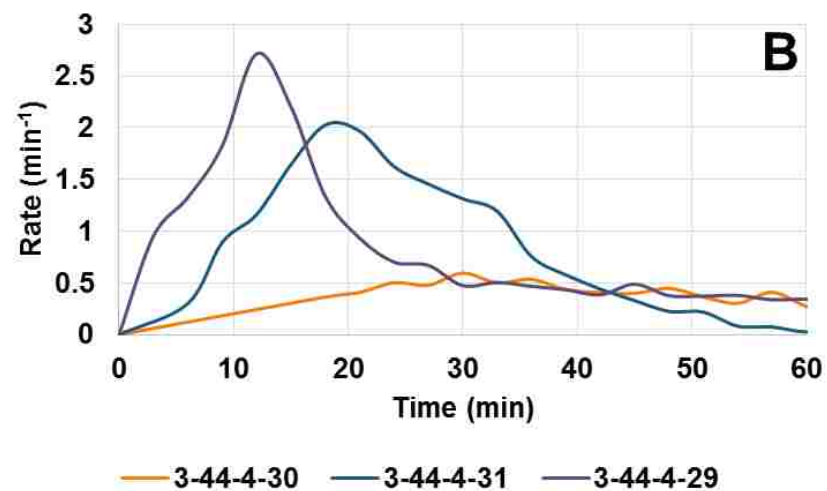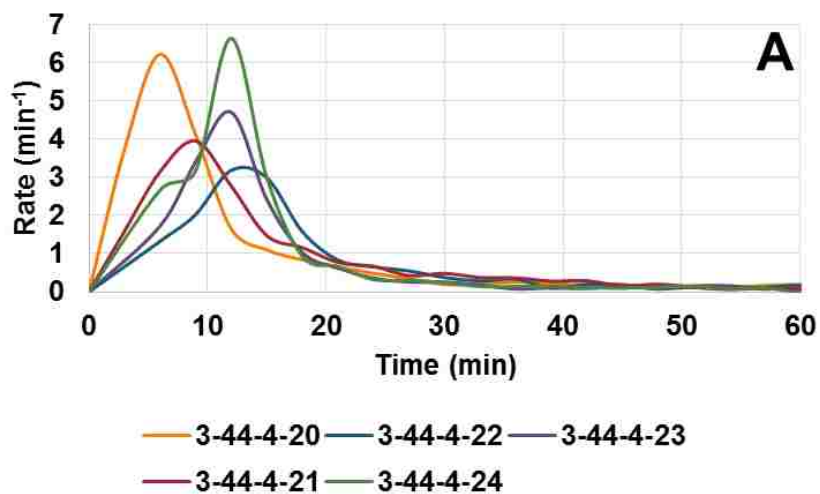
Figure 3.12. Rate versus time plots for MAA-ChCl samples measured at intensities of 14 mW*cm^{-2} (A), 11 mW*cm^{-2} (B), 9 mW*cm^{-2} (C), 5 mW*cm^{-2} (D).

3.4 PHOTOPOLYMERIZATION OF ACID DESS CONTAINING METHYL ESTER MONOMERS

In order to determine if the monomer has to be part of the DES to see the rate enhancement, DESs were made using nonreactive analogs of AA and MAA (see Figure 3.9) and the corresponding methyl ester monomer was polymerized, MeA and MMA, respectively. In most MeA samples (both pure and DES), the increases in conversion exceeded the aforementioned limit. The few samples at the lowest measured light intensity (measured at 365 nm) that potentially would exhibit measurable rates with pure MeA evaporated before polymerization was complete enough to calculate a rate—even after use of the glass slide covers. Because of this, slowing the rate further to study the MeA system with the NDF did not seem plausible.

The MMA-TPO and MMA-TPO-IBA-ChCl systems (Figures 3.13 and 3.14), however, gave consistent results to what was seen in the AA and MAA DESs. There is a definite rate enhancement in the samples that contain DES even though the monomer is not part of the DES. This indicates that the environment of the DES, even without the additional hydrogen bonding between the monomer and the HBA, is conducive to increased polymerization rate. Viscosity almost certainly does play some role, here, but the increased polarity of the DES versus bulk MMA cannot be ignored. As was shown for the ILs mentioned in section 3.2.2, the polarity of the system can play a role as well. The IBA-ChCl DES is much more polar than MMA, which almost certainly leads an increase in the k_p. The intensity of light and initiator concentration used for these samples is higher than those used for the original DES polymerizations. Because of these higher input values, the rates are approaching what is essentially a maximum for the system. Lower intensities should trend similarly to the monomer-containing DESs.
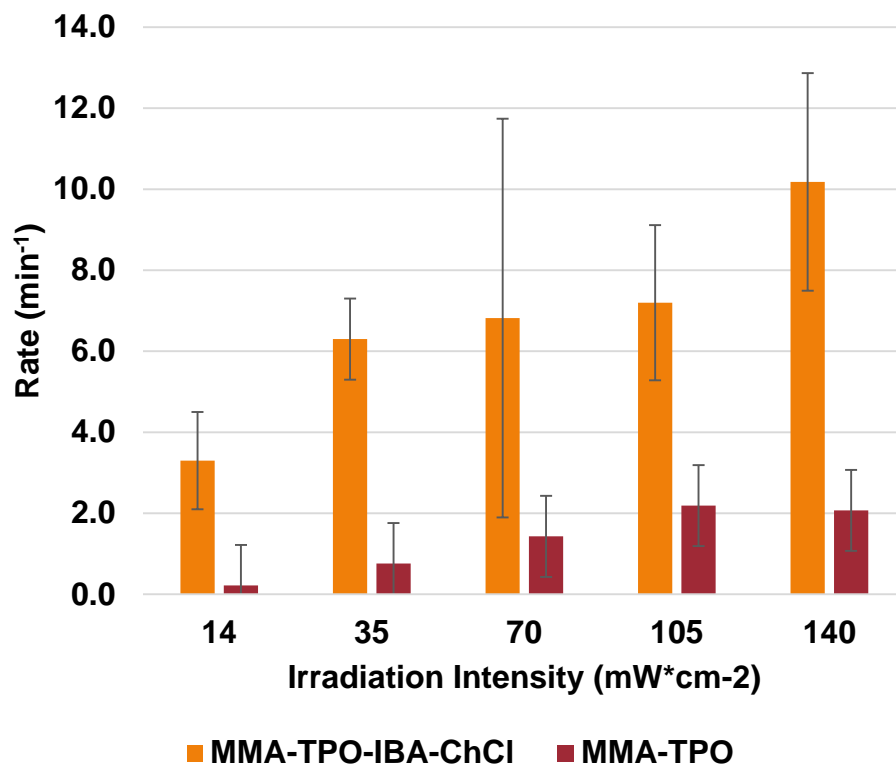
Figure 3.13. Initial rates for pure MMA and MMA in an IBA-ChCl DES.
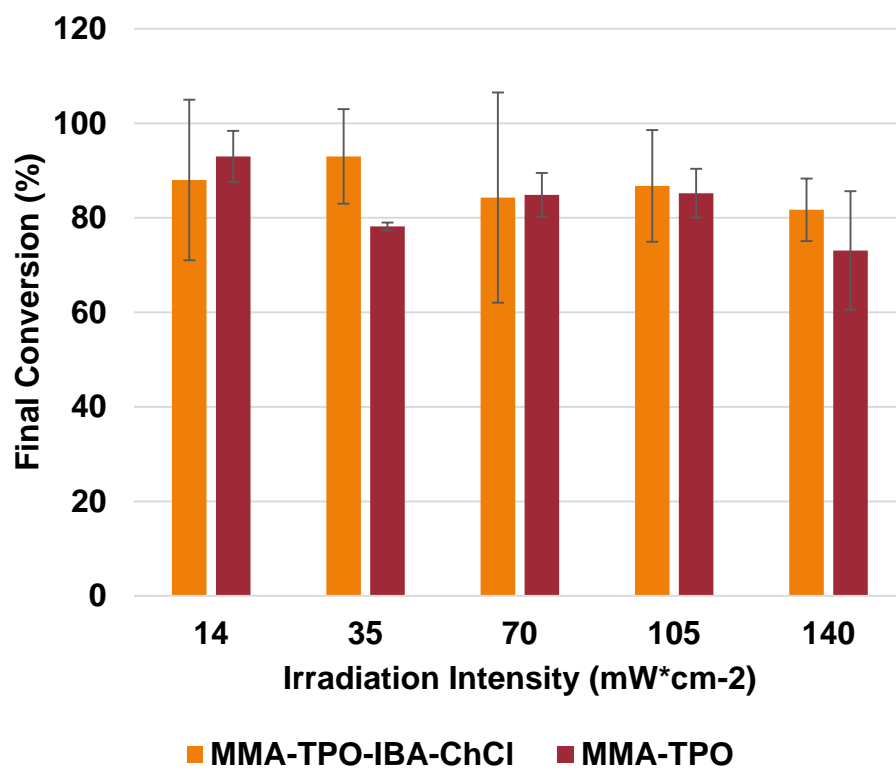
Figure 3.14. Final conversions for MMA and MMA in an IBA-ChCl DES.

3.5 CONCLUSIONS

  In order to determine if DESs cause polymerization rate enhancements similar to those seen in ILs, photopolymerizations of polymerizable DESs and DESs with monomer incorporated into them were performed and monitored via RTIR. Conversion and rate data obtained from the RTIR experiments indicate that rate enhancement occurs regardless of whether or not the monomer is a component of the DES. Viscosity measurements indicate that the enhanced rate is in part due to the increased viscosity found in the DES, but rate data indicates that even though DESs are known to be heterogeneous, the polymerization does not behave in an emulsion-like manner. This leaves the hydrogen bonding and polarity of the DESs versus their pure monomer states as the main factor that increases the rate.

IV. SUMMARY AND CONCLUSIONS

Deep eutectic solvents have a large presence and an even larger future in polymerization. In this work, deep eutectic solvents were synthesized using (meth)acrylic acid and choline chloride as the hydrogen bond donor and hydrogen bond acceptor, respectively. Unlike previous work which used crosslinkers in conjunction with the monomer HBD, the DESs in this work were polymerized using only the acid monomer HBD. The DESs were able to be polymerized using a range of initiator concentrations and exhibited frontal behavior that was unexpected. Due to this unusual behavior, a more in-depth study of these systems was performed by replacing the ChCl with inert analogs. These analogs were meant to impart typical phenomena that will alter the behavior of a frontal polymerization and included talc as a heat sink, stearic acid as an inert phase change material, lauric acid as a hydrogen bond capable diluent, and DMSO as an inert diluent. None of the analog systems produced results similar to the DESs, and methacrylic acid would not sustain a front with any of the analogs. This lead to the conclusion that the presence of a DES has a direct impact on the rate of a free-radical polymerization. To elucidate more about this rate enhancement, a step away from the complexity of frontal polymerization had to be taken.

In order to study the DES rate enhancement, DESs were photopolymerized while being monitored using real-time FTIR. The rates of the DES samples were much higher than those of the pure monomer due to the increased hydrogen bond complexation around the monomer. To study whether or not the monomer had to be part of the DES in order to experience rate enhancement, molecularly similar systems were employed in which the HBD was a nonpolymerizable analog to the monomer HBDs used previously: propionic acid in the place of acrylic acid and isobutyric acid in the place of methacrylic

57

acid. The monomers for these systems are methyl ester equivalents to the aforementioned monomers, methyl acrylate and methyl methacrylate, respectively. The rates from the methyl ester monomer-DES systems were also increased compared to their pure monomer counterparts. Placing a monomer that has no hydrogens to hydrogen bond into a DES still causes an increase in rate indicating that polarity as well as hydrogen bonding plays a role in rate enhancement by a DES.

If this work were to be pursued further, the next step would be to use one monomer in multiple DESs with the same HBD but differing HBAs to determine if DES heterogeneity has an impact on the polymerization. The polymer produced would be characterized by gel permeation chromatography so that molecular weight can be correlated to the polymerization data. Methyl methacrylate and hydroxyethylmethacrylate would both be desirable choices for these experiments. Another line of experimentation to pursue would be to test other hydrogen bond capable monomers such as hydroxyethylmethacrylate and carboxyethylacrylate to determine if monomer DES components with different dipole moments would experience rate enhancement to varying degrees. Dilution studies in which the monomer concentration is held constant and different nonreactive HBDs are used to tune viscosity would also be advantatgeous for understanding the impact of viscosity on polymerization kinetics.

REFERENCES

1. Moad, G.; Solomon, D. H., *The Chemistry of Radical Polymerization*. Pergamon: Oxford, 1995.

2. Odian, G., *Principles of Polymerization, 4th Ed.* 3rd ed. ed.; Wiley: New York, 2004.

3. Delaittre, G.; Rieger, J.; Charleux, B. *Macromolecules* **2011,** 44, (3), 462-470.

4. Matyjaszewski, K. Atom Transfer Radical Polymerization (ATRP). https://www.cmu.edu/maty/chem/fundamentals-atrp/atrp.html (2 February),

5. Perrier, S. *Macromolecules* **2017,** 50, 7433-7447.

6. Kubisa, P. *Prog. Polym. Sci.* **2009,** 34, (12), 1333-1347.

7. Gorke, J.; Srienc, F.; Kazlauskas, R. *Biotechnol Bioproc E* **2010,** 15, (1), 40-53.

8. Abbott, A. P.; Capper, G.; Davies, D. L.; Rasheed, R. K.; Tambyrajah, V. *Chem. Comm.* **2003**, (1), 70-71.

9. Smith, E. L.; Abbott, A. P.; Ryder, K. S. *Chemical Reviews* **2014,** 114, 11060-11082.

10. Carriazo, D.; Serrano, M. C.; Gutierrez, M. C.; Ferrer, M. L.; del Monte, F. *Chemical Society Reviews* **2012,** 41, (14), 4996-5014.

11. Zhang, Q.; De Oliveira Vigier, K.; Royer, S.; Jerome, F. *Chemical Society Reviews* **2012,** 41, (21), 7108-7146.

12. Mota-Morales, J. D.; Sánchez-Leija, R. J.; Carranza, A.; Pojman, J. A.; del Monte, F.; Luna-Bárcenas, G. *Progress in Polymer Science* **2018,** 78, 139-153.

13. Shishov, A.; Bulatov, A.; Locatelli, M.; Carradori, S.; Andruch, V. *Microchemical Journal* **2017,** 135, 33-38.

14. Paiva, A.; Craveiro, R.; Aroso, I.; Martins, M.; Reis, R. L.; Duarte, A. R. C. *ACS Sustainable Chemistry & Engineering* **2014,** 2, (5), 1063-1071.

15. Zainal-Abidin, M. H.; Hayyan, M.; Hayyan, A.; Jayakumar, N. S. *Analytica Chimica Acta* **2017,** 979, 1-23.

16. Qin, H.; Panzer, M. J. *ChemElectroChem* **2017,** 4, (10), 2556-2562.

17. Maugeri, Z.; Marıa, P. D. d. *RSC Advances* **2012,** 2, 421-425.

18. Abbott, A. P.; Boothby, D.; Capper, G.; Davies, D. L.; Rasheed, R. K. *J. Amer. Chem. Soc.* **2004,** 126, (29), 9142-9147.

19. Florindo, C.; Oliveira, F. S.; Rebelo, L. P. N.; Fernandes, A. M.; Marrucho, I. M. *ACS Sustainable Chemistry & Engineering* **2014,** 2, (10), 2416-2425.

20. Ribeiro, B. D.; Florindo, C.; Iff, L. C.; Coelho, M. A. Z.; Marrucho, I. M. *ACS Sustainable Chemistry & Engineering* **2015,** 3, (10), 2469-2477.

21. Isik, M.; Ruiperez, F.; Sardon, H.; Gonzalez, A.; Zulfiqar, S.; Mecerreyes, D. *Macromolecular Rapid Communications* **2016,** 37, (14), 1135-1142.

22. Isik, M.; Zulfiqar, S.; Edhaim, F.; Ruiperez, F.; Rothenberger, A.; Mecerreyes, D. *ACS Sustainable Chemistry & Engineering* **2016,** 4, (12), 7200-7208.

23. Sze, L. L.; Pandey, S.; Ravula, S.; Pandey, S.; Zhao, H.; Baker, G. A.; Baker, S. N. *ACS Sustainable Chemistry & Engineering* **2014,** 2, (9), 2117-2123.

24. Sanchez-Leija, R. J.; Pojman, J. A.; Luna-Barcenas, G.; Mota-Morales, J. D. *J. Mater. Chem. B* **2014,** 2, (43), 7495-7501.

25. Serrano, M. C.; Gutierrez, M. C.; Jimenez, R.; Ferrer, M. L.; Monte, F. d. *Chemical Communications* **2012,** 48, (4), 579-581.

26. Mukesh, C.; Upadhyay, K. K.; Devkar, R. V.; Chudasama, N. A.; Raol, G. G.; Prasad, K. *Macromolecular Chemistry and Physics* **2016,** 217, (17), 1899-1906.

27. Abbott, A. P.; Bell, T. J.; Handa, S.; Stoddart, B. *Green Chemistry* **2006,** 8, (9), 784-786.

28. Hong, S.; Lian, H.; Sun, X.; Pan, D.; Carranza, A.; Pojman, J. A.; Mota-Morales, J. D. *RSC Advances* **2016,** 6, (92), 89599-89608.

29. Lian, H.; Hong, S.; Carranza, A.; Mota-Morales, J. D.; Pojman, J. A. *RSC Adv.* **2015,** 5, (36), 28778-28785.

30. Sharma, M.; Mukesh, C.; Mondal, D.; Prasad, K. *RSC Advances* **2013,** 3, (39), 18149-18155.

31. Liu, Y.; Guo, B.; Xia, Q.; Meng, J.; Chen, W.; Liu, S.; Wang, Q.; Liu, Y.; Li, J.; Yu, H. *ACS Sustainable Chemistry & Engineering* **2017,** 5, (9), 7623-7631.

32. Cui, Y.; Li, M.-C.; Wu, Q.; Pojman, J. A.; Kuroda, D. G. *ACS Appl. Mater. Interfaces* **2017,** 9, (39), 33549-33553.

33. Warrag, S. E. E.; Peters, C. J.; Kroon, M. C. *Current Opinion in Green and Sustainable Chemistry* **2017,** 5, 55-60.

34. Bednarz, S.; Fluder, M.; Galica, M.; Bogdal, D.; Maciejaszek, I. *Journal of Applied Polymer Science* **2014,** 131, (16), 40608.

35.   Zahn, S.; Kirchner, B.; Mollenhauer, D. *ChemPhysChem* **2016,** 17, (21), 3354-3358.

36.   Cui, Y.; Kuroda, D. G. *The Journal of Physical Chemistry A* **2018,** 122, (5), 1185-1193.

37.   Hammond, O. S.; Bowron, D. T.; Edler, K. J. *Green Chemistry* **2016,** 18, (9), 2736-2744.

38.   Hammond, O. S.; Bowron, D. T.; Edler, K. J. *Angewandte Chemie International Edition* **2017,** 56, (33), 9782-9785.

39.   D'Agostino, C.; Harris, R. C.; Abbott, A. P.; Gladden, L. F.; Mantle, M. D. *Physical Chemistry Chemical Physics* **2011,** 13, (48), 21383-21391.

40.   Perkins, S. L.; Painter, P.; Colina, C. M. *Journal of Chemical & Engineering Data* **2014,** 59, (11), 3652-3662.

41.   Perez-Garcia, M. G.; Carranza, A.; Puig, J. E.; Pojman, J. A.; del Monte, F.; Luna-Barcenas, G.; Mota-Morales, J. D. *RSC Adv.* **2015,** 5, (30), 23255-23260.

42.   Abbott, A. P.; Boothby, D.; Capper, G.; Davies, D. L.; Rasheed, R. K. *Journal of the American Chemical Society* **2004,** 126, (29), 9142-9147.

43.   Carranza, A.; Pojman, J. A.; Mota-Morales, J. D. *RSC Advances* **2014,** 4, (78), 41584-41587.

44.   Gutiérrez, M. C.; Carriazo, D.; Tamayo, A.; Jiménez, R.; Picó, F.; Rojo, J. M.; Ferrer, M. L.; del Monte, F. *Chemistry – A European Journal* **2011,** 17, (38), 10533-10537.

45.   Mota-Morales, J. D.; Gutierrez, M. C.; Sanchez, I. C.; Luna-Barcenas, G.; del Monte, F. *Chem. Comm.* **2011,** 47, (18), 5328-5330.

46.   Mukesh, C.; Gupta, R.; Srivastava, D. N.; Nataraj, S. K.; Prasad, K. *RSC Advances* **2016,** 6, (34), 28586-28592.

47.   Wang, J.; Han, J.; Khan, M. Y.; He, D.; Peng, H.; Chen, D.; Xie, X.; Xue, Z. *Polymer Chemistry* **2017,** 8, (10), 1616-1627.

48.   Mendonça, P. V.; Lima, M. S.; Guliashvili, T.; Serra, A. C.; Coelho, J. F. J. *Polymer* **2017,** 132, 114-121.

49.   Maximiano, P.; Mendonça, P. V.; Santos, M. R. E.; Costa, J. R. C.; Guliashvili, T.; Serra, A. C.; Coelho, J. F. J. *Journal of Polymer Science Part A: Polymer Chemistry* **2017,** 55, (3), 371-381.

50. Sanchez-Leija, R. J.; Torres-Lubian, J. R.; Resendiz-Rubio, A.; Luna-Barcenas, G.; Mota-Morales, J. D. *RSC Advances* **2016,** 6, (16), 13072-13079.

51. Carranza, A.; Pérez-García, M. G.; Song, K.; Jeha, G. M.; Diao, Z.; Jin, R.; Bogdanchikova, N.; Soltero, A. F.; Terrones, M.; Wu, Q.; Pojman, J. A.; Mota-Morales, J. D. *ACS Appl. Mater. Interfaces* **2016,** 8, (45), 31295-31303.

52. Carranza, A.; Romero-Perez, D.; Almanza-Reyes, H.; Bogdanchikova, N.; Juarez-Moreno, K.; Pojman, J. A.; Velasquillo, C.; Mota-Morales, J. D. *Adv. Mater. Interfaces* **2017**, 1700094-n/a.

53. Gutiérrez, M. C.; Rubio, F.; del Monte, F. *Chemistry of Materials* **2010,** 22, (9), 2711-2719.

54. Carriazo, D.; Gutiérrez, M. C.; Ferrer, M. L.; del Monte, F. *Chemistry of Materials* **2010,** 22, (22), 6146-6152.

55. Gutierrez, M. C.; Carriazo, D.; Ania, C. O.; Parra, J. B.; Ferrer, M. L.; del Monte, F. *Energy & Environmental Science* **2011,** 4, (9), 3535-3544.

56. García-Argüelles, S.; Serrano, M. C.; Gutiérrez, M. C.; Ferrer, M. L.; Yuste, L.; Rojo, F.; del Monte, F. *Langmuir* **2013,** 29, (30), 9525-9534.

57. Li, R. a.; Chen, G.; He, M.; Tian, J.; Su, B. *Journal of Materials Chemistry C* **2017,** 5, (33), 8475-8481.

58. Mota-Morales, J. D.; Gutiérrez, M. C.; Ferrer, M. L.; Sanchez, I. C.; Elizalde-Peña, E. A.; Pojman, J. A.; Monte, F. D.; Luna-Bárcenas, G. *J. Polym. Sci. Part A: Polym. Chem.* **2013,** 51, 1767–1773.

59. Mota-Morales, J. D.; Gutierrez, M. C.; Ferrer, M. L.; Jimenez, R.; Santiago, P.; Sanchez, I. C.; Terrones, M.; Del Monte, F.; Luna-Barcenas, G. *J. Mater. Chem. A,* **2013,** 1, (12), 3970-3976.

60. Azizi, N.; Batebia, E. *Catalysis Science & Technology* **2012,** 2, 2445-2448.

61. Bednarz, S.; Błaszczyk, A.; Błazejewska, D.; Bogdał, D. *Catalysis Today* **2014**.

62. Pojman, J. A., Frontal Polymerization. In *Polymer Science: A Comprehensive Reference*, Matyjaszewski, K.; Möller, M., Eds. Elsevier BV: Amsterdam, 2012; Vol. 4, pp 957–980.

63. Trommsdorff, E.; Köhle, H.; Lagally, P. *Makromol. Chem.* **1948,** 1, 169-198.

64. Norrish, R. G. W.; Smith, R. R. *Nature* **1942,** 150, 336-337.

65. Jee, E.; Bánsági, T.; Taylor, A. F.; Pojman, J. A. *Angew. Chem.* **2016,** 128, (6), 2167-2171.

66.   Terrones, G.; Pearlstein, A. J. *Macromolecules* **2001,** 34, 3195-3204.

67.   Terrones, G.; Pearlstein, A. J. *Macromoleules* **2004,** 37, 1565-1575.

68.   Chechilo, N. M.; Khvilivitskii, R. J.; Enikolopyan, N. S. *Dokl. Akad. Nauk SSSR* **1972,** 204, (N5), 1180-1181.

69.   Chechilo, N. M.; Enikolopyan, N. S. *Dokl. Phys. Chem.* **1976,** 230, 840-843.

70.   Holt, T.; Fazende, K.; Jee, E.; Wu, Q.; Pojman, J. A. *J. Appl. Polym. Sci.* **2016,** 133, (40), 44064.

71.   Totaro, N. P.; Murphy, Z. D.; Burcham, A. E.; King, C. T.; Scherr, T. F.; Bounds, C. O.; Dasa, V.; Pojman, J. A.; Hayes, D. J. *J. Biomed. Mater. Res. Part A: Appl. Biomater.* **2016,** 104, 1152–1160.

72.   Alzari, V.; Monticelli, O.; Nuvoli, D.; Kenny, J. M.; Mariani, A. *Biomacromolecules* **2009,** 10, (9), 2672-2677.

73.   Scognamillo, S.; Alzari, V.; Nuvoli, D.; Illescas, J.; Marceddu, S.; Mariani, A. *J. Polym. Sci. Part A: Polym. Chem.* **2011,** 49, (5), 1228-1234.

74.   Sanna, R.; Alzari, V.; Nuvoli, D.; Scognamillo, S.; Marceddu, S.; Mariani, A. *J. Polym. Sci. Part A: Polym. Chem.* **2012,** 50, (8), 1515-1520.

75.   Nuvoli, L.; Sanna, D.; Alzari, V.; Nuvoli, D.; Sanna, V.; Malfatti, L.; Mariani, A. *J. Polym. Sci. A Polym. Chem.* **2016,** 54, (14), 2166-2170.

76.   Tang, W.-Q.; Mao, L.-H.; Zhou, Z.-F.; Wang, C.-F.; Chen, Q.-L.; Chen, S. *Colloid Polym. Sci.* **2014,** 292, 2529-2537.

77.   Tu, J.; Chen, L.; Fang, Y.; Wang, C.; Chen, S. *Journal of Polymer Science Part A: Polymer Chemistry* **2010,** 48, (4), 823-831.

78.   Du, X.-Y.; Liu, S.-S.; Wang, C.-F.; Wu, G.; Chen, S. *Journal of Polymer Science Part A: Polymer Chemistry* **2017**, n/a-n/a.

79.   Chekanov, Y. A.; Pojman, J. A. *J. Appl. Polym. Sci.* **2000,** 78, 2398-2404.

80.   Masere, J.; Lewis, L. L.; Pojman, J. A. *J. Appl. Polym. Sci.* **2001,** 80, 686-691.

81.   Nuvoli, D.; Alzari, V.; Pojman, J.; Sanna, V.; Ruiu, A.; Sanna, D.; Malucelli, G.; Mariani, A. *ACS Appl. Mater. Interfaces* **2015,** 7, 3600−3606.

82.   Scognamillo, S.; Bounds, C.; Luger, M.; Mariani, A.; Pojman, J. A. *J. Polym. Sci. Part A: Polym. Chem.* **2010,** 48, (9), 2000-2005.

83.   Scognamillo, S.; Bounds, C.; Thakuri, S.; Mariani, A.; Wu, Q.; Pojman, J. A. *J. Appl. Polym. Sci.* **2014,** 131, 40339-40349.

84.   Bomze, D.; Knaack, P.; Liska, R. *Polym. Chem.* **2015,** 6, 8161-8167.

85.   Mariani, A.; Bidali, S.; Fiori, S.; Sangermano, M.; Malucelli, G.; Bongiovanni, R.; Priola, A. *J. Poly. Sci. Part A. Polym. Chem.* **2004,** 42, 2066-2072.

86.   Chen, S.; Sui, J.; Chen, L.; Pojman, J. A. *J. Polym. Sci. Part A Polym. Chem.* **2005,** 43, 1670-1680.

87.   Z. Chen, P. L., L. Shi, Z. X. Huang, B. Y. Jiang. *Applied Mechanics and Materials* **2014,** 692, 416-419.

88.   Li, S.; Huang, H.; Tao, M.; Liu, X.; Cheng, T. *J. Appl. Poly. Sci.* **2013,** 129, (6), 3737-3745.

89.   Alzari, V.; Nuvoli, D.; Scognamillo, S.; Piccinini, M.; Gioffredi, E.; Malucelli, G.; Marceddu, S.; Sechi, M.; Sanna, V.; Mariani, A. *J. Mater. Chem.* **2011,** 21, (24), 8727-8733.

90.   Crivello, J. V.; Bulut, U. *Designed Monomers & Polymers* **2005,** 8, 517-531.

91.   Crivello, J. V.; Bulut, U. *J. Polym. Sci. Part A: Polym. Chem.* **2006,** 44, 6750-6764.

92.   Crivello, J. V.; Falk, B.; Zonca Jr., M. R. *J. Poly. Sci. Part A. Polym. Chem.* **2004,** 42, 1630-1646.

93.   Falk, B.; Zonca, M. R.; Crivello, J. V. *Macromolecular Symposia* **2005,** 226, 97-108.

94.   Mariani, A.; Fiori, S.; Chekanov, Y.; Pojman, J. A. *Macromolecules* **2001,** 34, 6539-6541.

95.   Ruiu, A.; Sanna, D.; Alzari, V.; Nuvoli, D.; Mariani, A. *J. Poly. Sci. Part A. Poly. Chem.* **2014,** 52, (19), 2776-2780.

96.   Bidali, S.; Fiori, S.; Malucelli, G.; Mariani, A. *e-Polymers* **2003,** 060, 1-12.

97.   Pojman, J. A.; Varisli, B.; Perryman, A.; Edwards, C.; Hoyle, C. *Macromolecules* **2004,** 37, 691-693.

98.   Hoyle, C. E.; Lee, T. Y.; Roper, T. *J. Poly. Sci. Part A. Polym. Chem.* **2004,** 52, 5301-5338.

99.   Viner, V.; Pojman, J. A. *J. Polym. Sci. Part A: Polym. Chem.* **2011,** 49, 4556–4561.

100.   Viner, V.; Viner, G. *J. Phys. Chem. B* **2011,** 115, 6862–6867.

101.   Crivello, J. V. *J. Polym. Sci. Part A Polym. Chem.* **2007,** 45, 4331–4340.

102. Carranza, A.; Gewin, M.; Pojman, J. A. *Chaos* **2014,** 24, 023118.

103. Washington, R. P.; Steinbock, O. *J. Am. Chem. Soc.* **2001,** 123, 7933-7934.

104. Pojman, J. A.; Curtis, G.; Ilyashenko, V. M. *J. Am. Chem. Soc.* **1996,** 118, 3783-3784.

105. Fortenberry, D. I.; Pojman, J. A. *Journal of Polymer Science Part A: Polymer Chemistry* **2000,** 38, (7), 1129-1135.

106. Asakura, K.; Nihei, E.; Harasawa, H.; Ikumo, A.; Osanai, S., Spontaneous Frontal Polymerization: Propagating Front Spontaneously Generated by Locally Autoaccelerated Free-Radical Polymerization. In *Nonlinear Dynamics in Polymeric Systems, ACS Symposium Series No. 869*, Pojman, J. A.; Tran-Cong-Miyata, Q., Eds. American Chemical Society: American Chemical Society, 2003; pp 135-146.

107. Wasserscheid, P.; Keim, W. *Angew. Chem Int. Ed. Engl.* **2000,** 39, 3772-3789.

108. Yan, T.; Burnham, C. J.; Popolo, M. G. D.; Voth, G. A. *Journal of Physical Chemistry B* **2004,** 108, (32), 11877-11881.

109. Abbott, A. P.; Capper, G.; Davies, D. L.; Rasheed, R. *Inorganic Chemistry* **2004,** 43, (11), 3447-3452.

110. Pojman, J. A.; Ilyashenko, V. M.; Khan, A. M. *J. Chem. Soc. Faraday Trans.* **1996,** 92, 2825-2837.

111. Pojman, J. A.; Willis, J. R.; Khan , A. M.; West, W. W. *J. Polym. Sci. Part A: Polym Chem.* **1996,** 34, 991-995.

112. Viner, V. G.; Pojman, J. A.; Golovaty, D. *Physica D: Nonlinear Phenomena* **2010,** 239, 838-847.

113. Strehmel, V.; Laschewsky, A.; Wetzel, H.; Gornitz, E. *Macromolecules* **2006,** 39, 923-930.

114. Woecht, I.; Schmidt-Naake, G.; Beuermann, S.; Buback, M.; García, N. *Journal of Polymer Science Part A: Polymer Chemistry* **2008,** 46, (4), 1460-1469.

115. Jeličić, A.; Köhler, F.; Winter, A.; Beuermann, S. *Journal of Polymer Science Part A: Polymer Chemistry* **2010,** 48, (14), 3188-3199.

116. DOW Acrylic Acid, Glacial. http://msdssearch.dow.com/PublishedLiteratureDOWCOM/dh_099c/0901b8038099c42d.pdf?filepath=acrylates/pdfs/noreg/745-00106.pdf&fromPage=GetDoc (25 February),

117.   Jansen, J.; Dias, A.; Dorschu, M.; Coussens, B. *Macromolecules* **2003,** 36, 3861-3873.

118.   Chemical, M. G. Methacrylic Acid. http://www.mgc.co.jp/eng/products/lm/08.html (25 February),

APPENDIX A. PERMISSION FOR REPRODUCTION OF CHAPTER 2

JOHN WILEY AND SONS LICENSE TERMS AND CONDITIONS

Apr 04, 2018

License Number	4322010794094
License date	Apr 04, 2018
Licensed Content Publisher	John Wiley and Sons
Licensed Content Publication	Journal of Polymer Science Part A: Polymer Chemistry
Licensed Content Title	Frontal Polymerization of Deep Eutectic Solvents Composed of Acrylic and Methacrylic Acids
Licensed Content Author	Kylee F. Fazende, Manysa Phachansitthi, Josué D. Mota-Morales, John A. Pojman
Licensed Content Date	Oct 12, 2017
Licensed Content Pages	5
Type of use	Dissertation/Thesis
Requestor type	Author of this Wiley article
Format	Electronic
Portion	Full article
Will you be translating?	No

Title of your thesis / dissertation	Free-Radical Polymerization of Acid-Containing Deep Eutectic Solvents
Expected completion date	Aug 2018
Expected size (number of pages)	100
Requestor Location	Kylee Fazende
	213 Choppin Hall
	BATON ROUGE, LA 70803
	United States
	Attn: Kylee Fazende
Publisher Tax ID	EU826007151
Total	0.00 USD

TERMS AND CONDITIONS

at the time that you opened your RightsLink account (these are available at any time at

http://myaccount.copyright.com).

Terms and Conditions

The materials you have requested permission to reproduce or reuse (the "Wiley

Materials") are protected by copyright.

You are hereby granted a personal, non-exclusive, non-sub licensable (on a stand-

alone basis), non-transferable, worldwide, limited license to reproduce the Wiley

Materials for the purpose specified in the licensing process. This license, and any

CONTENT (PDF or image file) purchased as part of your order, is for a one-time use

only and limited to any maximum distribution number specified in the license. The first

instance of republication or reuse granted by this license must be completed within two

years of the date of the grant of this license (although copies prepared before the end

date may be distributed thereafter). The Wiley Materials shall not be used in any other

manner or for any other purpose, beyond what is granted in the license. Permission is

granted subject to an appropriate acknowledgement given to the author, title of the

material/book/journal and the publisher. You shall also duplicate the copyright notice

that appears in the Wiley publication in your use of the Wiley Material. Permission is

also granted on the understanding that nowhere in the text is a previously published

source acknowledged for all or part of this Wiley Material. Any third party content is

expressly excluded from this permission.

With respect to the Wiley Materials, all rights are reserved. Except as expressly granted

by the terms of the license, no part of the Wiley Materials may be copied, modified,

adapted (except for minor reformatting required by the new Publication), translated,

reproduced, transferred or distributed, in any form or by any means, and no derivative works may be made based on the Wiley Materials without the prior permission of the respective copyright owner.For STM Signatory Publishers clearing permission under the terms of the STM Permissions Guidelines only, the terms of the license are extended to include subsequent editions and for editions in other languages, provided such editions are for the work as a whole in situ and does not involve the separate exploitation of the permitted figures or extracts, You may not alter, remove or suppress in any manner any copyright, trademark or other notices displayed by the Wiley Materials. You may not license, rent, sell, loan, lease, pledge, offer as security, transfer or assign the Wiley Materials on a stand-alone basis, or any of the rights granted to you hereunder to any other person.

The Wiley Materials and all of the intellectual property rights therein shall at all times remain the exclusive property of John Wiley & Sons Inc, the Wiley Companies, or their respective licensors, and your interest therein is only that of having possession of and the right to reproduce the Wiley Materials pursuant to Section 2 herein during the continuance of this Agreement. You agree that you own no right, title or interest in or to the Wiley Materials or any of the intellectual property rights therein. You shall have no rights hereunder other than the license as provided for above in Section 2. No right, license or interest to any trademark, trade name, service mark or other branding ("Marks") of WILEY or its licensors is granted hereunder, and you agree that you shall not assert any such right, license or interest with respect thereto

NEITHER WILEY NOR ITS LICENSORS MAKES ANY WARRANTY OR REPRESENTATION OF ANY KIND TO YOU OR ANY THIRD PARTY, EXPRESS,

IMPLIED OR STATUTORY, WITH RESPECT TO THE MATERIALS OR THE

ACCURACY OF ANY INFORMATION CONTAINED IN THE MATERIALS, INCLUDING,

WITHOUT LIMITATION, ANY IMPLIED WARRANTY OF MERCHANTABILITY,

ACCURACY, SATISFACTORY QUALITY, FITNESS FOR A PARTICULAR PURPOSE,

USABILITY, INTEGRATION OR NON-INFRINGEMENT AND ALL SUCH

WARRANTIES ARE HEREBY EXCLUDED BY WILEY AND ITS LICENSORS AND

WAIVED BY YOU.

WILEY shall have the right to terminate this Agreement immediately upon breach of this

Agreement by you.

You shall indemnify, defend and hold harmless WILEY, its Licensors and their

respective directors, officers, agents and employees, from and against any actual or

threatened claims, demands, causes of action or proceedings arising from any breach

of this Agreement by you.

IN NO EVENT SHALL WILEY OR ITS LICENSORS BE LIABLE TO YOU OR ANY

OTHER PARTY OR ANY OTHER PERSON OR ENTITY FOR ANY SPECIAL,

CONSEQUENTIAL, INCIDENTAL, INDIRECT, EXEMPLARY OR PUNITIVE

DAMAGES, HOWEVER CAUSED, ARISING OUT OF OR IN CONNECTION WITH

THE DOWNLOADING, PROVISIONING, VIEWING OR USE OF THE MATERIALS

REGARDLESS OF THE FORM OF ACTION, WHETHER FOR BREACH OF

CONTRACT, BREACH OF WARRANTY, TORT, NEGLIGENCE, INFRINGEMENT OR

OTHERWISE (INCLUDING, WITHOUT LIMITATION, DAMAGES BASED ON LOSS OF

PROFITS, DATA, FILES, USE, BUSINESS OPPORTUNITY OR CLAIMS OF THIRD

PARTIES), AND WHETHER OR NOT THE PARTY HAS BEEN ADVISED OF THE

POSSIBILITY OF SUCH DAMAGES. THIS LIMITATION SHALL APPLY

NOTWITHSTANDING ANY FAILURE OF ESSENTIAL PURPOSE OF ANY LIMITED

REMEDY PROVIDED HEREIN.

Should any provision of this Agreement be held by a court of competent jurisdiction to

be illegal, invalid, or unenforceable, that provision shall be deemed amended to achieve

as nearly as possible the same economic effect as the original provision, and the

legality, validity and enforceability of the remaining provisions of this Agreement shall

not be affected or impaired thereby.

The failure of either party to enforce any term or condition of this Agreement shall not

constitute a waiver of either party's right to enforce each and every term and condition

of this Agreement. No breach under this agreement shall be deemed waived or excused

by either party unless such waiver or consent is in writing signed by the party granting

such waiver or consent. The waiver by or consent of a party to a breach of any provision

of this Agreement shall not operate or be construed as a waiver of or consent to any

other or subsequent breach by such other party.

This Agreement may not be assigned (including by operation of law or otherwise) by

you without WILEY's prior written consent.

Any fee required for this permission shall be non-refundable after thirty (30) days from

receipt by the CCC.

These terms and conditions together with CCC's Billing and Payment terms and

conditions (which are incorporated herein) form the entire agreement between you and

WILEY concerning this licensing transaction and (in the absence of fraud) supersedes

all prior agreements and representations of the parties, oral or written. This Agreement

may not be amended except in writing signed by both parties. This Agreement shall be

binding upon and inure to the benefit of the parties' successors, legal representatives,

and authorized assigns.

In the event of any conflict between your obligations established by these terms and

conditions and those established by CCC's Billing and Payment terms and conditions,

these terms and conditions shall prevail.

WILEY expressly reserves all rights not specifically granted in the combination of (i) the

license details provided by you and accepted in the course of this licensing transaction,

(ii) these terms and conditions and (iii) CCC's Billing and Payment terms and conditions.

This Agreement will be void if the Type of Use, Format, Circulation, or Requestor Type

was misrepresented during the licensing process.

This Agreement shall be governed by and construed in accordance with the laws of the

State of New York, USA, without regards to such state's conflict of law rules. Any legal

action, suit or proceeding arising out of or relating to these Terms and Conditions or the

breach thereof shall be instituted in a court of competent jurisdiction in New York

County in the State of New York in the United States of America and each party hereby

consents and submits to the personal jurisdiction of such court, waives any objection to

venue in such court and consents to service of process by registered or certified mail,

return receipt requested, at the last known address of such party.

Other Terms and Conditions:

v1.10 Last updated September 2015

Questions? customercare@copyright.com or +1-855-239-3415 (toll free in the US) or

+1-978-646-2777.

APPENDIX B. FRONT TEMPERATURE PROFILES

This appendix gives all front temperature profiles for the experiments in Chapter 2. Figures B.1 – B.6 are AA-ChCl, and Figures B.7 – B.12 are MAA-ChCl. Figures B.13 – B.15 are the AA-Analog samples. MAA-Analog and stearic acid in general have no profiles as no fronts were successful.

B.1 FT PROFILES FOR AA-CHCL VARIED INITIATOR SAMPLES
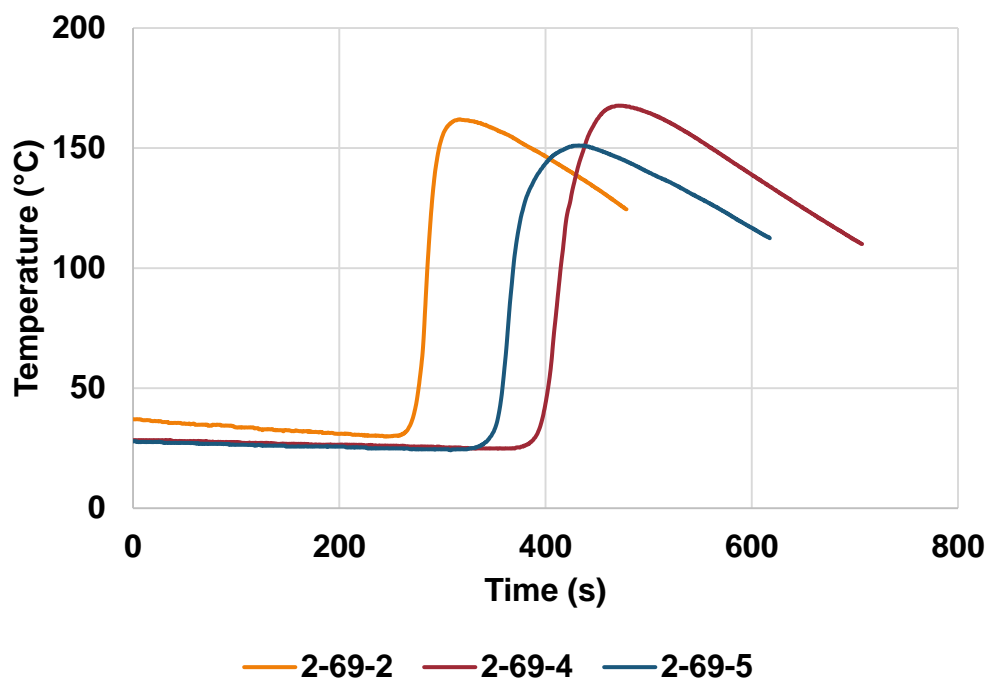
Figure B.1. FT profiles for 0.2% L231 AA-ChCl FP.
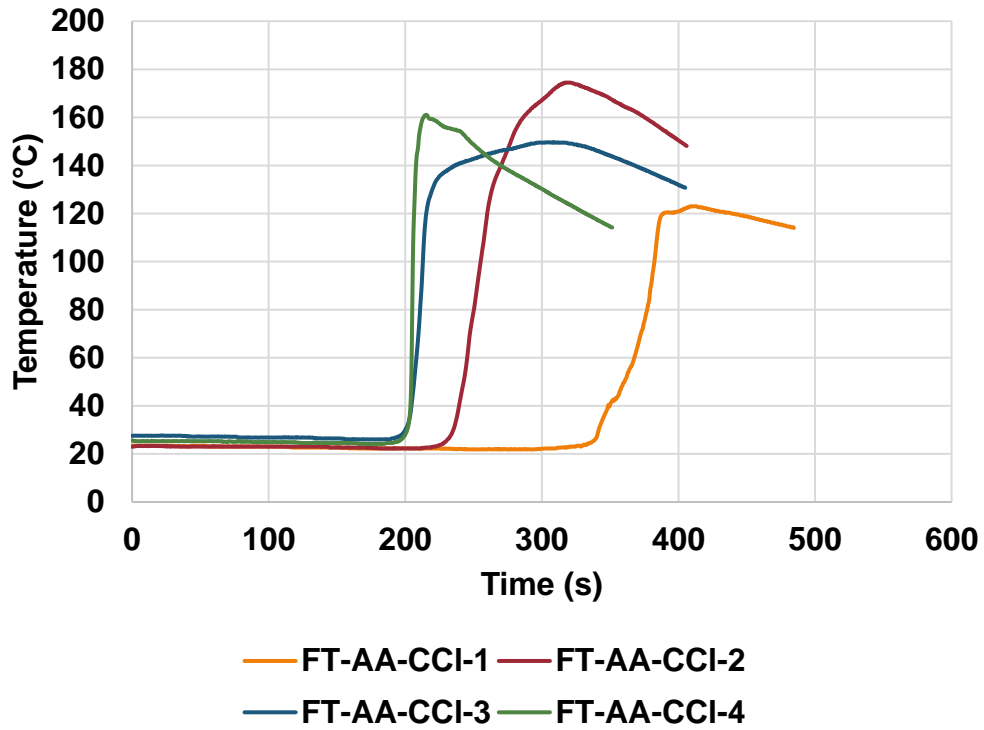
Figure B.2. FT profiles for 0.3% L231 AA-ChCl FP.
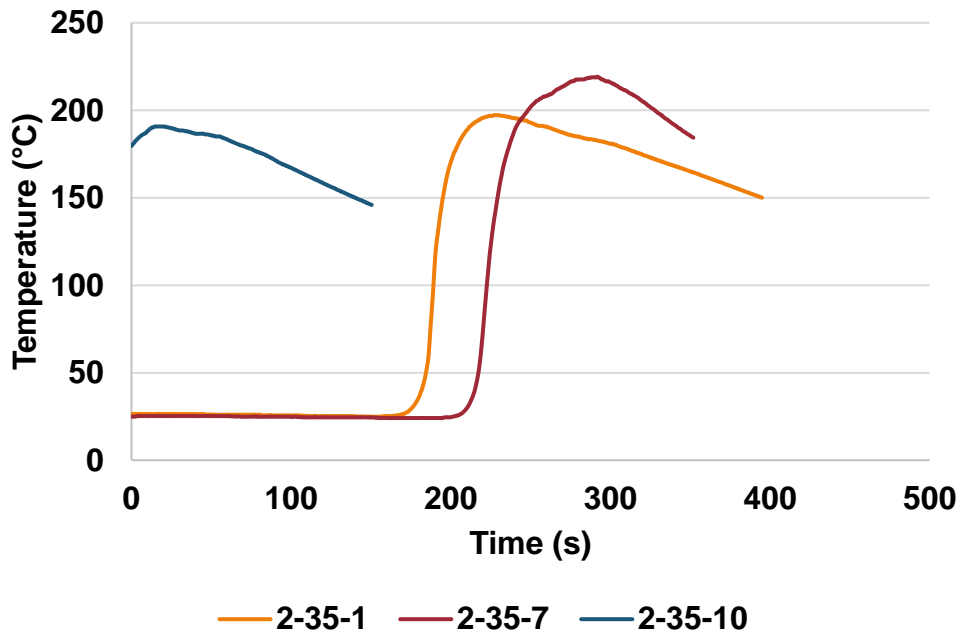
Figure B.3. FT profiles for 0.8% L231 AA-ChCl FP.
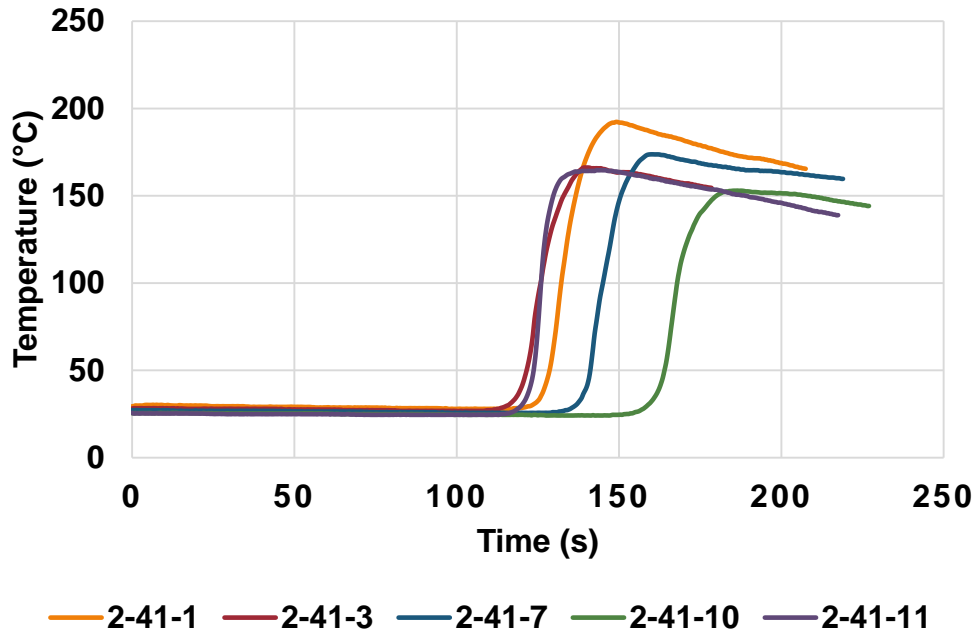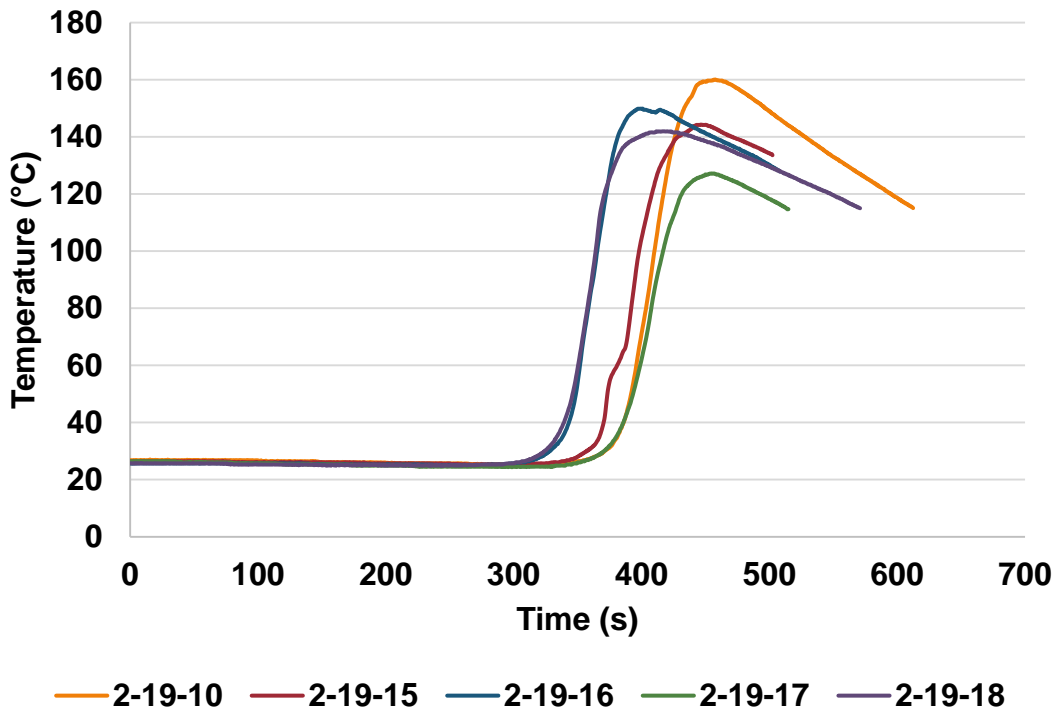
Figure B.4. FT profiles for 1.7% L231 AA-ChCl FP.
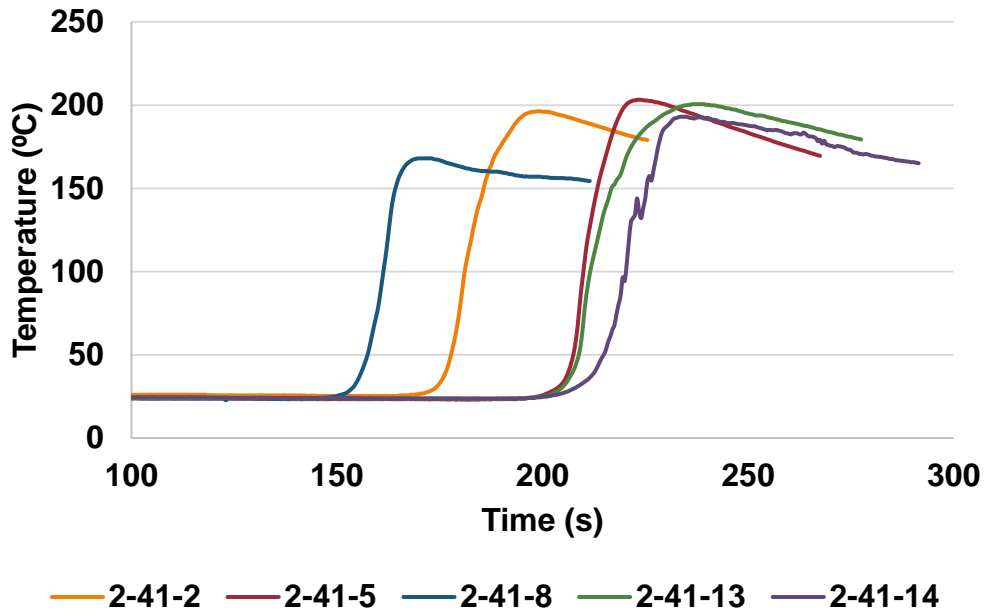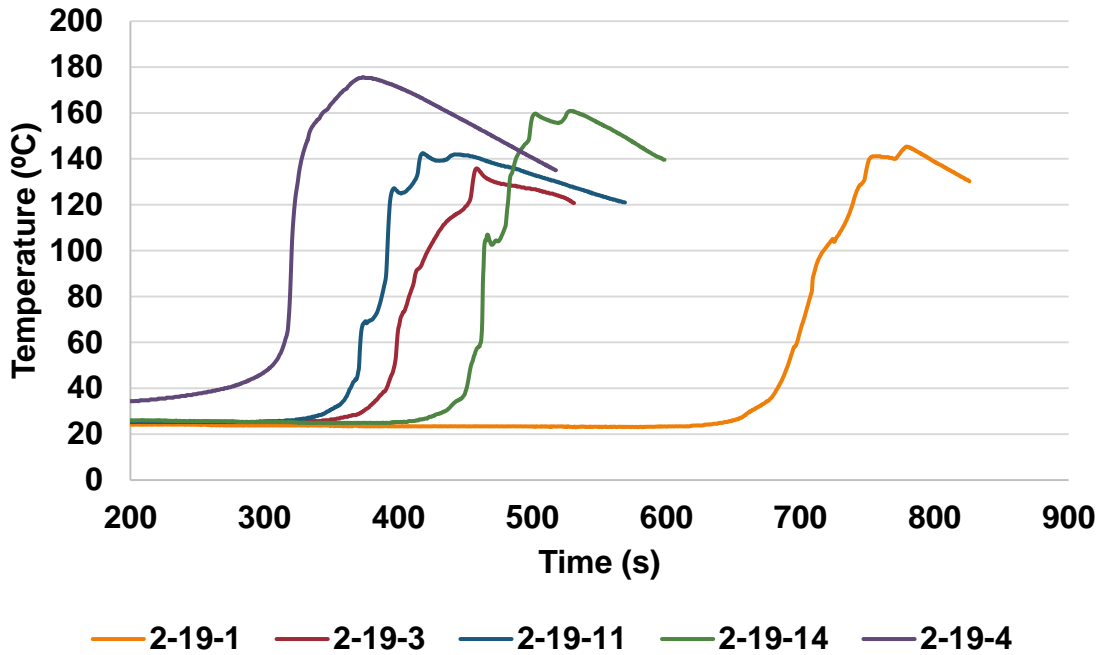

Figure B.5. FT profiles for 2.5% L231 AA-ChCl FP.
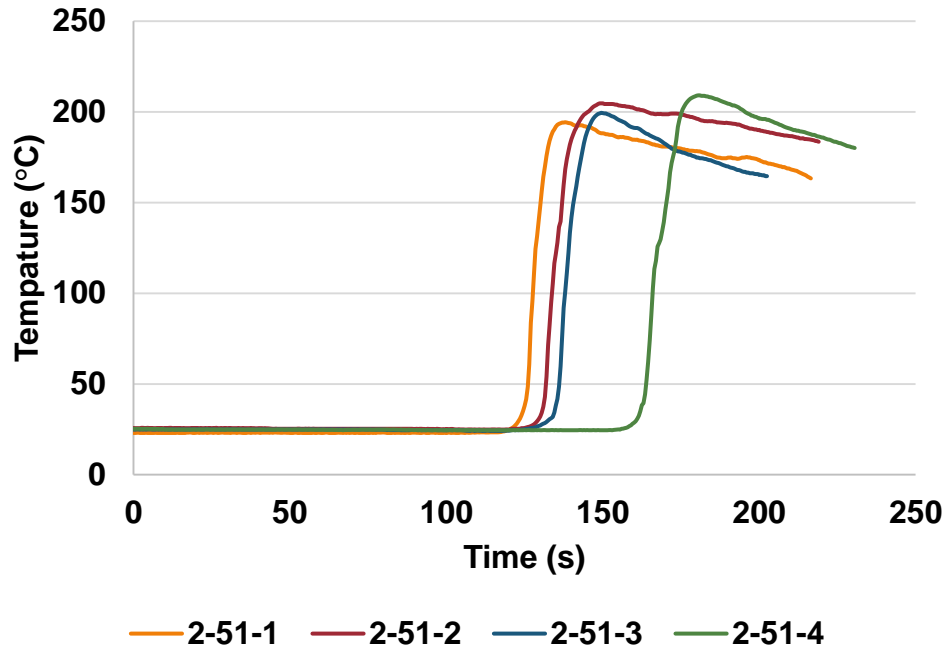
Figure B.6. FT profiles for 3.3% L231 AA-ChCl FP.

B.2 FT Profiles for MAA-ChCl Varied Initiator Samples
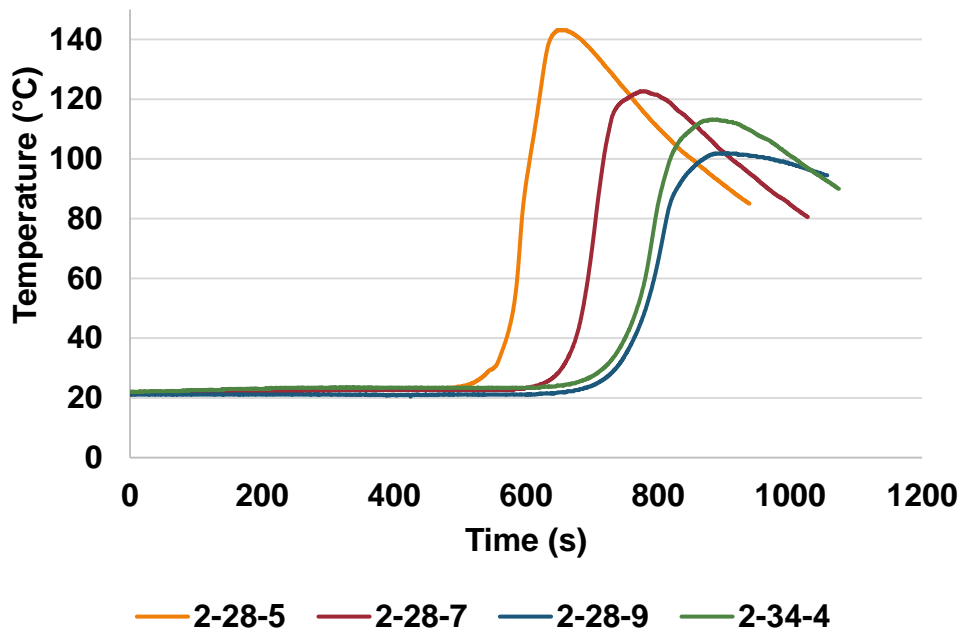
Figure B.7. FT profiles for 0.2% L231 MAA-ChCl FP.
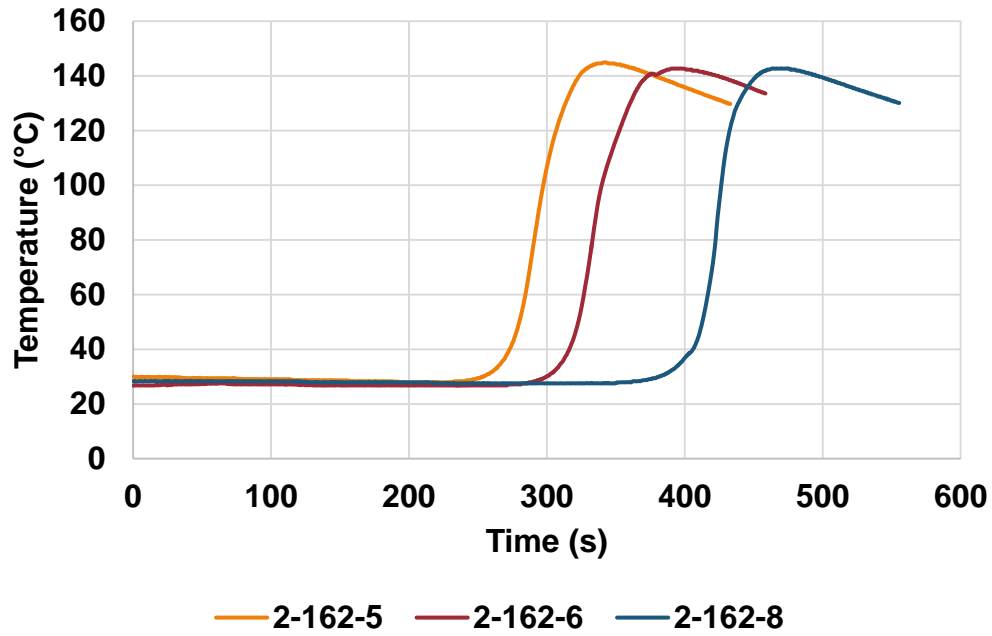
Figure B.8. FT profiles for 0.3% L231 MAA-ChCl FP.
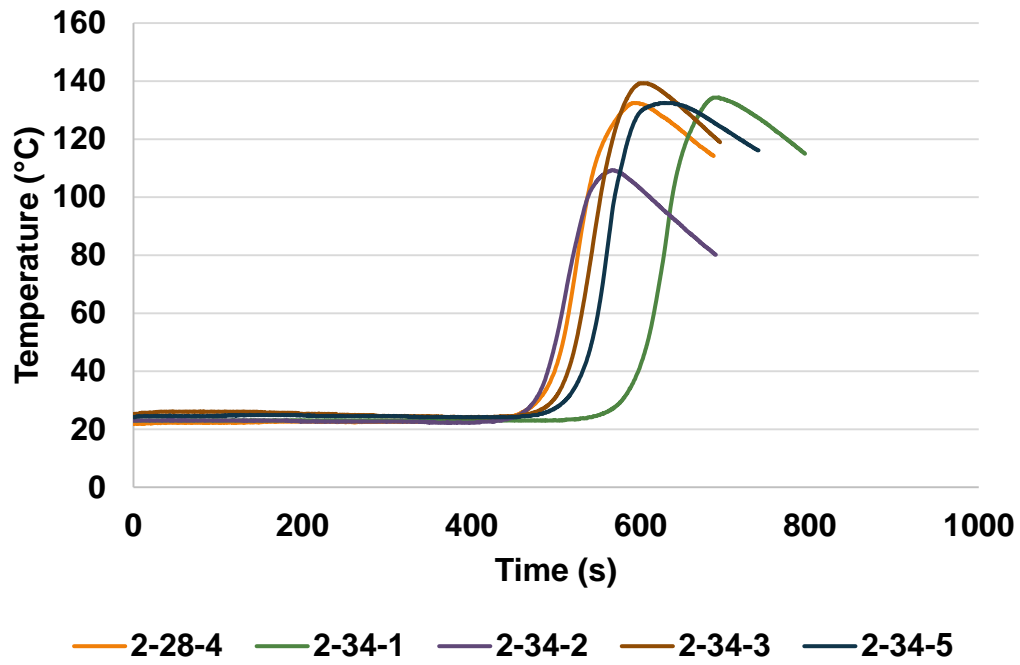
Figure B.9. FT profiles for 0.8% L231 MAA-ChCl FP.
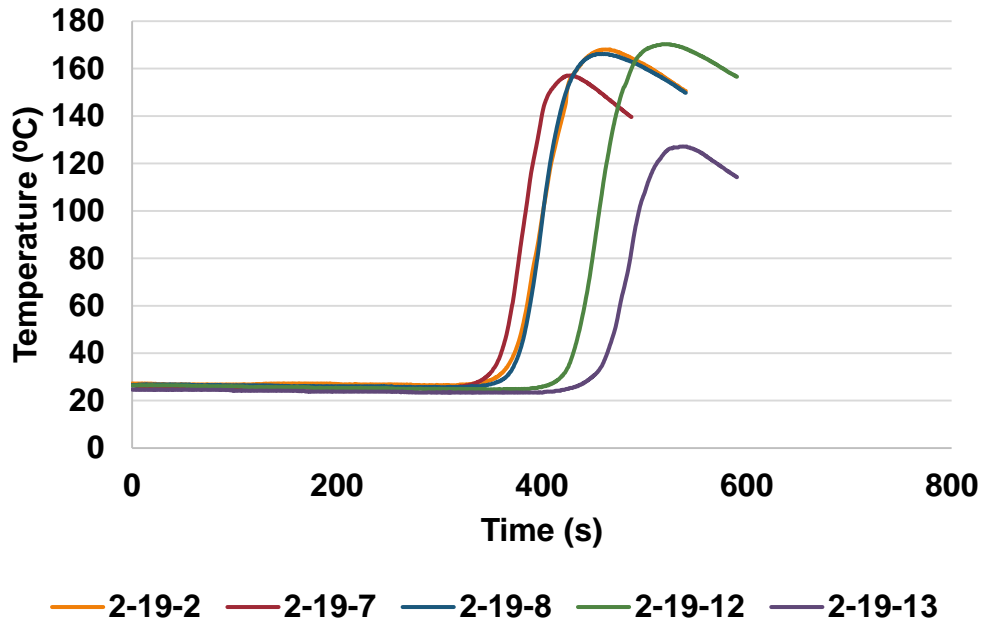
Figure B.10. FT profiles for 1.7% L231 MAA-ChCl FP.

Figure B.11. FT profiles for 2.5% L231 MAA-ChCl FP.

Figure B.12. FT profiles for 3.3% L231 MAA-ChCl FP.

B.3 FT PROFILES FOR AA-ANALOG SAMPLES
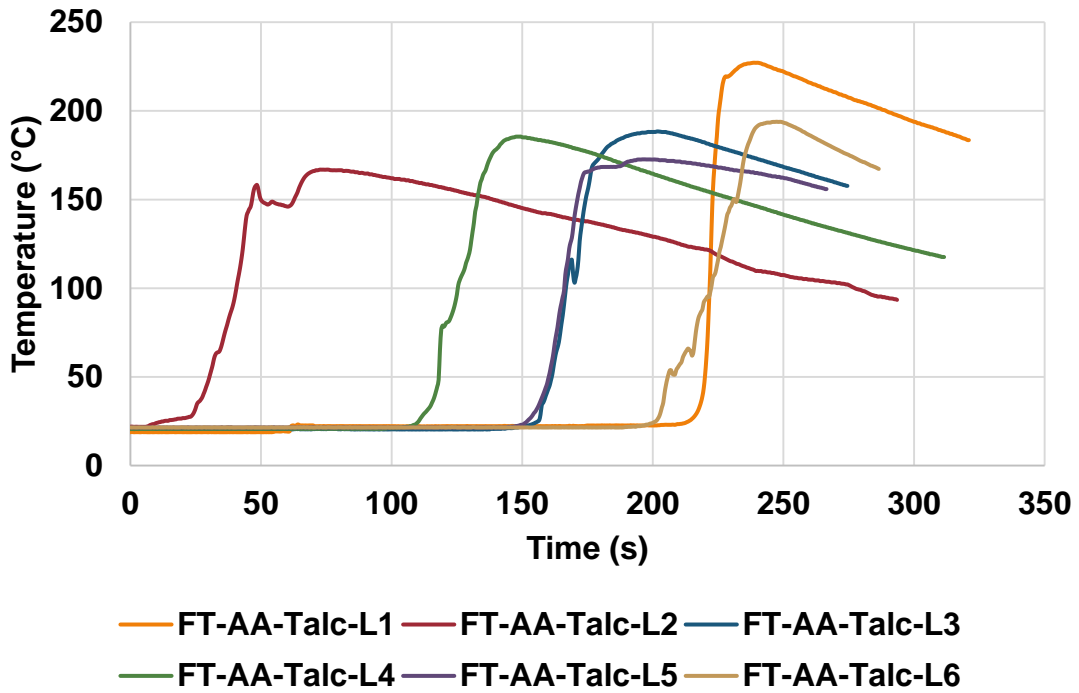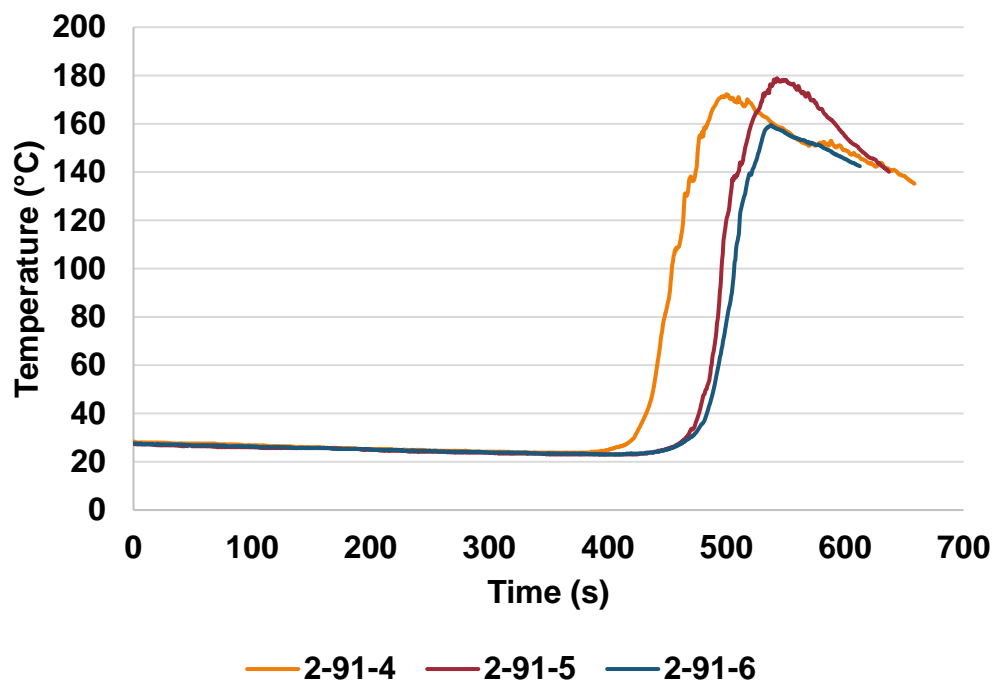

Figure B.13. FT profiles for AA-Talc samples.

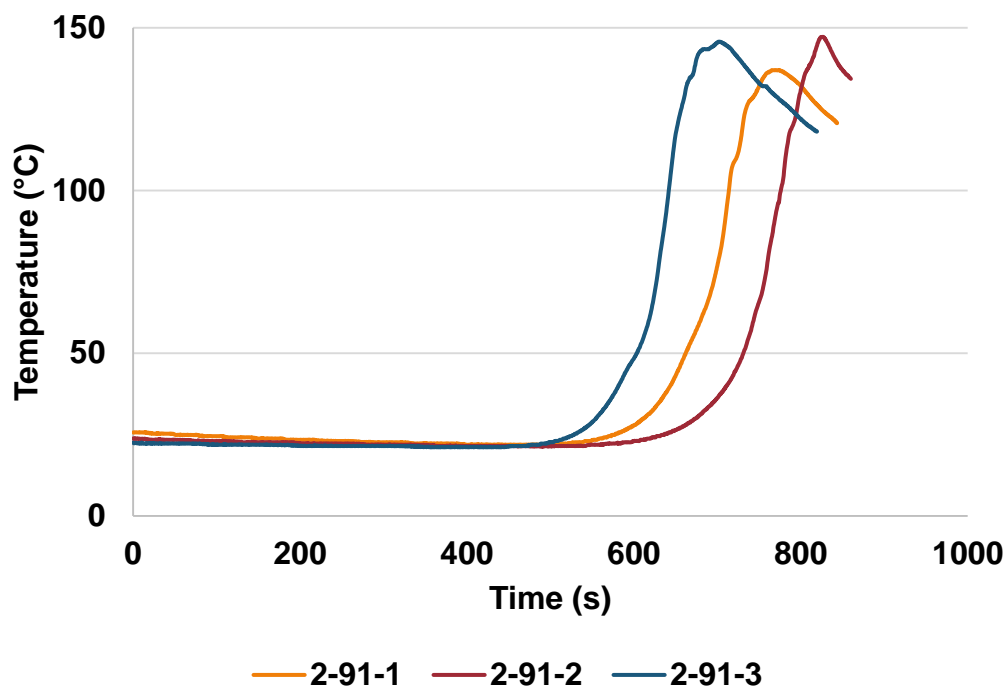Figure B.14. FT profiles for AA-DMSO samples with increased silica.

Figure B.15. FT profiles for AA-LA with increased silica.

APPENDIX C. FRONT VELOCITY POSITION VERSUS TIME PLOTS

For all front velocity plots, the unit of time plotted is seconds due to the method of data recording from the video. The conversion to the reported units of $cm \cdot min^{-1}$ is performed after the FV is calculated from the slope of the line. Figures C.1 – C.6 are AA-ChCl at the various monomer concentrations, and Figures C.7 – C.12 are MAA-ChCl. Figures C.13 – C.15 are the AA-Analog samples. Again, MAA-Analog and stearic acid in general have no plots as no fronts were successful.

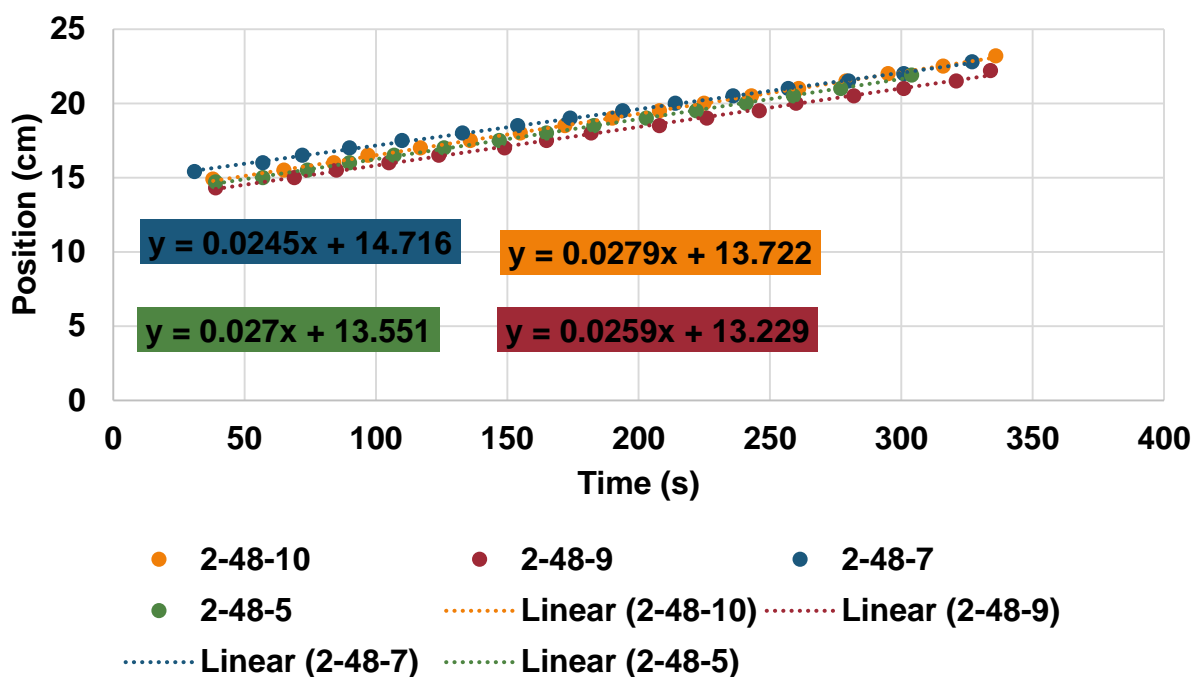C.1 FV PROFILES FOR AA-CHCL VARIED INITIATOR SAMPLES

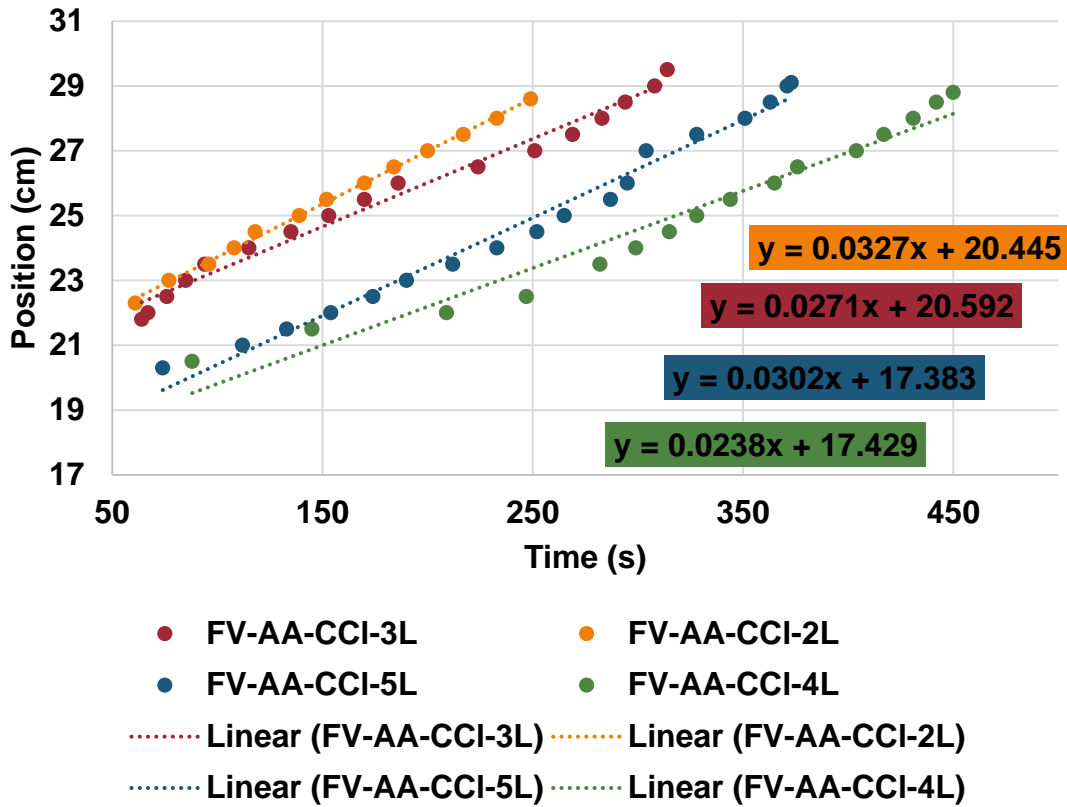Figure C.1. Position versus time plots for 0.2% L231 AA-ChCl FP.

Figure C.2. Position versus time plots for 0.3% L231 AA-ChCl FP.
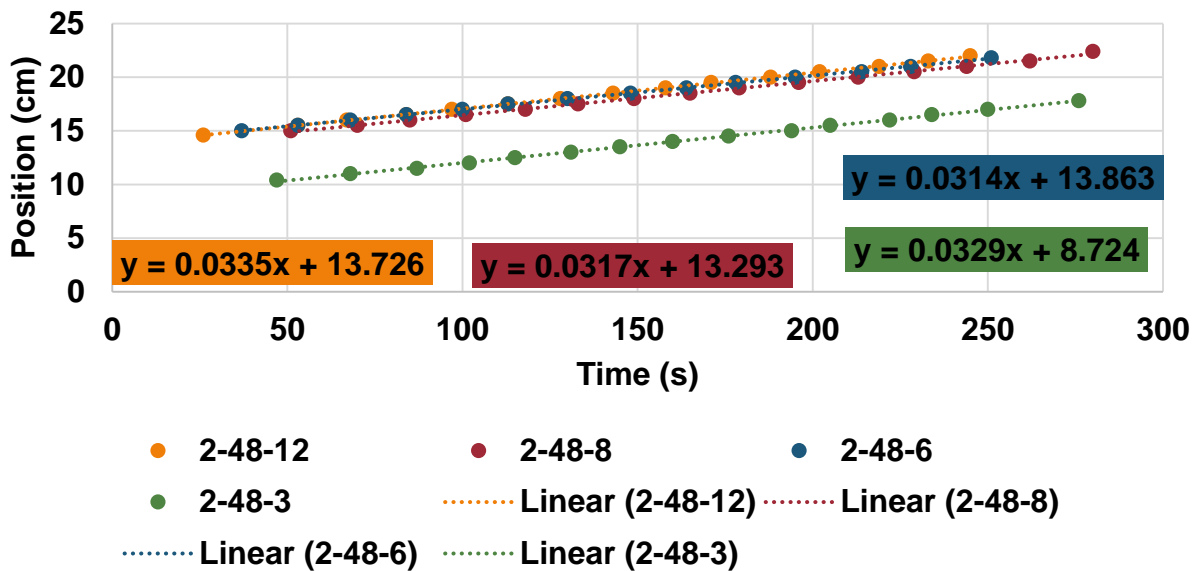

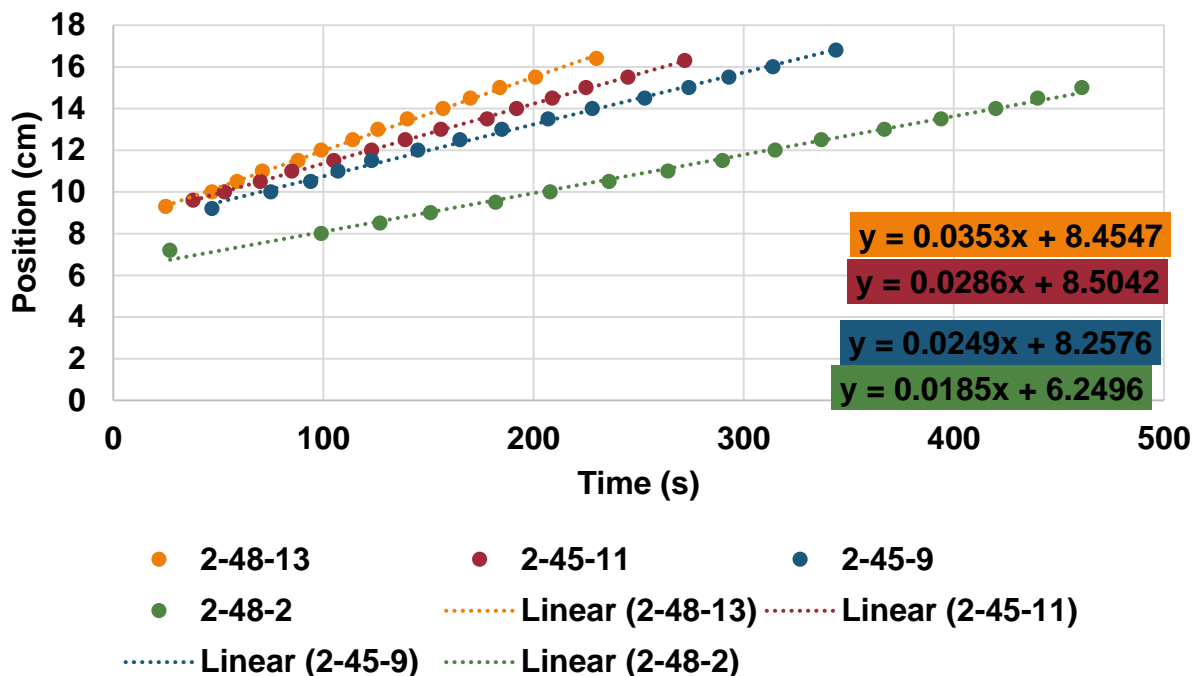Figure C.3. Position versus time plots for 0.8% L231 AA-ChCl FP.

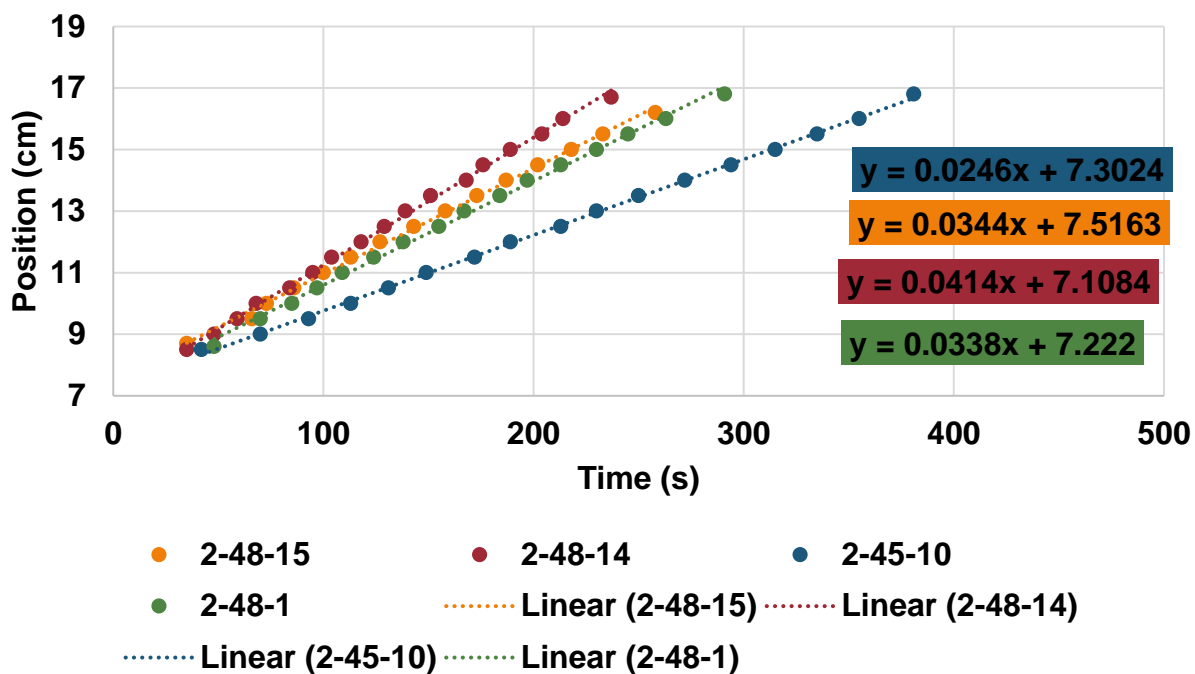Figure C.4. Position versus time plots for 1.7% L231 AA-ChCl FP.

Figure C.5. Position versus time plots for 2.5% L231 AA-ChCl FP.

Figure C.6. Position versus time plots for 3.3% L231 AA-ChCl FP.

C.2 FV Profiles for MAA-ChCl Varies Initiator Samples

Figure C.7. Position versus time plots for 0.2% L231 MAA-ChCl FP.
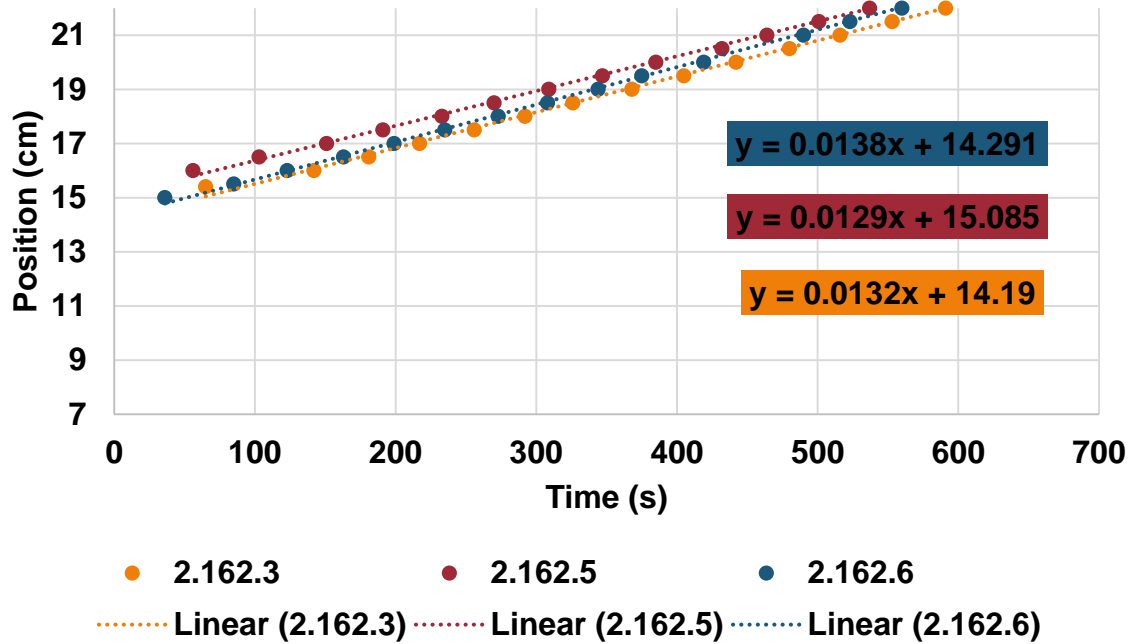
Figure C.8. Position versus time plots for 0.3% L231 MAA-ChCl FP.
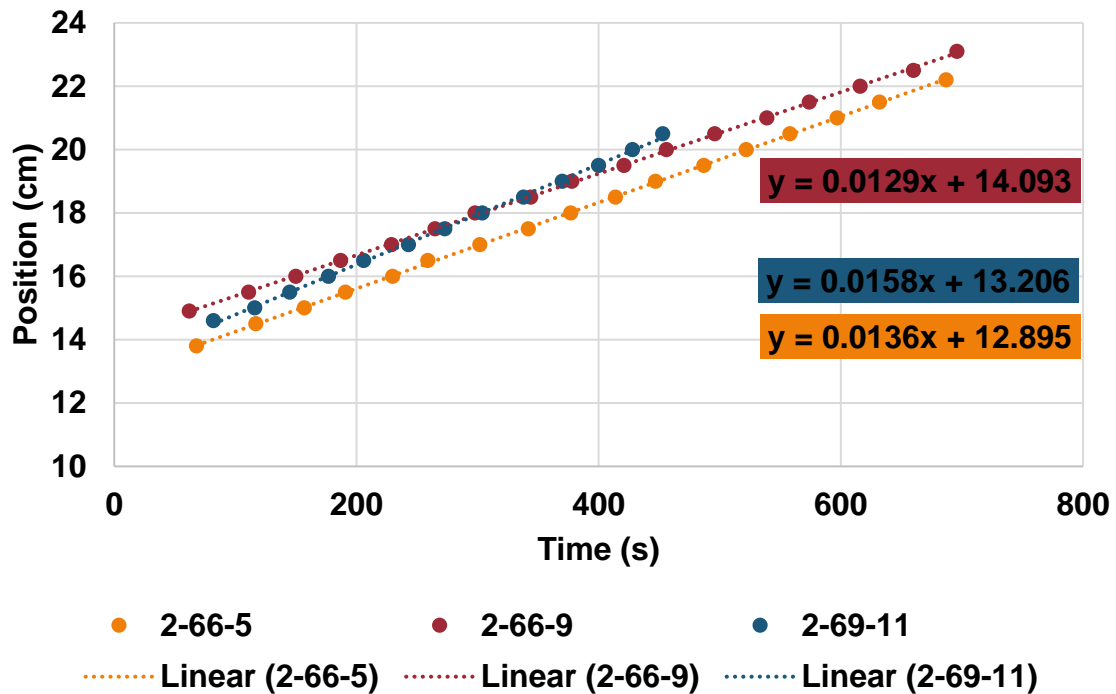
Figure C.9. Position versus time plots for 0.8% L231 MAA-ChCl FP.
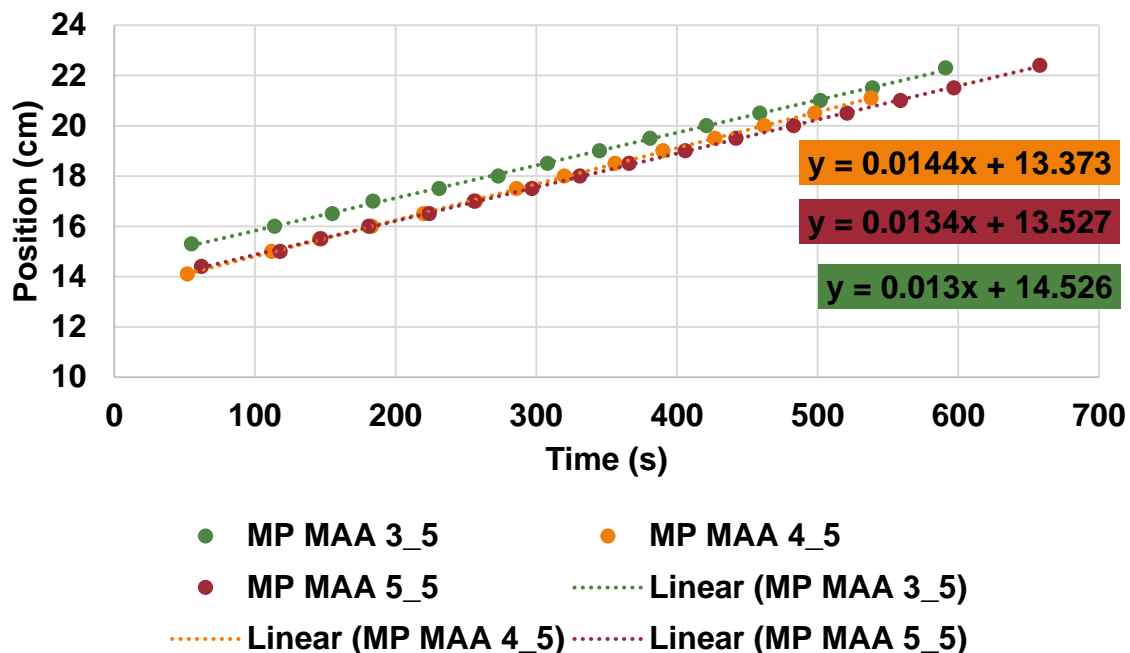
Figure C.10. Position versus time plots for 1.7% L231 MAA-ChCl FP.

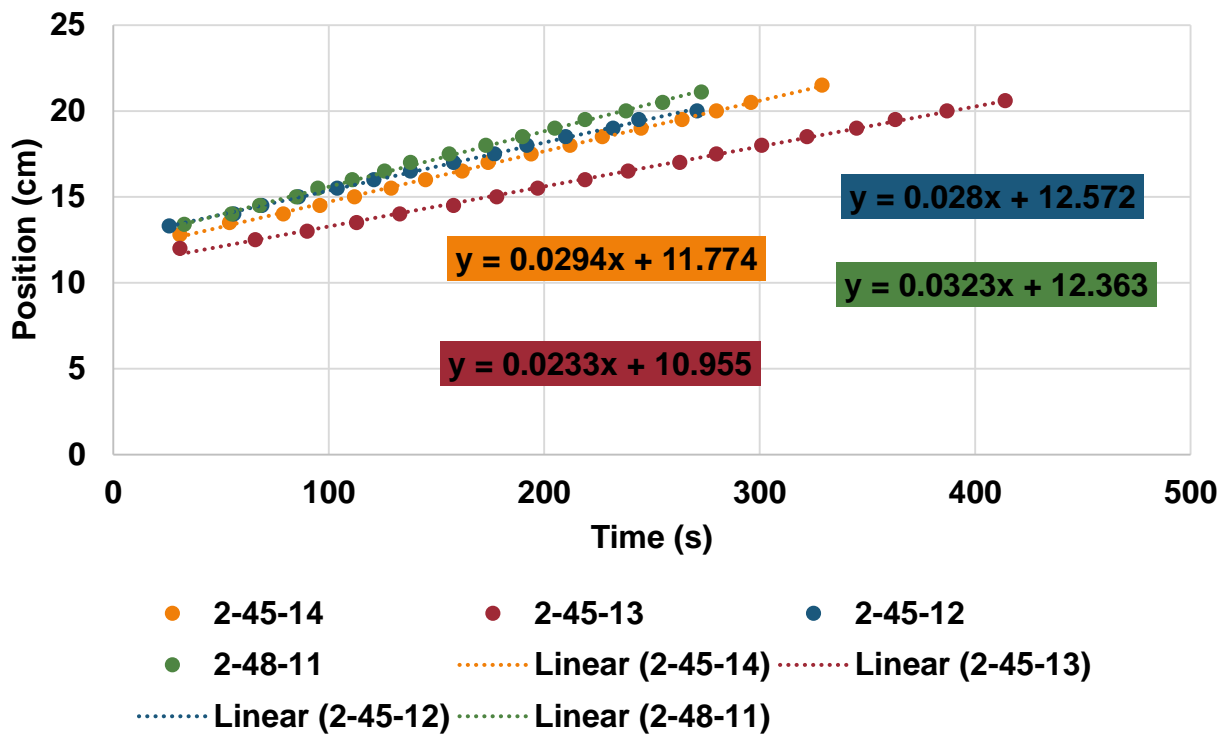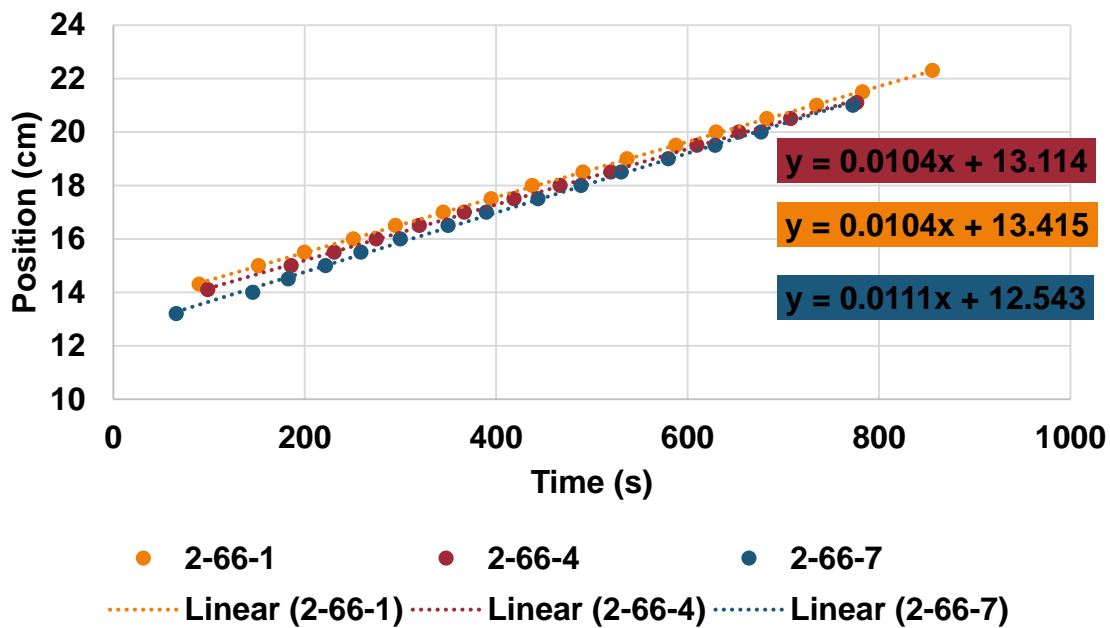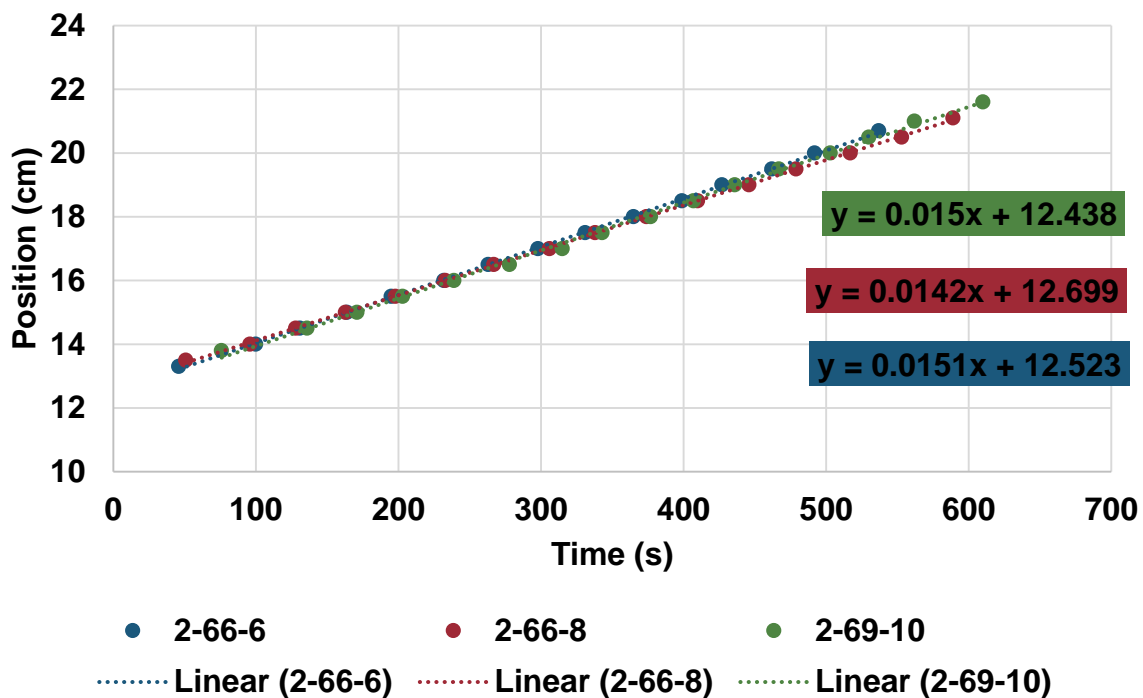Figure C.11. Position versus time plots for 2.5% L231 MAA-ChCl FP.

y = 0.0129x + 13.695

y = 0.0161x + 13.787

y = 0.0124x + 13.114

y = 0.0128x + 12.456
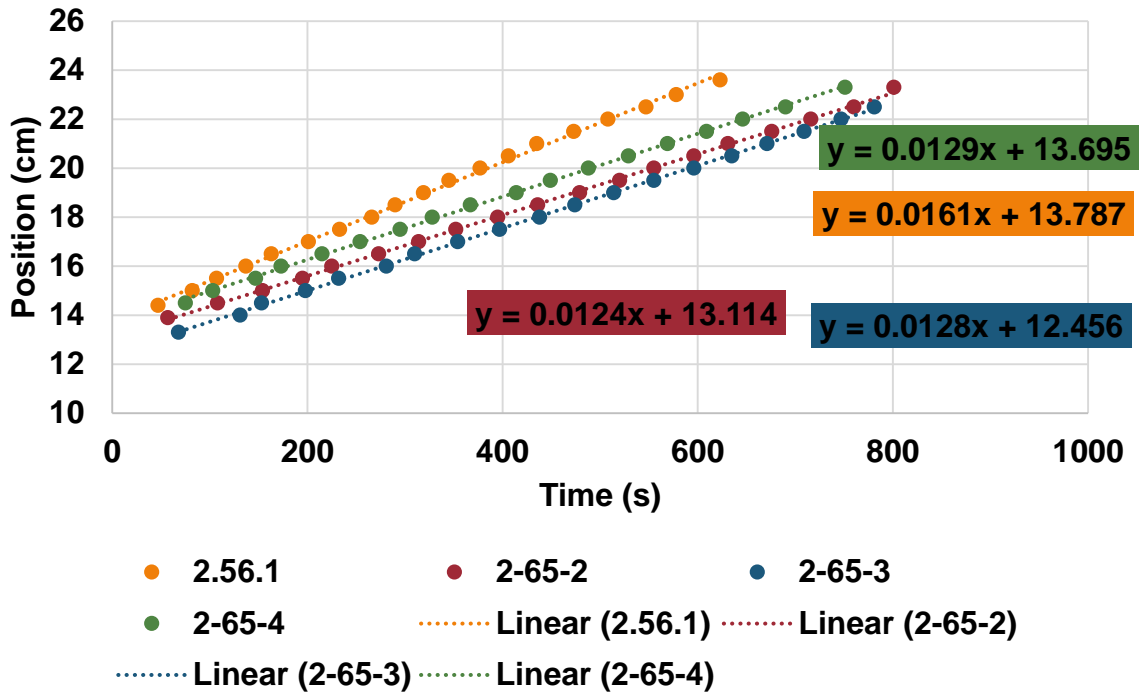
Figure C.12. Position versus time plots for 3.3% L231 MAA-ChCl FP.

C.3 FV PROFILES FOR AA-ANALOG SAMPLES

y = 0.0333x + 12.997

y = 0.0358x + 12.561

y = 0.0292x + 11.891

y = 0.0366x + 12.09

y = 0.0373x + 11.111
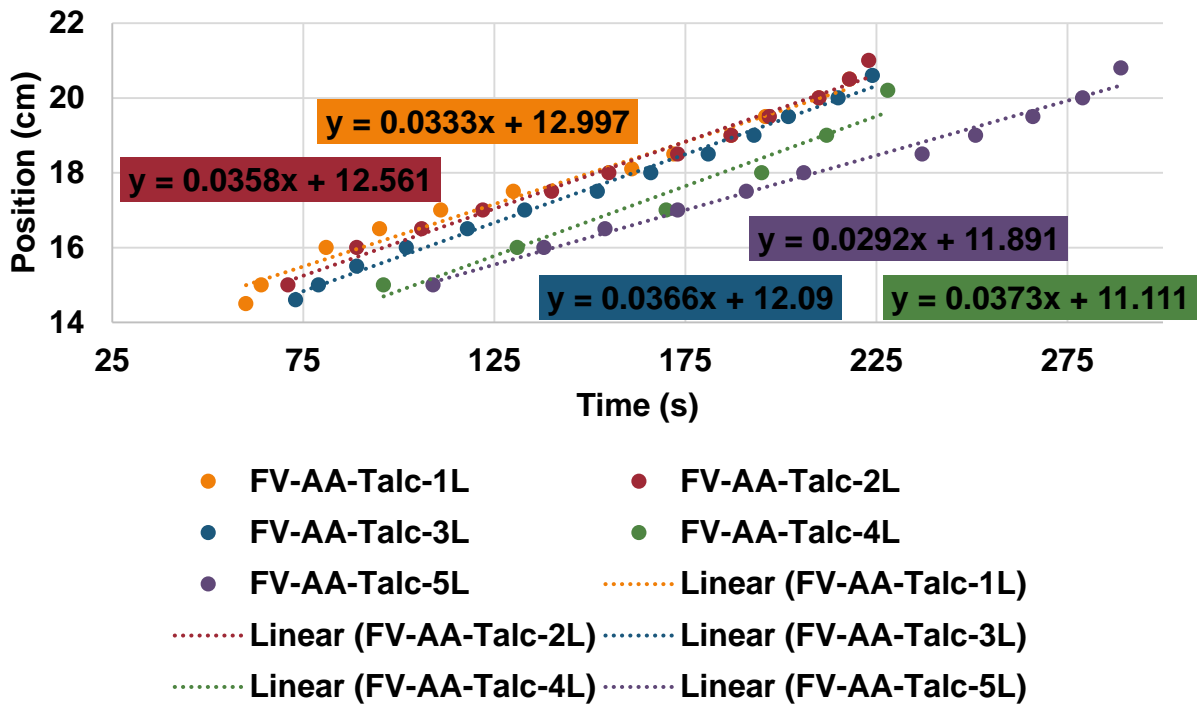
Figure C.13. Position versus time plots for AA-Talc samples.

89

y = 0.0151x + 11.028

y = 0.0145x + 10.428

y = 0.0154x + 10.522
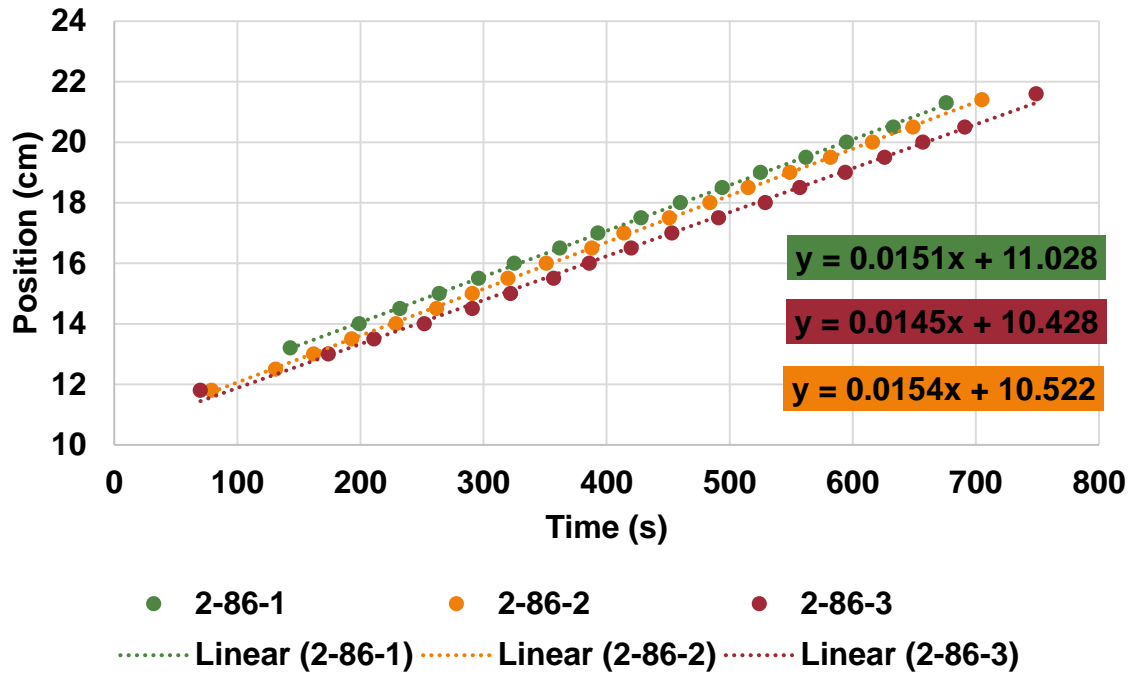
Figure C.14. FV plots for AA-DMSO samples with increased silica.

y = 0.012x + 11.152

y = 0.0071x + 10.732

y = 0.0118x + 11.148

Figure C.15. FV plots for AA-LA with increased silica.

APPENDIX D. RTIR SAMPLE SET INFORMATION

D.1 CAMPHORQUINONE SAMPLE SETS (365 NM MEASUREMENTS)

Table D.1 Camphorquinone RTIR parameters.

Sample set	Measured Intensity (mW)	Interval time (s)	Number of spectra	Total time (min)
AA-CQ	1180	60	30	30
AA-ChCl-CQ	1180	60	15	15
AA-ChCl-CQ	750	60	20	20
AA-ChCl-CQ-TEA	1180	30	60	30
MAA-CQ	1180	60	60	60
MAA-ChCl-CQ	1180	60	60	60
MAA-ChCl-CQ	750	60	75	75
MAA-ChCl-CQ-TEA	1180	60	60	60
MAA-ChCl-CQ-TEA	750	60	75	75

D.2. 1% DESS AND PURE MONOMERS (365 NM MEASUREMENTS)

Table D.2. RTIR parameters for DES and pure monomer samples with 1% TPO and light intensity measured at 365 nm.

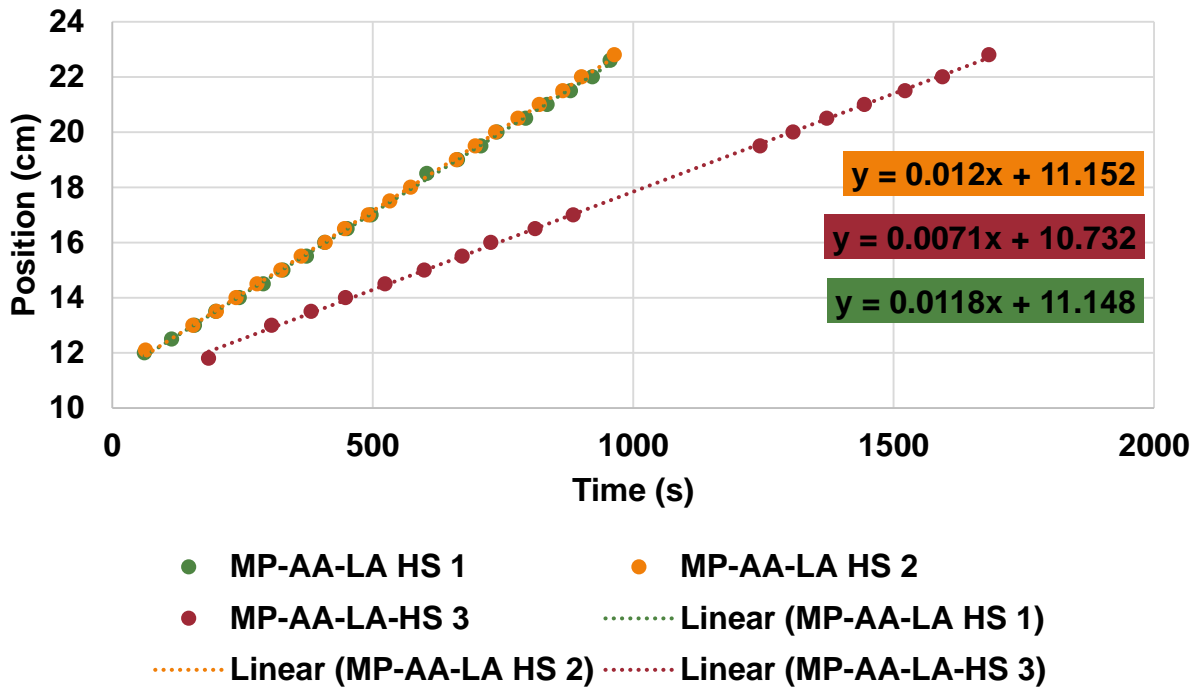| Sample set	Measured Intensity (mW)	Interval time (s)	Number of spectra	Total time (min)
AA-TPO	500	60	60	60
AA-TPO	375	60	60	60
AA-TPO	250	60	60	60
AA-TPO	50	60	60	60
AA-ChCl-TPO	500	60	30	30
AA-ChCl-TPO	375	60	30	30
AA-ChCl-TPO	250	60	30	30
AA-ChCl-TPO	50	60	30	30
MAA-TPO	500	60	60	60
MAA-TPO	375	60	90	90
MAA-TPO	250	60	90	90
MAA-TPO	125	60	120	120
MAA-TPO	50	60	120	120
MAA-ChCl-TPO	500	60	45	45
MAA-ChCl-TPO	375	60	90	90
MAA-ChCl-TPO	250	60	90	90
MAA-ChCl-TPO	125	60	120	120
MAA-ChCl-TPO	50	60	120	120

D.3. 0.1% DESs AND PURE MONOMERS (365 NM MEASUREMENTS)

Table D.3. RTIR parameters for DES and pure monomer samples with 0.1% TPO and light intensity measured at 365 nm.

Sample set	Measured Intensity (mW)	Interval time (s)	Number of spectra	Total time (min)
AA-TPO	500	30	40	20
AA-TPO	375	30	60	30
AA-TPO	250	30	120	60
AA-TPO	125	30	120	60
AA-TPO	50	30	120	60
AA-ChCl-TPO	500	30	30	15
AA-ChCl-TPO	375	30	30	15
AA-ChCl-TPO	250	30	30	15
AA-ChCl-TPO	125	30	30	15
AA-ChCl-TPO	50	30	40	20
MAA-TPO	500	30	60	30
MAA-TPO	375	30	120	60
MAA-TPO	250	30	120	60
MAA-TPO	125	30	120	60
MAA-TPO	50	30	120	60
MAA-ChCl-TPO	500	30	30	15
MAA-ChCl-TPO	375	30	30	15
MAA-ChCl-TPO	250	30	30	15
MAA-ChCl-TPO	125	30	30	15
MAA-ChCl-TPO	50	30	60	30

D.4. 0.1% DESs AND PURE MONOMERS (400 nm MEASUREMENTS)

Table D.4. RTIR parameters for DES and pure monomer samples with 0.1% TPO and light intensity measured at 400 nm.

Sample set	Measured Intensity (mW)	Interval time (s)	Number of spectra	Total time (min)
AA-TPO	50	300	120	600
AA-ChCl-TPO	50	45	120	90
AA-ChCl-TPO (0.1 OD NDF)	50	45	120	90
AA-ChCl-TPO (0.2 OD NDF)	50	45	120	90
AA-ChCl-TPO (0.5 OD NDF)	50	45	120	90
MAA-TPO	50	300	120	600
MAA-ChCl-TPO	50	45	120	90
MAA-ChCl-TPO (0.1 OD NDF)	50	45	120	90
MAA-ChCl-TPO (0.2 OD NDF)	50	45	120	90
MAA-ChCl-TPO (0.5 OD NDF)	50	45	120	90

D.5. METHYL ESTER MONOMER SAMPLE SETS (365 NM MEASUREMENTS)

Table D.5. RTIR parameters for DES and pure monomer methyl ester samples with 1% TPO and light intensity measured at 365 nm.

Sample set	Measured Intensity (mW)	Interval time (s)	Number of spectra	Total time (min)
MeA-TPO	500	30	60	30
MeA-TPO	375	30	60	30
MeA-TPO	250	30	120	60
MeA-TPO	125	30	120	60
MeA-TPO	50	30	120	60
MeA-TPO-PA-ChCl	500	30	30	15
MeA-TPO-PA-ChCl	375	30	30	15
MeA-TPO-PA-ChCl	250	30	30	15
MeA-TPO-PA-ChCl	125	30	30	15
MeA-TPO-PA-ChCl	50	30	30	15
MMA-TPO	500	30	60	30
MMA-TPO	375	30	120	60
MMA-TPO	250	30	120	60
MMA-TPO	125	30	120	60
MMA-TPO	50	30	120	60
MMA-TPO-IBA-ChCl	500	30	60	30
MMA-TPO-IBA-ChCl	375	30	60	30
MMA-TPO-IBA-ChCl	250	30	60	30
MMA-TPO-IBA-ChCl	125	30	60	30
MMA-TPO-IBA-ChCl	50	30	60	30

VITA

   Kylee Fazende is a native of South Louisiana. After graduating valedictorian from Hammond High School, she attended the University of Southern Mississippi to obtain her Bachelor's degree in Polymer Science, graduating Summa Cum Laude. Upon completing her studies at Southern Miss, she decided to return home to Louisiana to pursue her doctorate at Louisiana State University. In 2014, she joined the Pojman Research Team with an initial intent to study frontal polymerizations in thin layers, but after becoming a PhD candidate, she changed her focus to the kinetics of polymerizations of deep eutectic solvents. She has presented her research at several conferences including two American Chemical Society National Meetings. She has also served as a conference coordinator for two conferences, the 2014 National Graduate Research Polymer Conference and the 2016 APTEC Annual Meeting. After five years of study in the LSU Chemistry Department, she is pleased to be completing her doctoral studies with two publications and a third currently being written. Kylee anticipates graduating in August of 2018